

Supporting Information

Nickel Catalyzed C(sp²)-H Borylation of Arenes

Arpan Das, Pradip Kumar Hota, and Swadhin K. Mandal*

Department of Chemical Sciences, Indian Institute of Science Education and Research Kolkata, Mohanpur 741246, India

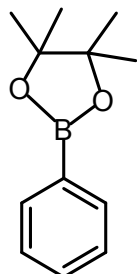
E-mail: swadhin.mandal@iiserkol.ac.in

Contents

A) ¹ H, ¹³ C, and ¹¹ B NMR data of borylated products 4a–4t	S2-S12
B) ¹ H, ¹³ C, and ¹¹ B NMR spectra of 2 and 3	S12-S15
C) ¹ H, ¹³ C, and ¹¹ B NMR spectra of borylated products 4a–4t	S16-S45
D) ¹ H NMR spectra of stoichiometric reactions	S46-S48
E) Crystallographic and data collection parameters for 2 and 3	S49-S50
F) References.....	S51-S52

A) ^1H , ^{13}C and ^{11}B NMR data for borylated compounds 4a–4t:

4,4,5,5-tetramethyl-2-phenyl-1,3,2-dioxaborolane (4a)¹:



4a

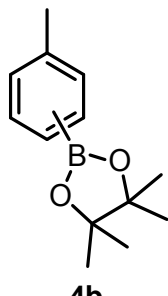
Colourless liquid. Yield 88%. The crude product was purified through silica gel column chromatography (100-200 mesh) using 0.5% EtOAc in hexane as eluent.

^1H NMR (400 MHz, CDCl_3 , 298 K) δ (ppm) 7.82 (d, $J = 6.8$ Hz, 2H), 7.49-7.45 (m, 1H), 7.38 (t, $J = 7.2$ Hz, 2H) 1.36 (s, 12H).

^{13}C NMR (100 MHz, CDCl_3 , 298 K) δ (ppm) 134.7, 131.2, 127.7, 83.7, 24.8.

^{11}B NMR (160 MHz, CDCl_3 , 298 K) δ (ppm) 31.2.

4,4,5,5-tetramethyl-2-(m-tolyl)-1,3,2-dioxaborolane (4b)²:



4b

m:p = 69:31

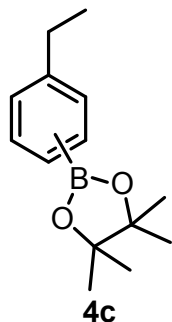
Colourless liquid. Yield 83%. The crude product was purified through silica gel column chromatography (100-200 mesh) using 0.5% EtOAc in hexane as eluent. The percentage of different regioisomers was calculated by relative integration of the protons arising from the respective isomers in ^1H NMR spectroscopy.

^1H NMR (400 MHz, CDCl_3 , 298 K) δ (ppm) 7.72 (d, $J = 8$ Hz, 2H, para), 7.20 (d, $J = 7.6$ Hz, 2H, para), 2.38 (s, 3H, para), 1.35 (s, 12H, para); 7.66 (s, 1H, meta), 7.63 (t, $J = 5.2$ Hz, 1H, meta), 7.29-7.28 (m, 2H, meta), 2.37 (s, 3H, meta), 1.36 (s, 12H, meta).

^{13}C NMR (100 MHz, CDCl_3 , 298 K) δ (ppm) 141.4, 134.8, 128.5, 83.6, 24.8, 21.7 (para); 137.1, 135.3, 132.0, 131.8, 127.7, 83.6, 24.8, 21.2 (meta).

¹¹B NMR (160 MHz, CDCl₃, 298 K) δ (ppm) 33.3, 31.2.

2-(3-ethylphenyl)-4,4,5,5-tetramethyl-1,3,2-dioxaborolane (4c)³⁻⁴:



m:p = 60:40

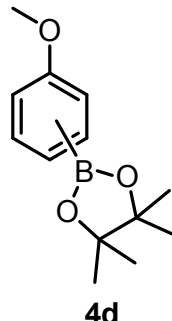
Colourless liquid. Yield 82 %. The crude product was purified through silica gel column chromatography (100-200 mesh) using 0.5% EtOAc in hexane as eluent. The percentage of different regioisomers was calculated by relative integration of the protons arising from the respective isomers in ¹H NMR spectroscopy.

¹H NMR (400 MHz, CDCl₃, 298 K) δ (ppm) 7.78 (d, *J* = 8 Hz, 2H, para), 7.70 (s, 1H, meta), 7.68- 7.66 (m, 1H, meta), 7.24 (d, *J* = 8 Hz, 2H, para), 2.72-2.66 (m, meta and para), 1.38 (s, 12H, meta), 1.37 (s, 12 H, para), 1.30-1.25 (m, meta and para).

¹³C NMR (100 MHz, CDCl₃, 298 K) δ (ppm) 147.6, 134.9, 127.3, 83.5, 29.1, 24.5, 15.4 (para); 143.4, 134.2, 132.1, 130.8, 127.7, 83.6, 28.8, 24.8, 15.7 (meta).

¹¹B NMR (160 MHz, CDCl₃, 298 K) δ (ppm) 33.7, 31.2.

2-(3-methoxyphenyl)-4,4,5,5-tetramethyl-1,3,2-dioxaborolane (4d)²:



m:p = 87:13

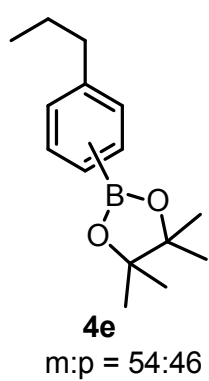
Colourless liquid. Yield 76%. The crude product was purified through silica gel column chromatography (100-200 mesh) using 1% EtOAc in hexane as eluent. The percentage of different regioisomers was calculated by relative integration of the protons arising from the respective isomers in ¹H NMR spectroscopy.

¹H NMR (400 MHz, CDCl₃, 298 K) δ (ppm) 7.40 (d, *J* = 6.4 Hz, 1H, meta), 7.33-7.27 (m, 2H, meta), 7.03- 7.00 (m, 1H, meta), 3.84 (s, 3H, meta), 1.34 (s, 12H, meta); 7.75 (d, *J* = 8.4 Hz, 2H, para), 6.89 (d, *J* = 8.4 Hz, 2H, para), 3.82 (s, 3H, para), 1.33 (s, 12H, para).

¹³C NMR (100 MHz, CDCl₃, 298 K) δ (ppm) 159.0, 128.9, 127.2, 118.7, 117.9, 83.8, 55.3, 24.8 (meta); 162.1, 136.5, 113.3, 83.5, 55.2, 24.8 (para).

¹¹B NMR (160 MHz, CDCl₃, 298 K) δ (ppm) 31.0.

4,4,5,5-tetramethyl-2-(3-propylphenyl)-1,3,2-dioxaborolane (4e)⁵⁻⁶:



m:p = 54:46

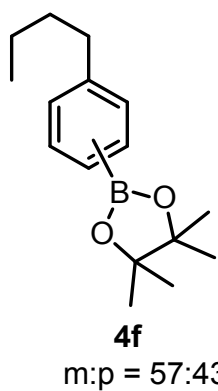
Colourless liquid. Yield 74 %. The crude product was purified through silica gel column chromatography (100-200 mesh) using 1% EtOAc in hexane as eluent. The percentage of different regioisomers was calculated by relative integration of the protons arising from the respective isomers in ¹H NMR spectroscopy.

¹H NMR (400 MHz, CDCl₃, 298 K) δ (ppm) 7.75 (d, 2H, *J* = 7.6 Hz, para), 7.66 (br s, 2H, meta), 7.30-7.28 (m, 2H, meta), 7.20 (d, *J* = 7.6 Hz, 2H, para), 2.63-2.59 (t, *J* = 7.6 Hz, 4H, meta and para), 1.70-1.62 (m, 4H, meta and para), 1.36 (s, 12H, meta), 1.34 (s, 12H, para), 0.97-0.93 (m, 6H, meta and para).

¹³C NMR (100 MHz, CDCl₃, 298 K) δ (ppm) 146.1, 141.9, 134.8, 132.1, 131.4, 127.9, 127.6, 83.6, 83.5, 38.2, 38.0, 24.8, 24.7, 24.4, 13.9, 13.8 (meta and para).

¹¹B NMR (160 MHz, CDCl₃, 298 K) δ (ppm) 30.6.

2-(3-butylphenyl)-4,4,5,5-tetramethyl-1,3,2-dioxaborolane (4f)⁷:



m:p = 57:43

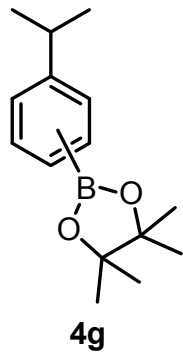
Colourless liquid. Yield 69%. The product was purified through silica gel column chromatography (100-200 mesh) using 1% EtOAc in hexane as eluent. The percentage of different regioisomers was calculated by relative integration of the protons arising from the respective isomers in ¹H NMR spectroscopy.

¹H NMR (400 MHz, CDCl₃, 298 K) δ (ppm) 7.75 (d, *J* = 7.6 Hz, 2H, para), 7.66-7.64 (m, 2H, meta), 7.31-7.29 (m, 2H, meta), 7.21 (d, *J* = 7.6 Hz, 2H, para), 2.66-2.62 (m, 4H, meta and para), 1.67-1.59 (m, 4H, meta and para), 1.37-1.35 (m, 28H, meta and para), 0.97-0.92 (dt, *J* = 7.6 Hz, 2.4 Hz, 6H, meta and para).

¹³C NMR (100 MHz, CDCl₃, 298 K) δ (ppm) 146.4, 142.2, 134.8, 134.7, 132.1, 131.4, 127.9, 127.6, 83.7, 83.6, 35.9, 35.6, 33.8, 33.5, 24.8, 22.5, 22.3, 14.0, 13.9 (meta and para).

¹¹B NMR (160 MHz, CDCl₃, 298 K) δ (ppm) 31.4.

2-(3-isopropylphenyl)-4,4,5,5-tetramethyl-1,3,2-dioxaborolane (4g)^{4,8}:



m:p = 55:45

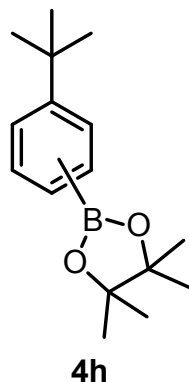
Colourless liquid. Yield 67%. The crude product was purified by column chromatography over silica gel (100-200 mesh) using 1% of EtOAc in hexane. The percentage of different regioisomers was calculated by relative integration of the protons arising from the respective isomers in ¹H NMR spectroscopy.

¹H NMR (400 MHz, CDCl₃, 298 K) δ (ppm) 7.76 (d, *J* = 6.4 Hz, 2H, para), 7.68 (s, 1H, meta), 7.65 (d, *J* = 5.6 Hz, 1H, meta), 7.36-7.30 (m, 2H, meta), 7.25 (d, *J* = 6.4 Hz, 2H, para) 2.98-2.89 (m, 2H, meta and para), 1.36 (s, 12H, meta), 1.34 (s, 12H, para), 1.28-1.26 (m, 12H, meta and para).

¹³C NMR (100 MHz, CDCl₃, 298 K) δ (ppm) 148.0, 132.9, 132.3, 129.3, 127.8, 83.7, 34.1, 24.8, 24.0 (meta); 152.3, 134.9, 125.9, 83.6, 34.3, 24.8, 23.8 (para).

¹¹B NMR (160 MHz, CDCl₃, 298 K) δ (ppm) 31.3.

2-(3-(tert-butyl)phenyl)-4,4,5,5-tetramethyl-1,3,2-dioxaborolane (4h)⁹⁻¹⁰:



m:p = 54:46

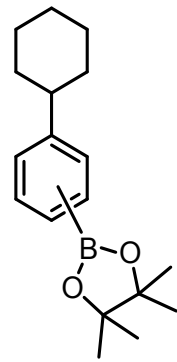
Colourless liquid. Yield 63%. The crude product was purified by column chromatography over silica gel (100-200 mesh) using 1% of EtOAc in hexane. The percentage of different regioisomers was calculated by relative integration of the protons arising from the respective isomers in ¹H NMR spectroscopy.

¹H NMR (400 MHz, CDCl₃, 298 K) δ (ppm) 7.83 (s, 1H, meta), 7.76 (d, *J* = 8.0 Hz, 2H, para), 7.64 (d, *J* = 6.8 Hz, 1H, meta), 7.50 (dd, *J* = 8.0 Hz, 1.6 Hz, 1H, meta), 7.41 (d, *J* = 8.0 Hz, 2H, para), 7.32 (t, *J* = 7.6 Hz, 1H, meta), 1.35 (s, 24H, meta and para), 1.34 (s, 9H, meta), 1.33 (s, 9H, para).

¹³C NMR (100 MHz, CDCl₃, 298 K) δ (ppm) 150.2, 132.0, 131.4, 128.4, 127.5, 83.7, 34.7, 31.4, 24.9 (meta); 154.5, 134.7, 124.7, 83.6, 34.7, 31.2, 24.8 (para).

¹¹B NMR (160 MHz, CDCl₃, 298 K) δ (ppm) 31.3.

2-(3-cyclohexylphenyl)-4,4,5,5-tetramethyl-1,3,2-dioxaborolane (4i)¹¹⁻¹²:



m:p = 58:42

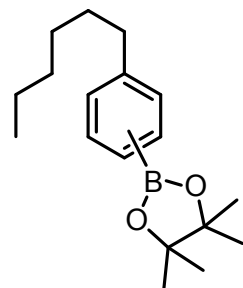
Colourless liquid. Yield 58 %. The crude product was purified by column chromatography over silica gel (100-200 mesh) using 1% of EtOAc in hexane. The percentage of different regioisomers was calculated by relative integration of the protons arising from the respective isomers in ¹H NMR spectroscopy.

¹H NMR (400 MHz, CDCl₃, 298 K) δ (ppm) 7.76 (d, *J* = 8.0 Hz, 1H, para), 7.66 (s, 1H, meta), 7.649-7.634 (m, 1H, meta), 7.32-7.30 (m, 2H, meta), 7.24 (d, *J* = 8.0 Hz, 1H, para), 2.56-2.49 (m, 2H, meta and para), 1.89-1.83 (m, 10H, meta and para), 1.52-1.37 (m, 8H, meta and para), 1.35 (s, 12H, meta), 1.34 (s, 12H, para), 1.27-1.24 (m, 2H, meta and para).

¹³C NMR (100 MHz, CDCl₃, 298 K) δ (ppm) 151.5, 147.2, 134.9, 133.3, 132.3, 129.8, 127.7, 126.3, 83.7, 83.6, 44.8, 44.6, 34.4, 34.2, 26.9, 26.8, 26.1, 24.9, 24.8 (meta and para).

¹¹B NMR (160 MHz, CDCl₃, 298 K) δ (ppm) 31.3.

2-(3-hexylphenyl)-4,4,5,5-tetramethyl-1,3,2-dioxaborolane (**4j**)¹²:



4j
m:p = 57:43

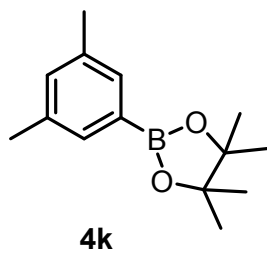
Colourless liquid. Yield 57%. The crude product was purified through silica gel column chromatography (100-200 mesh) using 1% EtOAc in hexane as eluent. The percentage of different regioisomers was calculated by relative integration of the protons arising from the respective isomers in ¹H NMR spectroscopy.

¹H NMR (400 MHz, CDCl₃, 298 K) δ (ppm) 7.76 (d, *J* = 7.6 Hz, 2H, para), 7.67- 7.65 (m, 2H, meta), 7.32-7.30 (m, 2H, meta), 7.22 (d, 2H, *J* = 7.6 Hz, para), 2.65-2.62 (m, 4H, meta and para), 1.68-1.61 (m, 4H, meta and para), 1.38-1.33 (m, 36H, meta and para), 0.916-0.902 (m, 6H, meta and para).

¹³C NMR (100 MHz, CDCl₃, 298 K) δ (ppm) 146.4, 142.2, 134.8, 134.7, 132.1, 131.4, 127.9, 127.6, 83.6, 83.5, 36.2, 35.9, 31.8, 31.7, 31.6, 31.3, 29.1, 28.9, 24.8, 22.6, 22.6, 14.1 (meta and para).

¹¹B NMR (160 MHz, CDCl₃, 298 K) δ (ppm) 31.3.

2-(3,5-dimethylphenyl)-4,4,5,5-tetramethyl-1,3,2-dioxaborolane (**4k**)²:



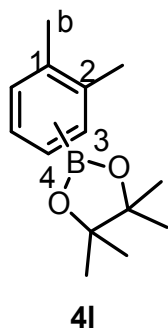
White solid. Yield 68%. The crude product was purified through silica gel column chromatography (100-20 mesh) using 1% EtOAc in hexane.

¹H NMR (400 MHz, CDCl₃, 298 K) δ (ppm) 7.44 (s, 2H), 7.11 (s, 1H), 2.32 (s, 6H), 1.35 (s, 12H).

¹³C NMR (100 MHz, CDCl₃, 298 K) δ (ppm) 137.1, 133.0, 132.4, 83.7, 24.8, 21.1.

¹¹B NMR (160 MHz, CDCl₃, 298 K) δ (ppm) 31.3.

2-(3,4-dimethylphenyl)-4,4,5,5-tetramethyl-1,3,2-dioxaborolane (**4l**)²:



4:3:b = 79:15:6

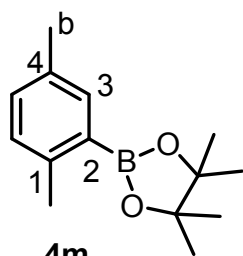
Colourless liquid. Yield 70%. All isomeric products (4, 3 and b) were collected together from other reaction impurities by column chromatography over silica gel (100-200 mesh) using 1% EtOAc in hexane mixture. The percentage of different regioisomers was calculated by relative integration of the protons arising from the respective isomers in ¹H NMR spectroscopy.

¹H NMR (400 MHz, CDCl₃, 298 K) δ (ppm) 7.59 (s, 1H), 7.55 (d, *J* = 7.2 Hz, 1H), 7.15 (d, *J* = 7.6 Hz, 1H), 2.29 (s, 3H), 2.28 (s, 3H), 1.34 (s, 12H) (borylation at 4th position); 7.62 (d, *J* = 7.6 Hz, 1H), 7.21 (d, *J* = 7.6 Hz, 1H), 7.09 (t, *J* = 7.6 Hz, 1H), 2.48 (s, 3H), 2.28 (s, 3H) 1.35 (s, 12H) (borylation at 3rd position); peak at 1.24 ppm belongs to the borylated product at benzylic position.

¹³C NMR (100 MHz, CDCl₃, 298 K) δ (ppm) 140.1, 135.9, 135.8, 132.4, 129.1, 83.6, 24.8, 20.0, 19.4 (borylation at 4th position).

¹¹B NMR (160 MHz, CDCl₃, 298 K) δ (ppm) 30.5.

2-(2,5-dimethylphenyl)-4,4,5,5-tetramethyl-1,3,2-dioxaborolane (**4m**)²:



2:b = 86:14

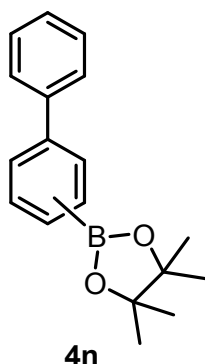
Colourless liquid. Yield 54%. The crude product was purified by column chromatography over silica gel (100-200 mesh) using 1% of EtOAc in hexane. The percentage of different regioisomers was calculated by relative integration of the protons arising from the respective isomers in ^1H NMR spectroscopy.

^1H NMR (400 MHz, CDCl_3 , 298 K) δ (ppm) 7.58 (s, 1H), 7.13 (d, J = 7.6 Hz, 1H), 7.06 (d, J = 7.6 Hz, 1H), 2.50 (s, 3H), 2.31 (s, 3H), 1.35 (s, 12H) (borylation at 3rd position). Peak at 1.24 ppm belongs to the borylated product at benzylic position.

^{13}C NMR (100 MHz, CDCl_3 , 298 K) δ (ppm) 141.7, 136.3, 133.9, 131.5, 129.8, 83.3, 24.9, 23.9, 21.7, 20.8 (borylation at 3rd position).

^{11}B NMR (160 MHz, CDCl_3 , 298 K) δ (ppm) 34.6, 31.4.

2-([1,1'-biphenyl]-3-yl)-4,4,5,5-tetramethyl-1,3,2-dioxaborolane (**4n**)^{9,13}:



m:p = 63:37

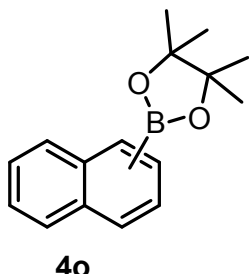
White solid. Yield 66%. The crude product was purified by column chromatography over silica gel (100-200 mesh) using 1% of EtOAc in hexane. The percentage of different regioisomers was calculated by relative integration of the protons arising from the respective isomers in ^1H NMR spectroscopy.

^1H NMR (400 MHz, CDCl_3 , 298 K) δ (ppm) 8.05 (s, 1H, meta), 7.80 (d, J = 6.8 Hz, 1H, meta), 7.70 (dd, J = 8.0 Hz, 1.6 Hz, 1H, meta), 7.65-7.61 (m, 2H, meta), 7.47-7.41 (m, 3H, meta), 7.33-7.31 (m, 1H, meta), 1.37 (s, 12H, meta); 7.89 (d, J = 8 Hz, 2H, para), 7.64-7.60 (m, 4H, para), 7.47-7.41 (m, 2H, para), 7.38-7.35 (m, 1H, para), 1.37 (s, 12H, para).

¹³C NMR (100 MHz, CDCl₃, 298 K) δ (ppm) 143.9, 141.1, 141.0, 140.5, 135.2, 133.6, 133.5, 130.0, 128.7, 128.6, 128.1, 127.5, 127.2, 127.1, 126.4, 83.9, 83.8, 24.9 (meta and para).

¹¹B NMR (160 MHz, CDCl₃, 298 K) δ (ppm) 31.1.

4,4,5,5-tetramethyl-2-(naphthalen-2-yl)-1,3,2-dioxaborolane (4o)¹⁴⁻¹⁵:



4o

β :α = 86:14

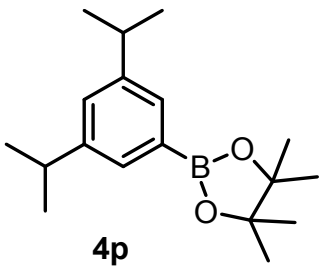
White solid. Yield 61%. The crude product was purified by column chromatography over silica gel (100-200 mesh) using 1% of EtOAc in hexane. The percentage of different regioisomers was calculated by relative integration of the protons arising from the respective isomers in ¹H NMR spectroscopy.

¹H NMR (400 MHz, CDCl₃, 298 K) δ (ppm) 8.37 (s, 1H, β isomer), 7.88 (d, *J* = 7.6 Hz, 1H, β isomer), 7.85-7.81 (m, 3H, β isomer), 7.53-7.45 (m, 2H, β isomer), 1.39 (s, 12H, β isomer); 8.76 (d, *J* = 8.4 Hz, α isomer), 1.43 (s, 12H, α isomer).

¹³C NMR (100 MHz, CDCl₃, 298 K) δ (ppm) 136.2, 135.0, 132.8, 130.4, 128.6, 127.7, 126.9, 126.9, 125.8, 83.9, 24.9 (β isomer), 136.9, 135.6, 133.2, 131.6, 128.4, 128.3, 126.3, 125.5, 124.9, 83.7, 24.9 (α isomer).

¹¹B NMR (160 MHz, CDCl₃, 298 K) δ (ppm) 31.5.

2-(3,5-diisopropylphenyl)-4,4,5,5-tetramethyl-1,3,2-dioxaborolane (4p)¹⁶:



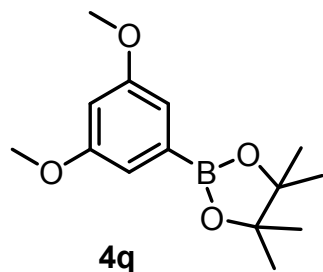
White solid. Yield 43%. The crude product was purified by column chromatography over silica gel (100-200 mesh) using 1% of EtOAc in hexane.

¹H NMR (400 MHz, CDCl₃, 298 K) δ (ppm) 7.50 (s, 2H), 7.19 (s, 1H), 2.94-2.87 (m, 2H), 1.35 (s, 12H), 1.26 (d, *J* = 6.8 Hz, 12H).

¹³C NMR (100 MHz, CDCl₃, 298 K) δ (ppm) 148.1, 130.4, 127.7, 85.6, 34.2, 24.8, 24.1.

¹¹B NMR (160 MHz, CDCl₃, 298 K) δ (ppm) 31.3.

2-(3,5-dimethoxyphenyl)-4,4,5,5-tetramethyl-1,3,2-dioxaborolane (4q)¹⁷:



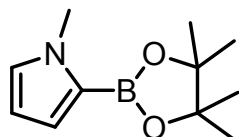
White solid. Yield 46 %. The crude product was purified by column chromatography over silica gel (100-200 mesh) using 2.5% of EtOAc in hexane.

¹H NMR (400 MHz, CDCl₃, 298 K) δ (ppm) 6.95 (d, *J* = 2.4 Hz, 2H), 6.56 (t, *J* = 2.4 Hz, 1H), 3.81 (s, 6H), 1.34 (s, 12H).

¹³C NMR (100 MHz, CDCl₃, 298 K) δ (ppm) 160.4, 111.6, 104.5, 83.9, 55.4, 24.8.

¹¹B NMR (160 MHz, CDCl₃, 298 K) δ (ppm) 31.0.

1-methyl-2-(4,4,5,5-tetramethyl-1,3,2-dioxaborolan-2-yl)-1H-pyrrole (4r)¹:



4r

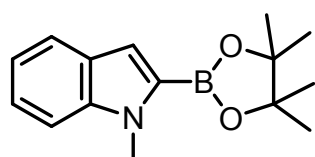
Colourless liquid. Yield 92%. The crude product was purified by column chromatography over silica gel (100-200 mesh) using 0.5% of EtOAc in hexane.

¹H NMR (400 MHz, CDCl₃, 298 K) δ (ppm) 6.82 (m, 2H), 6.16 (s, 1H), 3.84 (s, 3H), 1.32 (s, 12H).

¹³C NMR (100 MHz, CDCl₃, 298 K) δ (ppm) 128.1, 121.9, 108.3, 83.0, 36.5, 24.7.

¹¹B NMR (160 MHz, CDCl₃, 298 K) δ (ppm) 28.1.

1-methyl-2-(4,4,5,5-tetramethyl-1,3,2-dioxaborolan-2-yl)-1H-indole (4s)¹:



4s

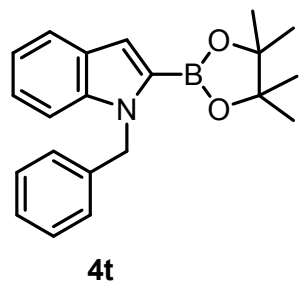
White solid. Yield 77%. The crude product was purified through a silica gel column chromatography (100-200 mesh) using 1% EtOAc in hexane as eluent.

¹H NMR (400 MHz, CDCl₃, 298 K) δ (ppm) 7.67 (d, *J* = 8.4 Hz, 1H), 7.37 (d, *J* = 8.4 Hz, 1H), 7.29 (t, *J* = 7.2 Hz, 1H), 7.16 (s, 1H), 7.11 (t, *J* = 8.0 Hz, 1H), 3.99 (s, 12H), 1.39 (s, 12H)

¹³C NMR (100 MHz, CDCl₃, 298 K) δ (ppm) 140.1, 127.8, 123.1, 121.5, 119.2, 114.2, 109.6, 83.6, 32.2, 24.8.

¹¹B NMR (160 MHz, CDCl₃, 298 K) δ (ppm) 28.7.

1-benzyl-2-(4,4,5,5-tetramethyl-1,3,2-dioxaborolan-2-yl)-1H-indole (4t)¹:



White solid. Yield 79%. The crude product was purified through a silica gel column chromatography (100-200 mesh) using 1% EtOAc in hexane as eluent.

¹H NMR (400 MHz, CDCl₃, 298 K) δ (ppm) 7.67 (d, *J* = 8.0 Hz, 1H), 7.31 (d, *J* = 8.0 Hz, 1H), 7.24- 7.18 (m, 5H), 7.09 (d, *J* = 7.6 Hz, 1H), 7.05 (d, *J* = 6.8 Hz, 2H), 5.67 (s, 2H), 1.28 (s, 12 H).

¹³C NMR (100 MHz, CDCl₃, 298 K) δ (ppm) 139.8, 139.3, 128.3, 127.2, 126.8, 126.5, 123.4, 121.7, 119.5, 115.0, 110.3, 83.7, 48.9, 24.7.

¹¹B NMR (160 MHz, CDCl₃, 298 K) δ (ppm) 29.0.

B) ^1H , ^{13}C , ^{11}B NMR spectra of 2 and 3:

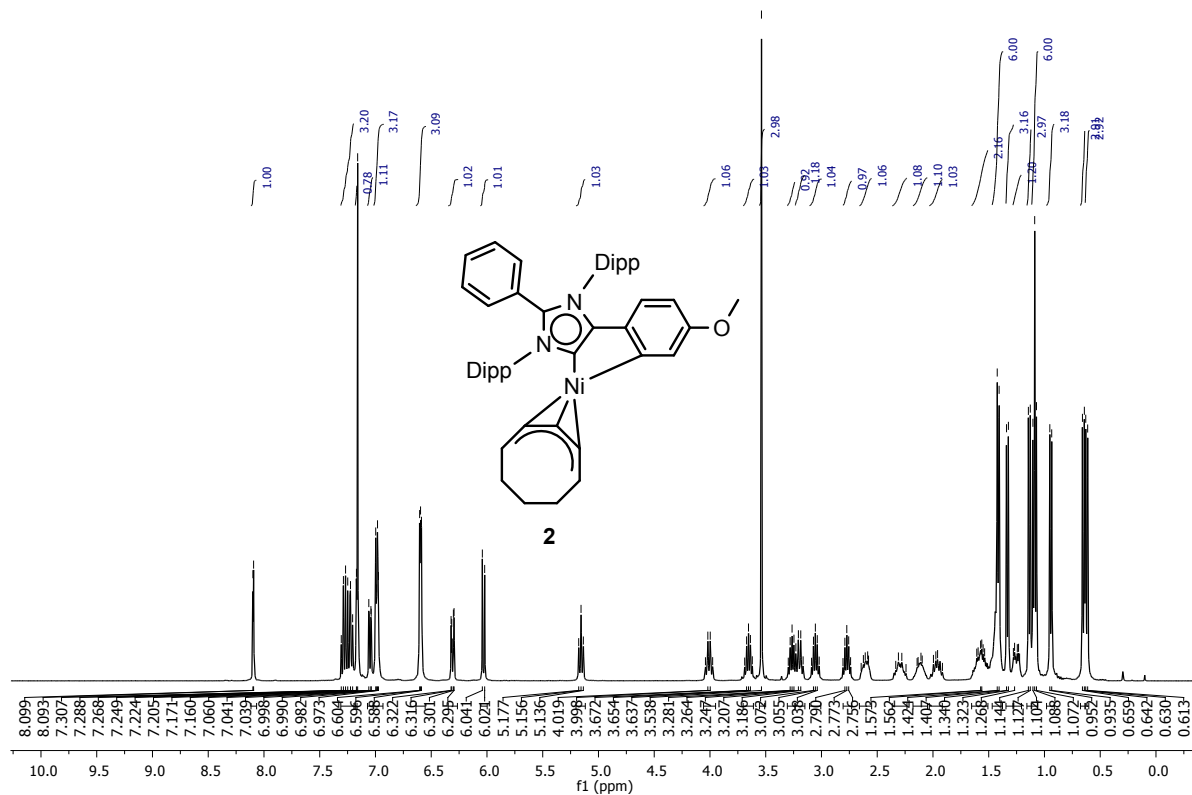


Figure S1. ^1H NMR (C_6D_6) spectrum of nickel complex **2**.

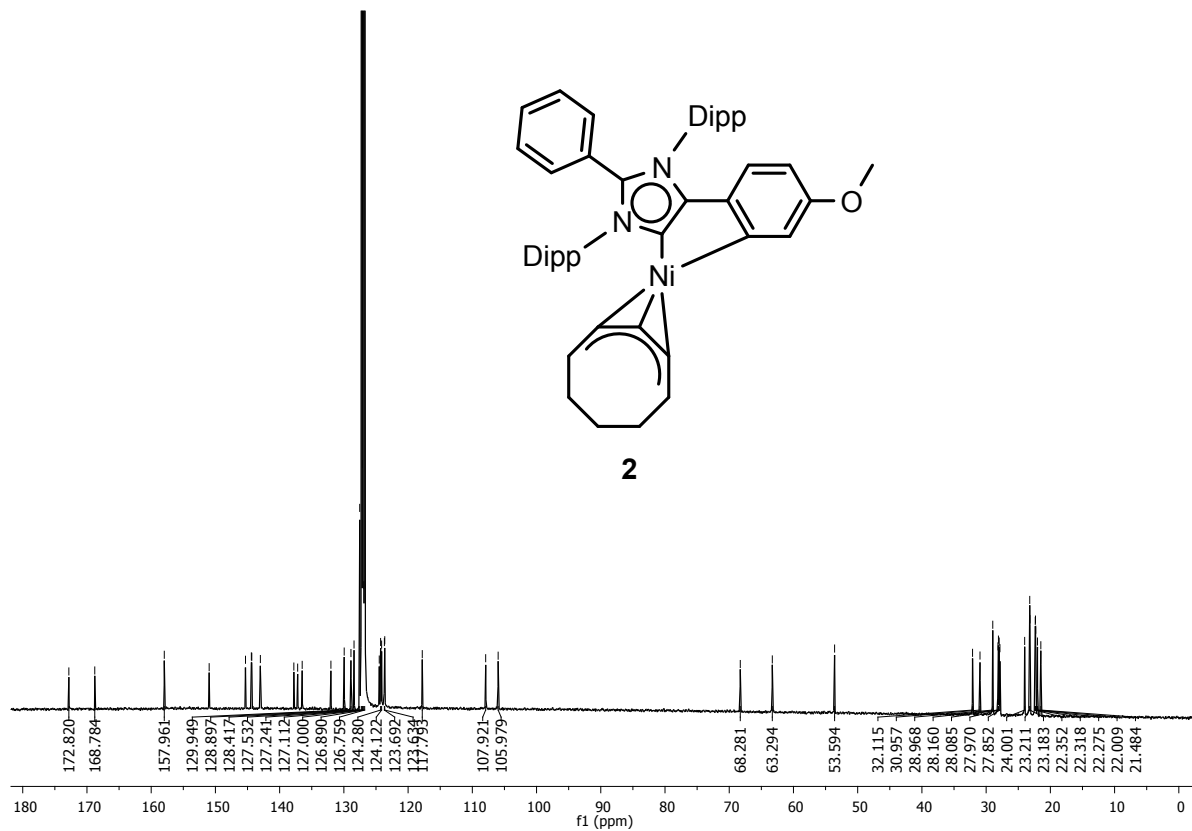


Figure S2. ^{13}C NMR (C_6D_6) spectrum of nickel complex **2**.

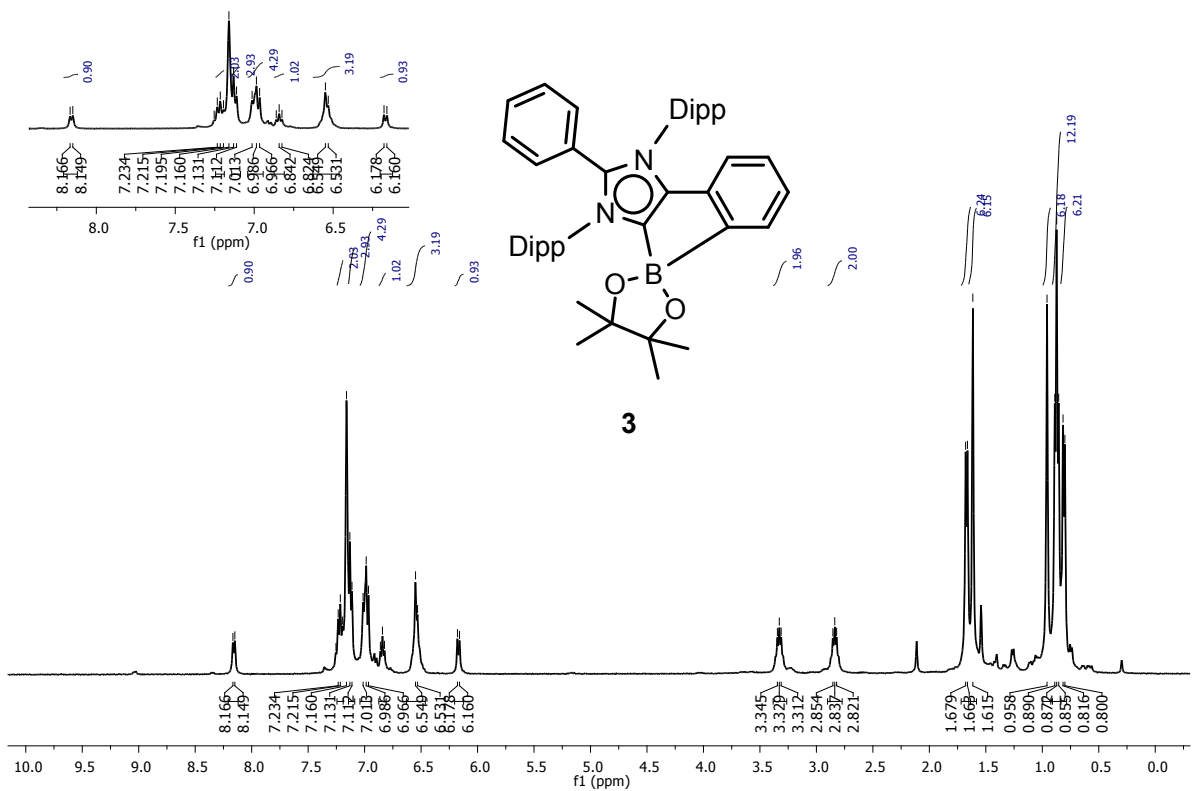


Figure S3. ^1H NMR (C_6D_6) spectrum of **3**.

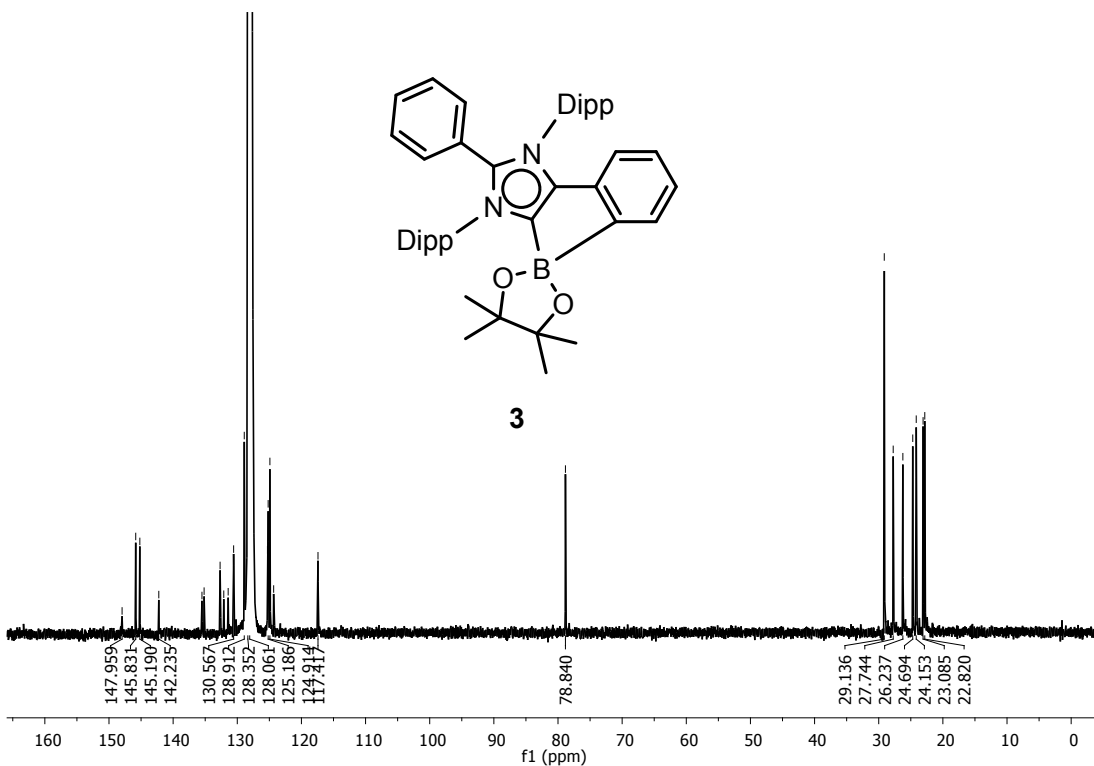


Figure S4. ^{13}C NMR (C_6D_6) spectrum of **3**.

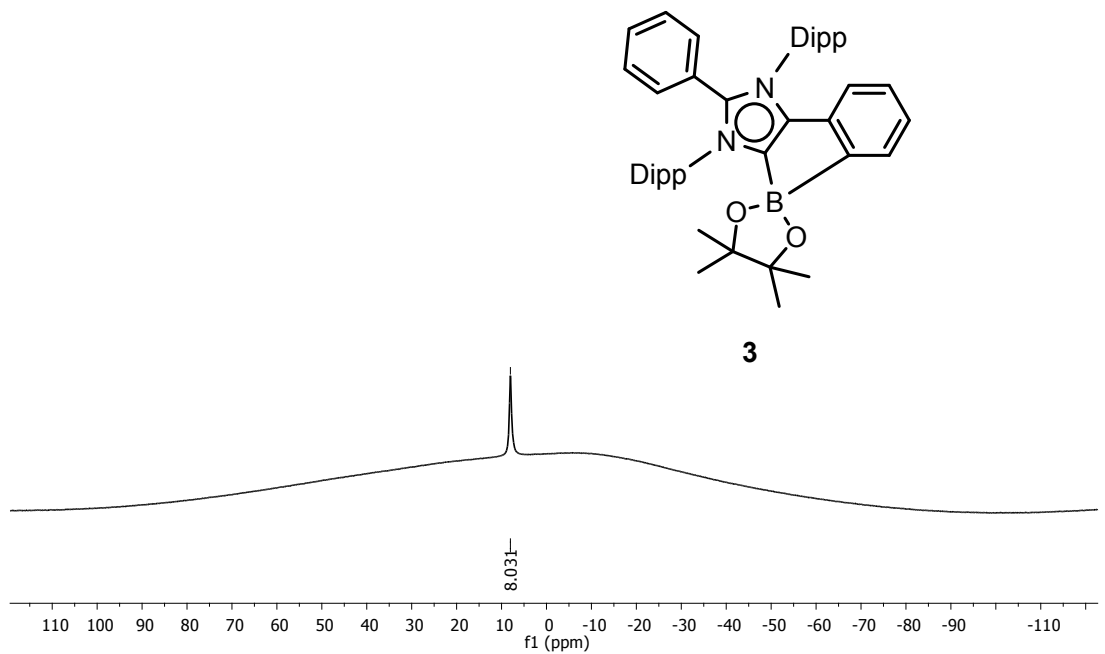


Figure S5. ^{11}B NMR (C_6D_6) spectrum of **3**.

C) ^1H , ^{13}C , ^{11}B NMR spectra of borylated products 4a–4t:

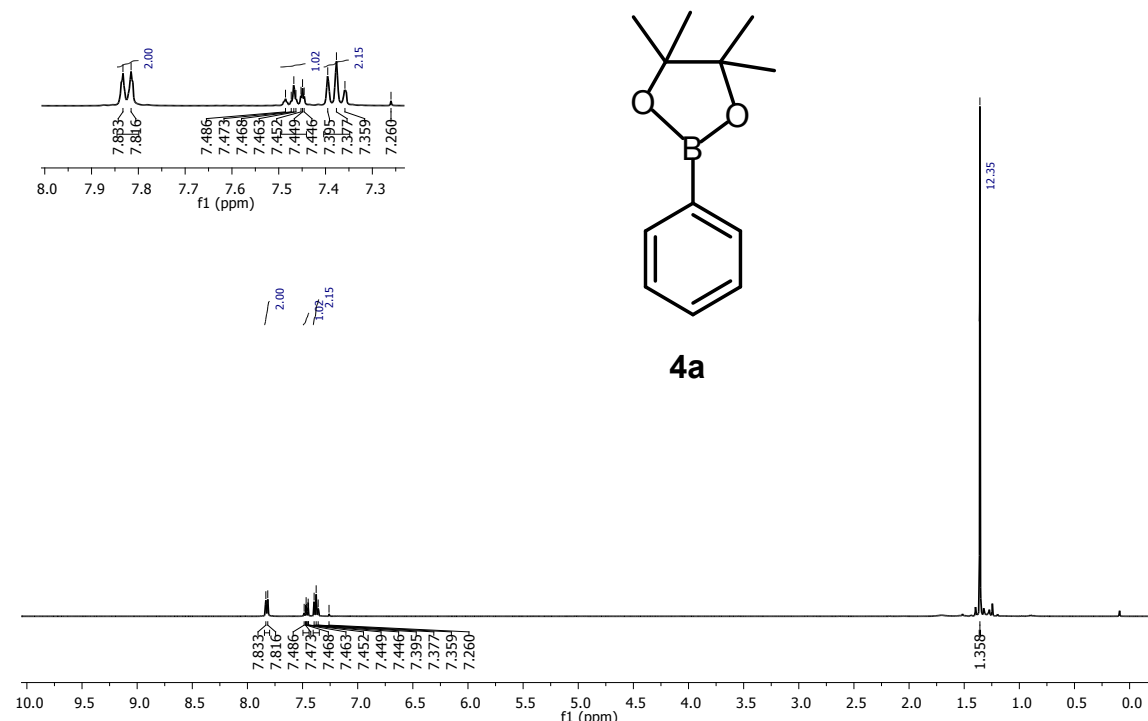


Figure S6. ^1H NMR (CDCl_3) spectrum of 4,4,5,5-tetramethyl-2-phenyl-1,3,2-dioxaborolane (**4a**).

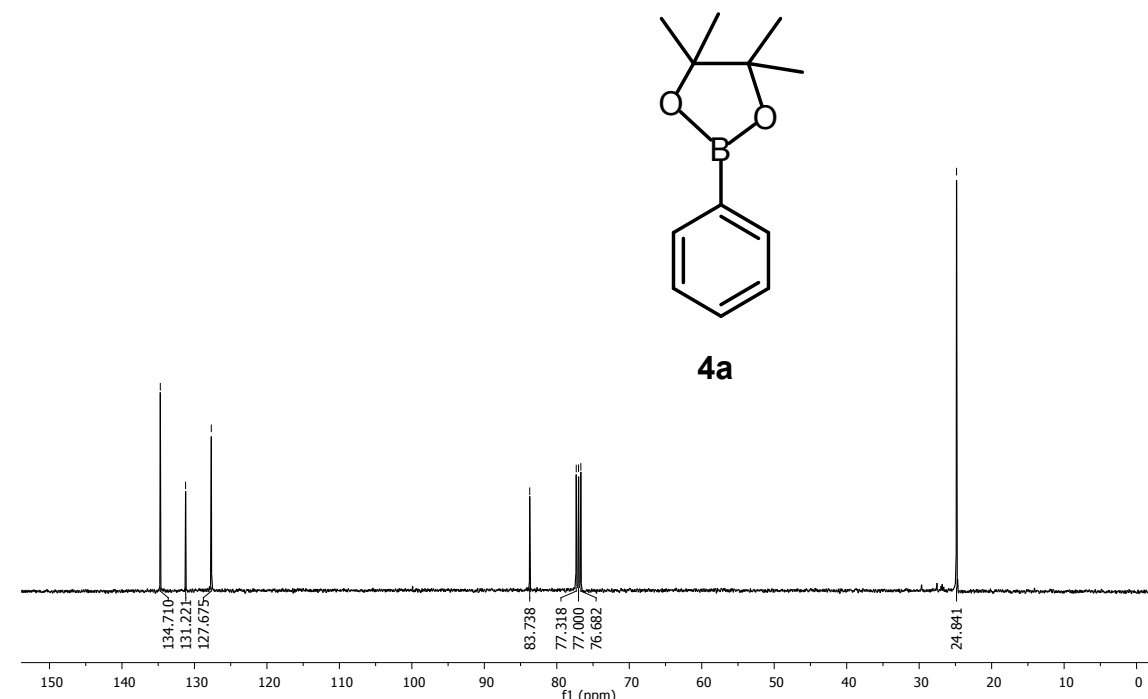


Figure S7. ^{13}C NMR (CDCl_3) spectrum of 4,4,5,5-tetramethyl-2-phenyl-1,3,2-dioxaborolane (**4a**).

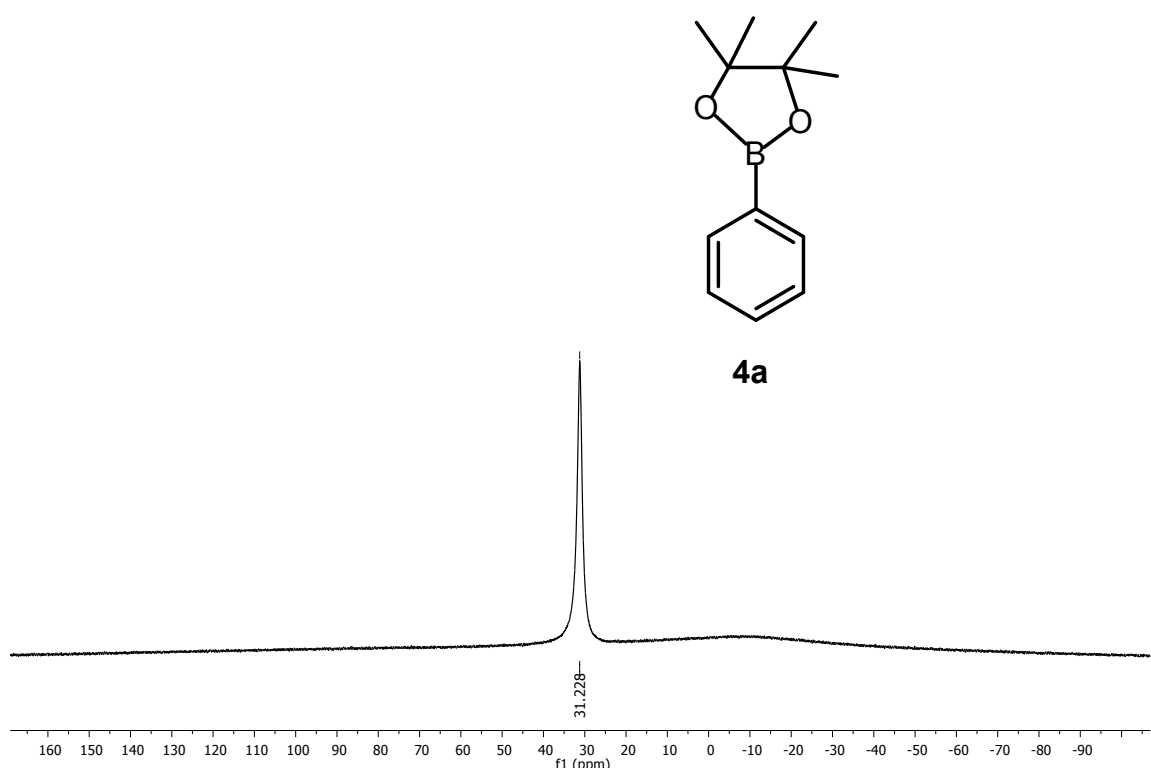


Figure S8. ^{11}B NMR (CDCl_3) spectrum of 4,4,5,5-tetramethyl-2-phenyl-1,3,2-dioxaborolane (**4a**).

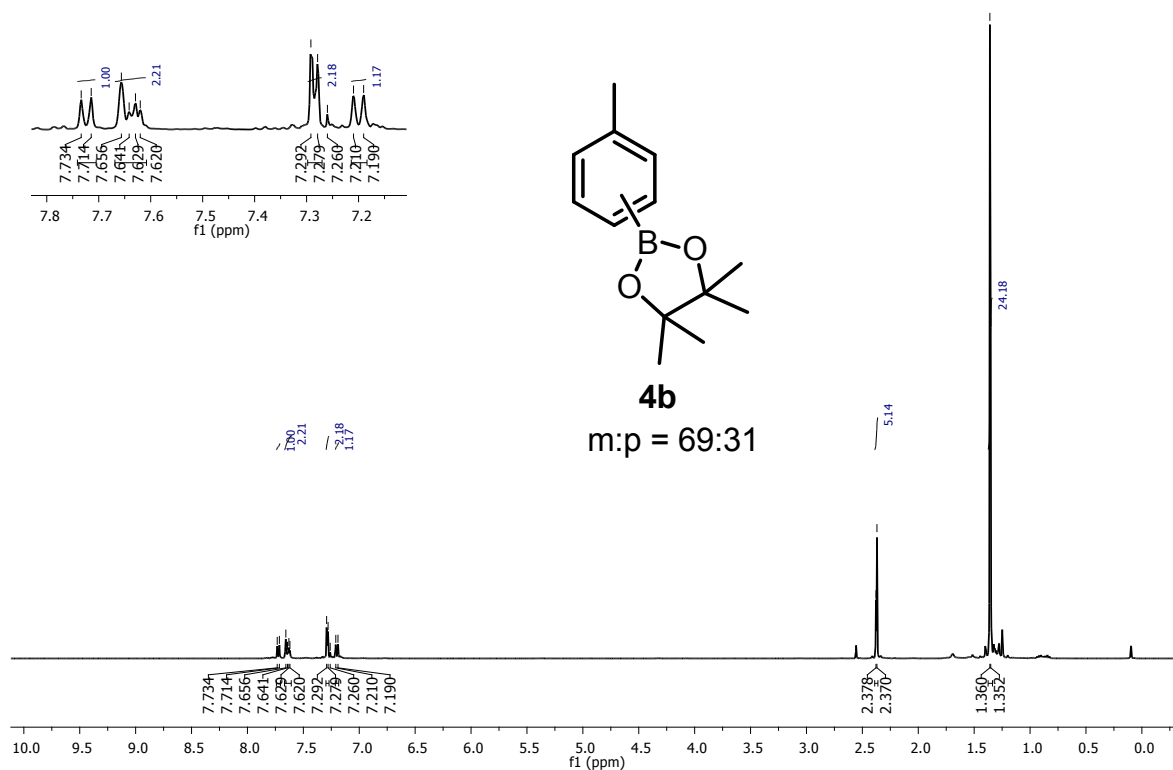


Figure S9. ^1H NMR (CDCl_3) spectrum of 4,4,5,5-tetramethyl-2-(m-tolyl)-1,3,2-dioxaborolane (**4b**).

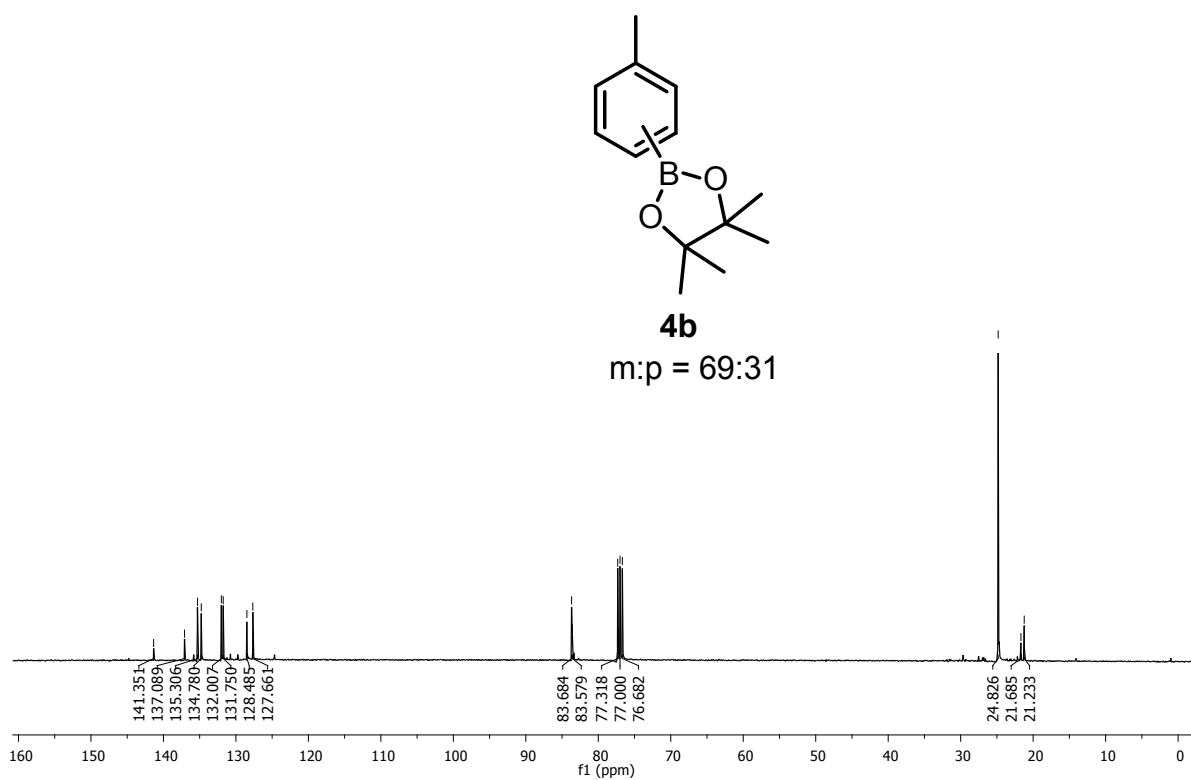


Figure S10. ^{13}C NMR (CDCl_3) spectrum of 4,4,5,5-tetramethyl-2-(m-tolyl)-1,3,2-dioxaborolane (**4b**).

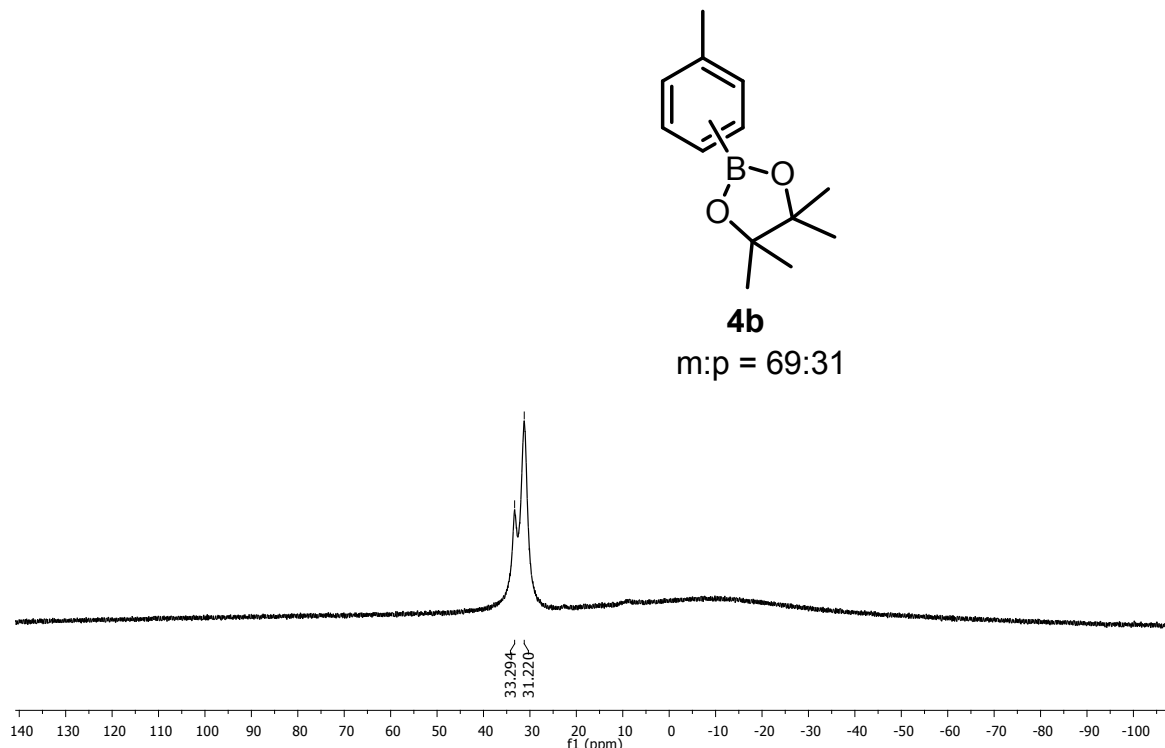


Figure S11. ^{11}B NMR (CDCl_3) spectrum of 4,4,5,5-tetramethyl-2-(m-tolyl)-1,3,2-dioxaborolane (**4b**).

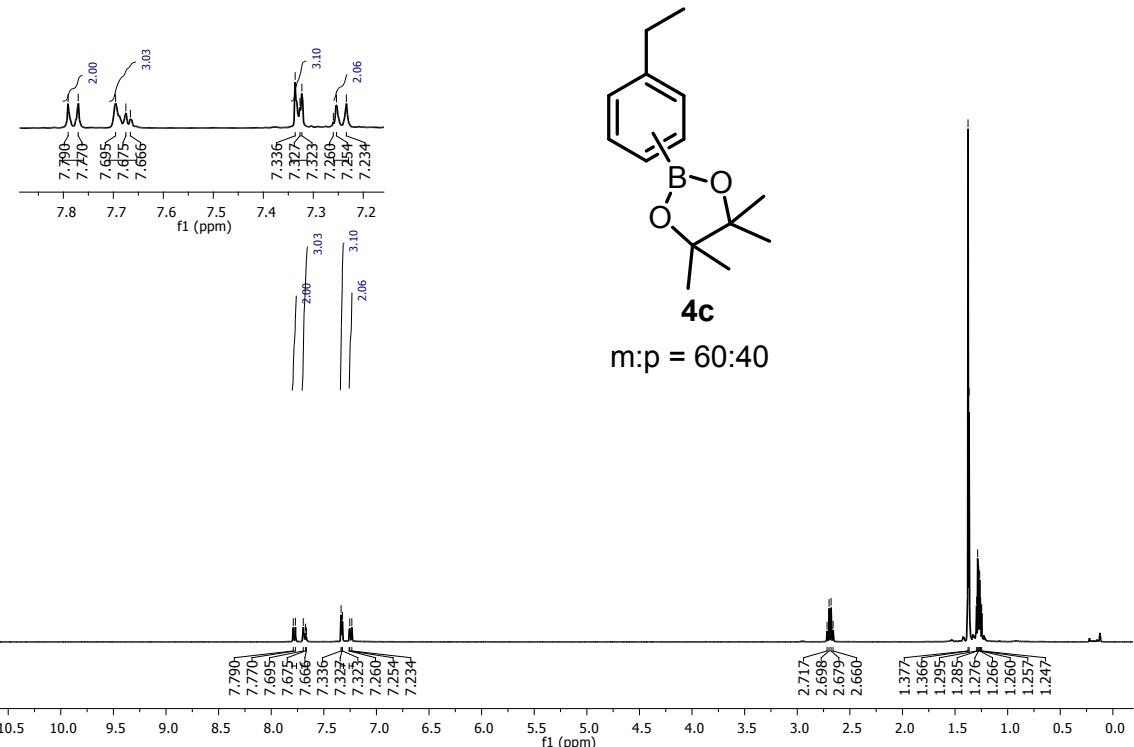


Figure S12. ¹H NMR (CDCl₃) spectrum of 2-(3-ethylphenyl)-4,4,5,5-tetramethyl-1,3,2-dioxaborolane (**4c**).

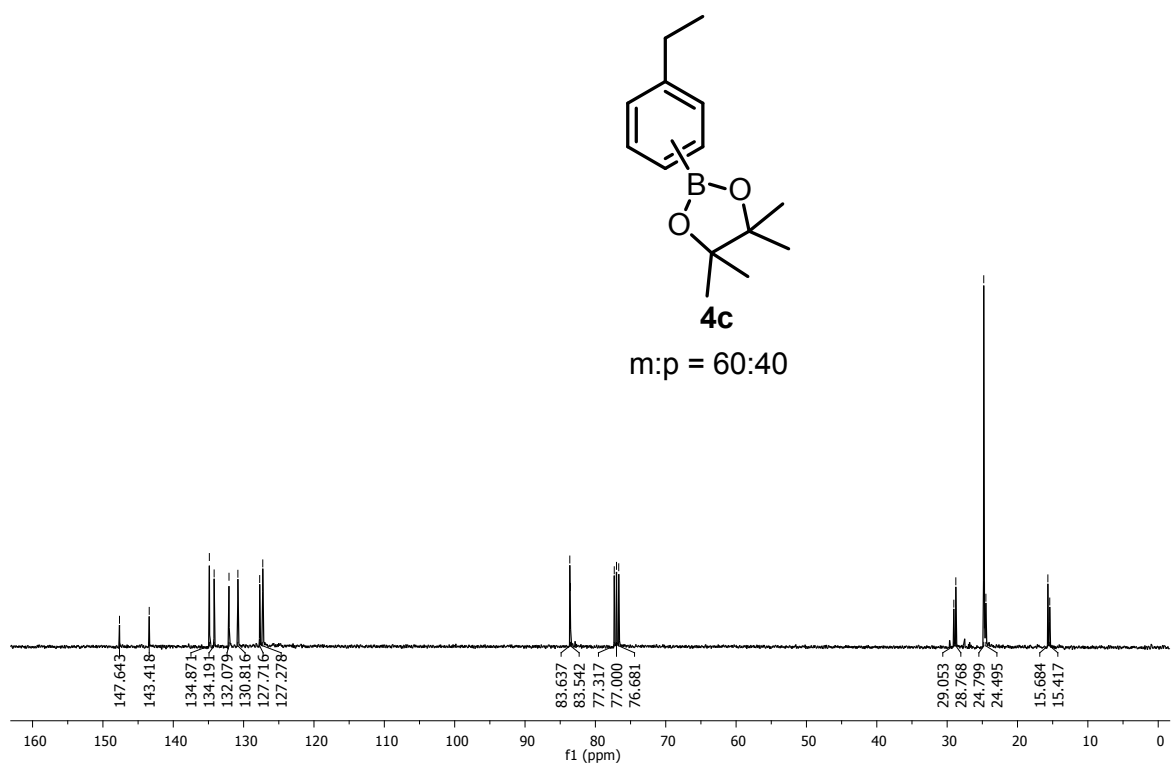


Figure S13. ¹³C NMR (CDCl₃) spectrum of 2-(3-ethylphenyl)-4,4,5,5-tetramethyl-1,3,2-dioxaborolane (**4c**).

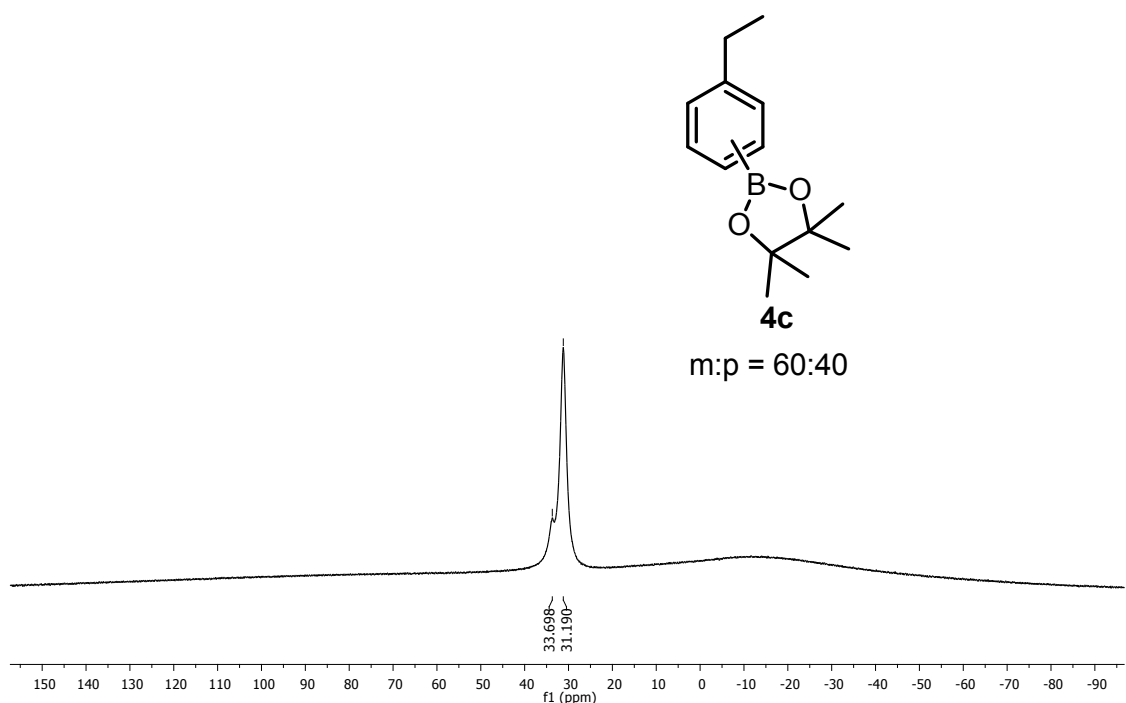


Figure S14. ^{11}B NMR (CDCl_3) spectrum of 2-(3-ethylphenyl)-4,4,5,5-tetramethyl-1,3,2-dioxaborolane (**4c**).

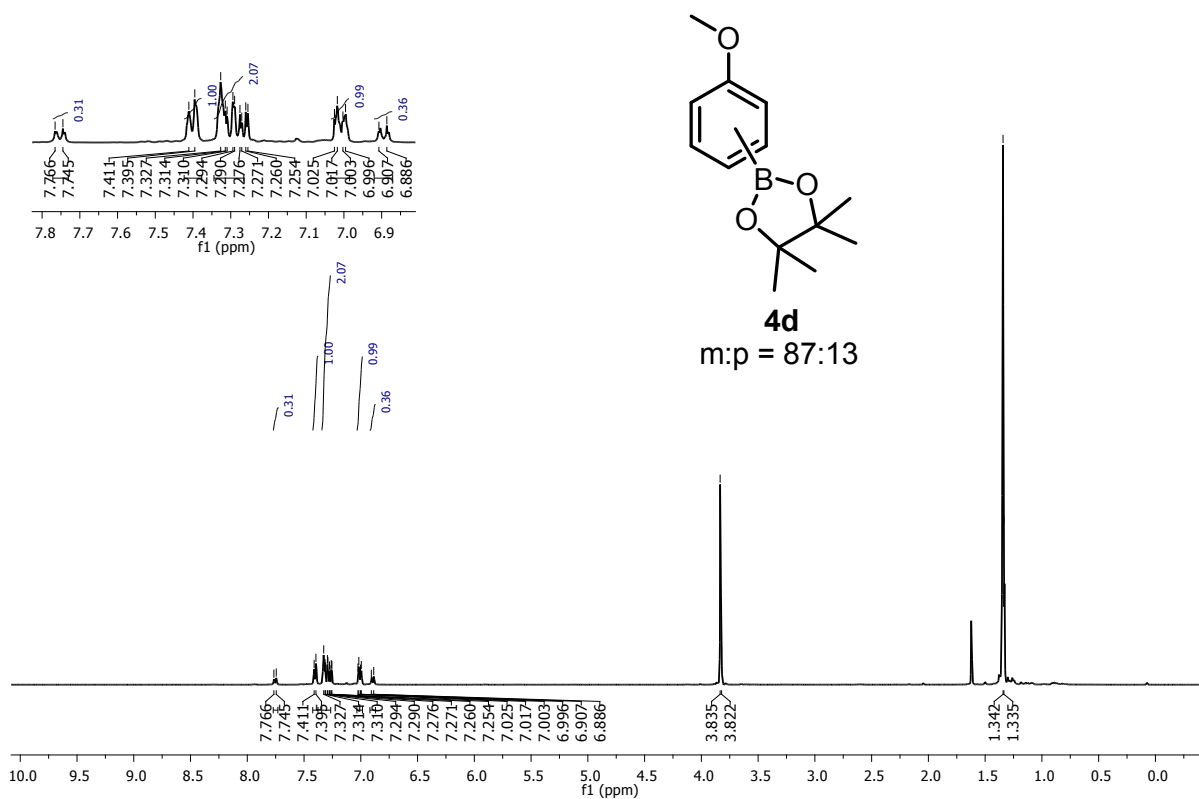


Figure S15. ^1H NMR (CDCl_3) spectrum of 2-(3-methoxyphenyl)-4,4,5,5-tetramethyl-1,3,2-dioxaborolane (**4d**).

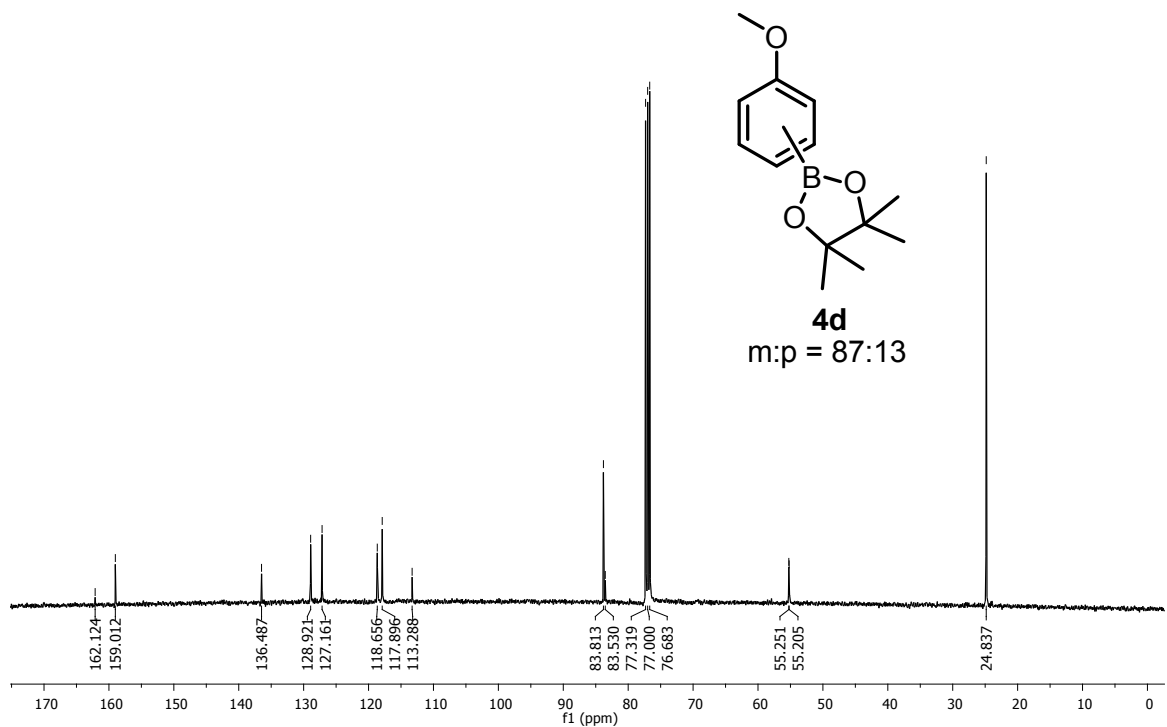


Figure S16. ^{13}C NMR (CDCl_3) spectrum of 2-(3-methoxyphenyl)-4,4,5,5-tetramethyl-1,3,2-dioxaborolane (**4d**).

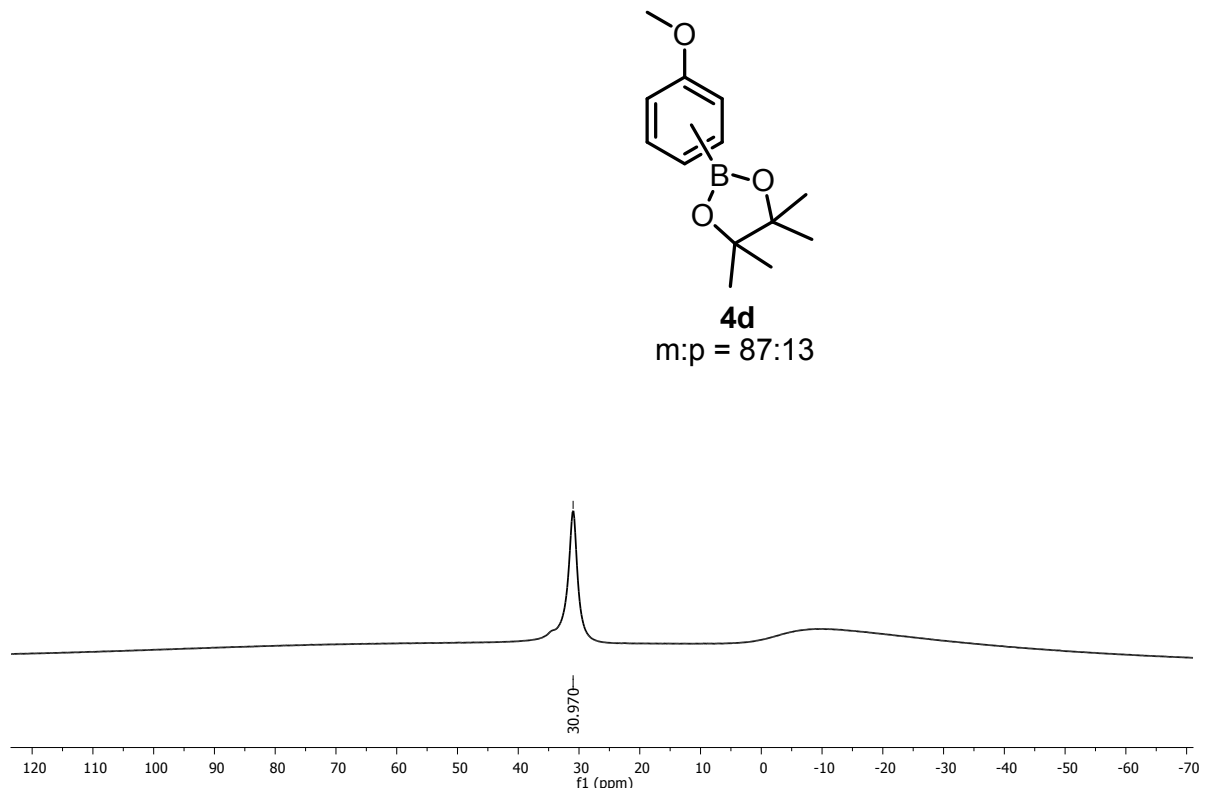


Figure S17. ^{11}B NMR (CDCl_3) spectrum of 2-(3-methoxyphenyl)-4,4,5,5-tetramethyl-1,3,2-dioxaborolane (**4d**).

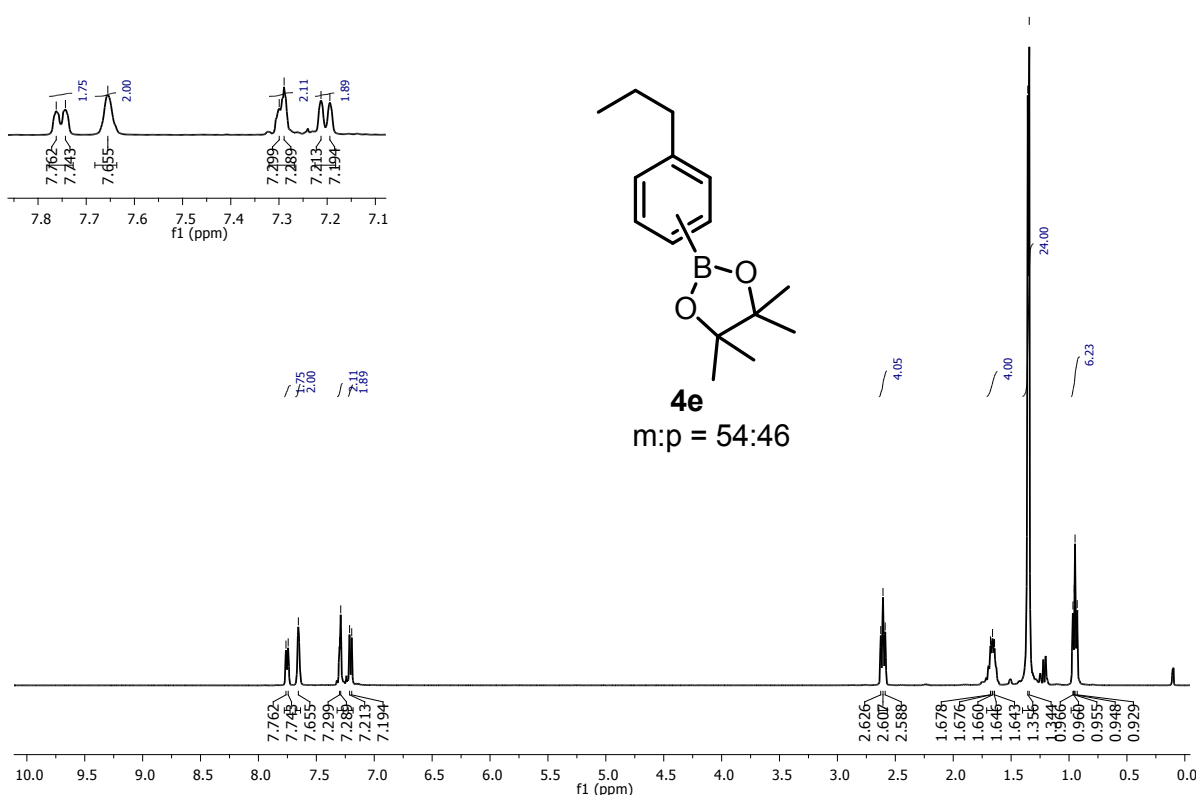


Figure S18. ^1H NMR (CDCl_3) spectrum of 4,4,5,5-tetramethyl-2-(3-propylphenyl)-1,3,2-dioxaborolane (**4e**).

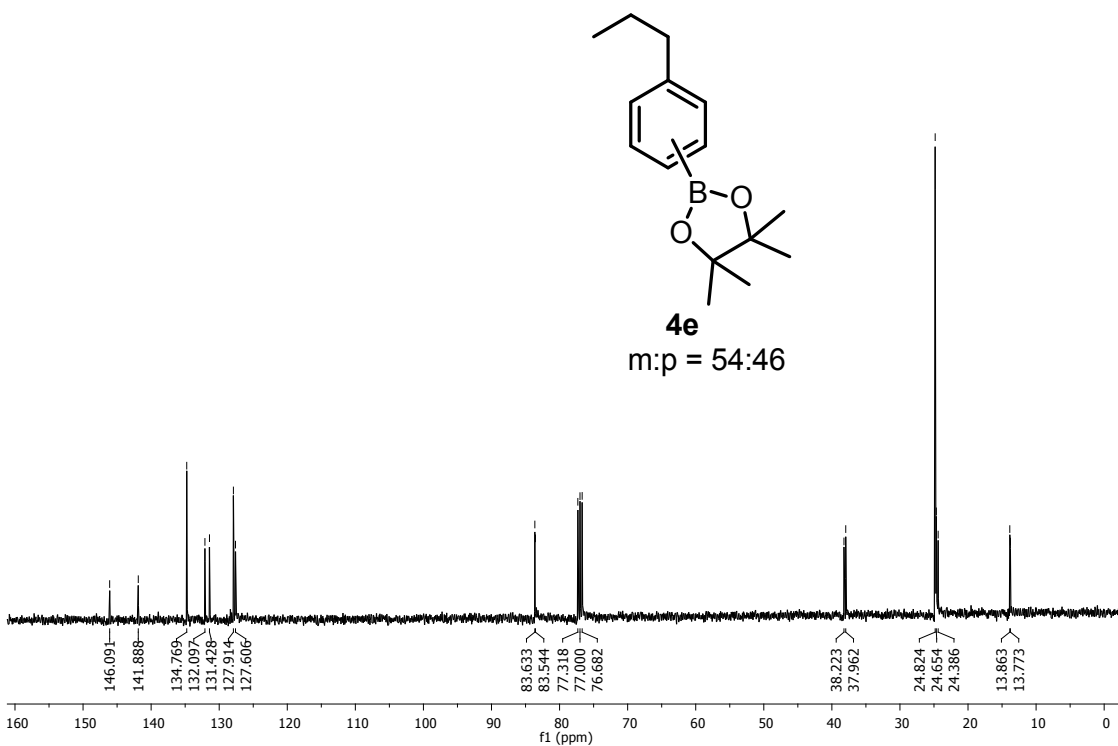


Figure S19. ^{13}C NMR (CDCl_3) spectrum of 4,4,5,5-tetramethyl-2-(3-propylphenyl)-1,3,2-dioxaborolane (**4e**).

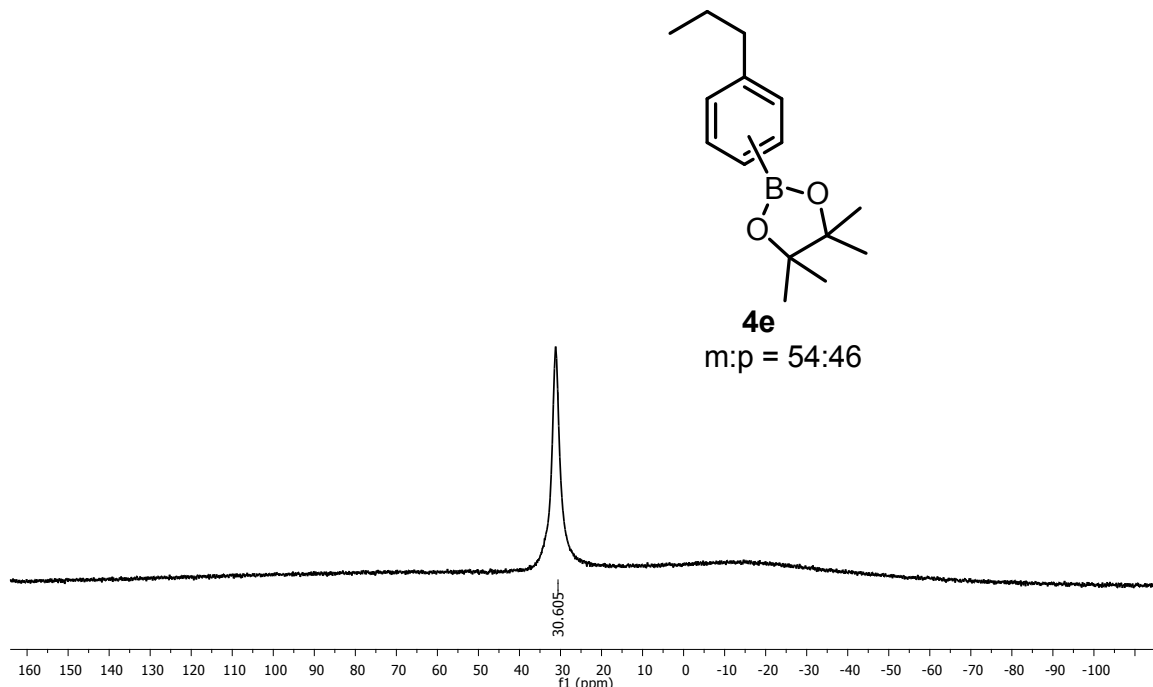


Figure S20. ^{11}B NMR (CDCl_3) spectrum of 4,4,5,5-tetramethyl-2-(3-propylphenyl)-1,3,2-dioxaborolane (**4e**).

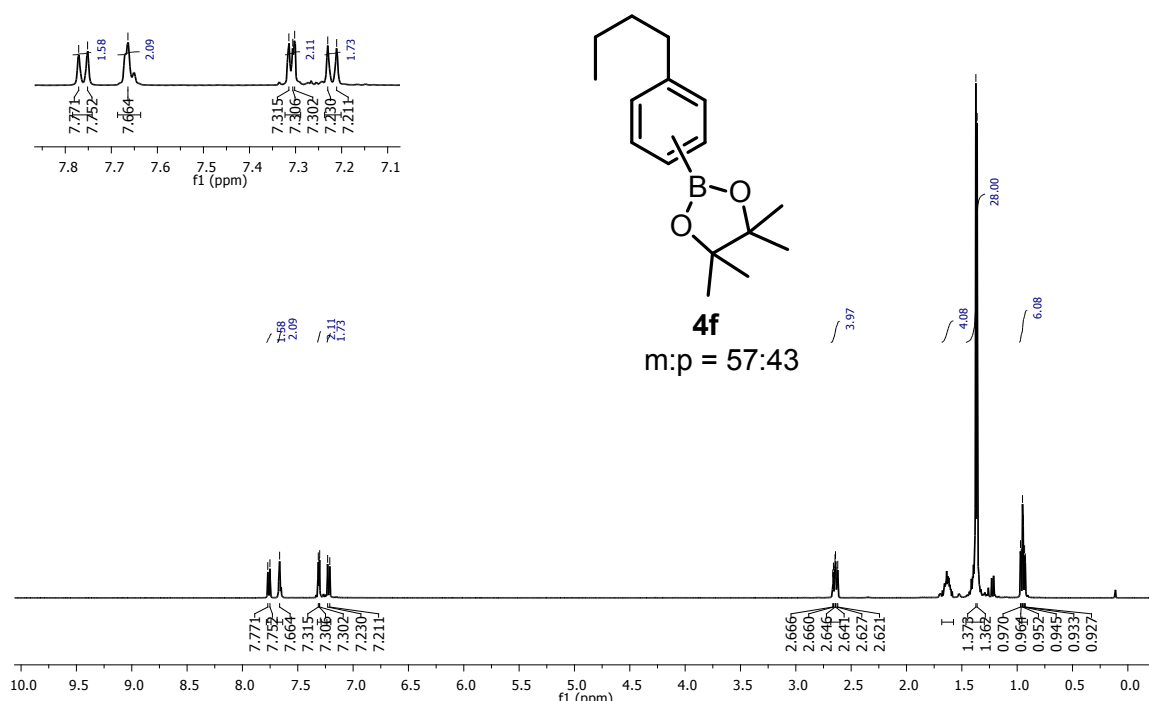


Figure S21. ^1H NMR (CDCl_3) spectrum of 2-(3-butylphenyl)-4,4,5,5-tetramethyl-1,3,2-dioxaborolane (**4f**).

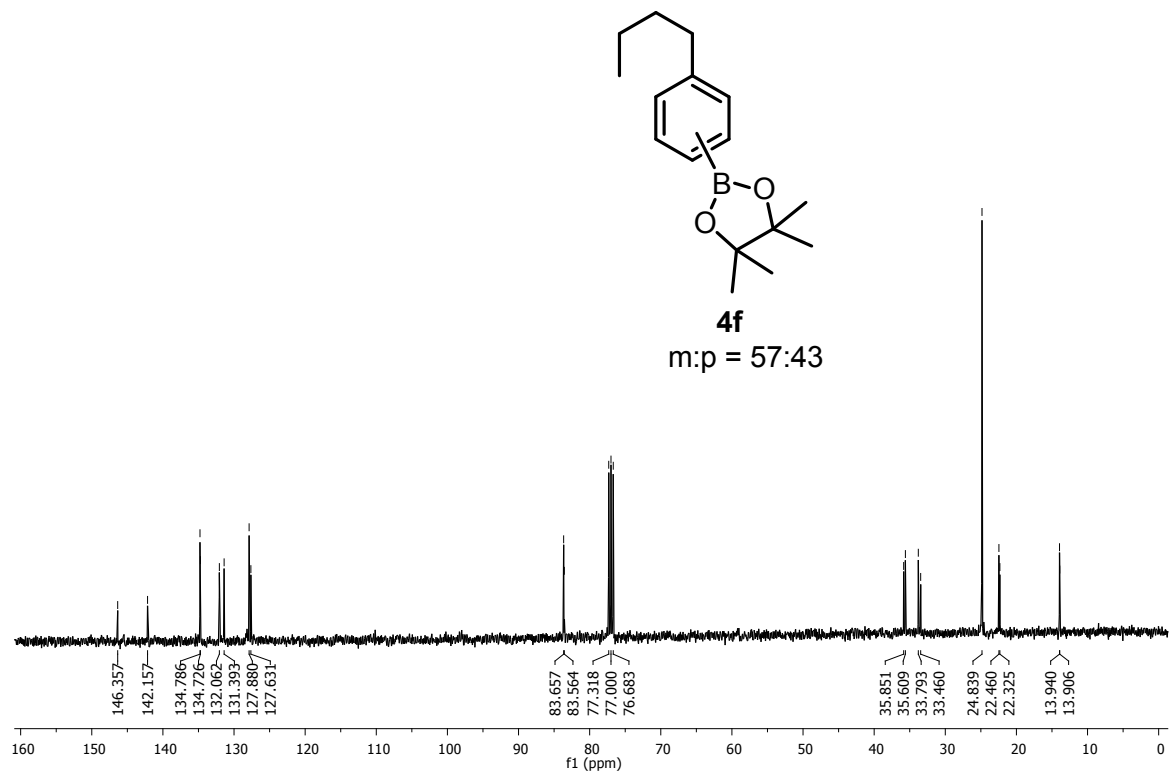


Figure S22. ^{13}C NMR (CDCl_3) spectrum of 2-(3-butylphenyl)-4,4,5,5-tetramethyl-1,3,2-dioxaborolane (**4f**).

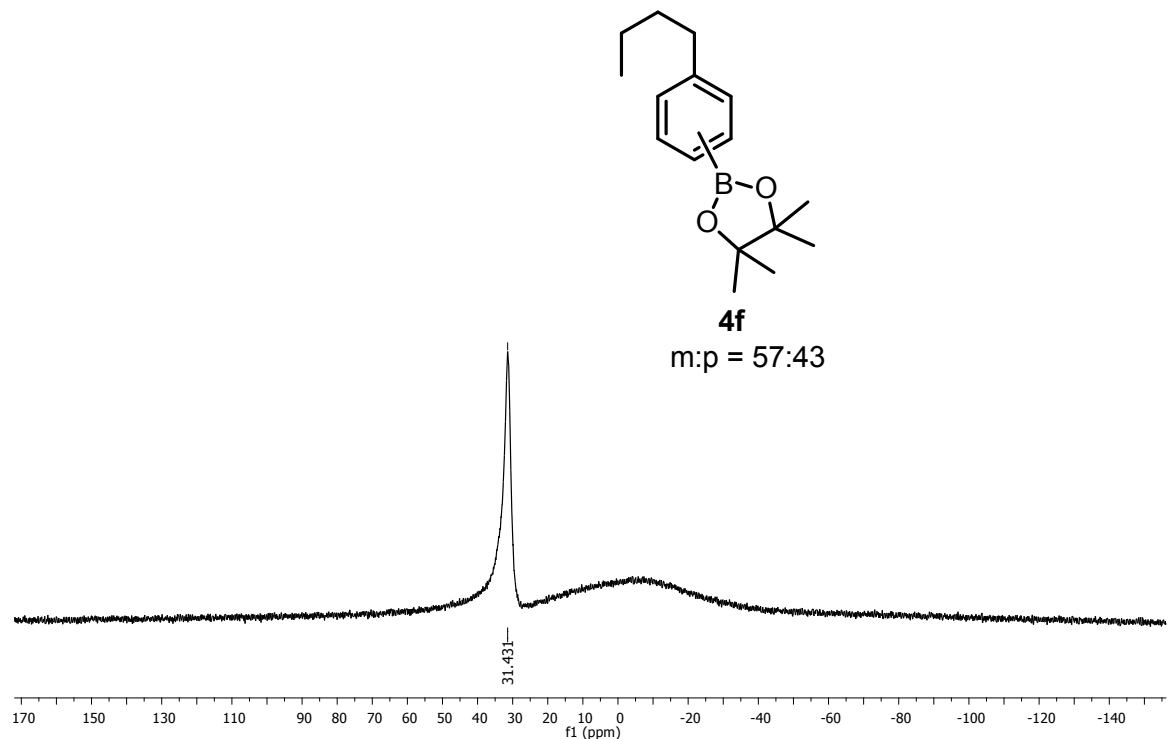


Figure S23. ^{11}B NMR (CDCl_3) spectrum of 2-(3-butylphenyl)-4,4,5,5-tetramethyl-1,3,2-dioxaborolane (**4f**).

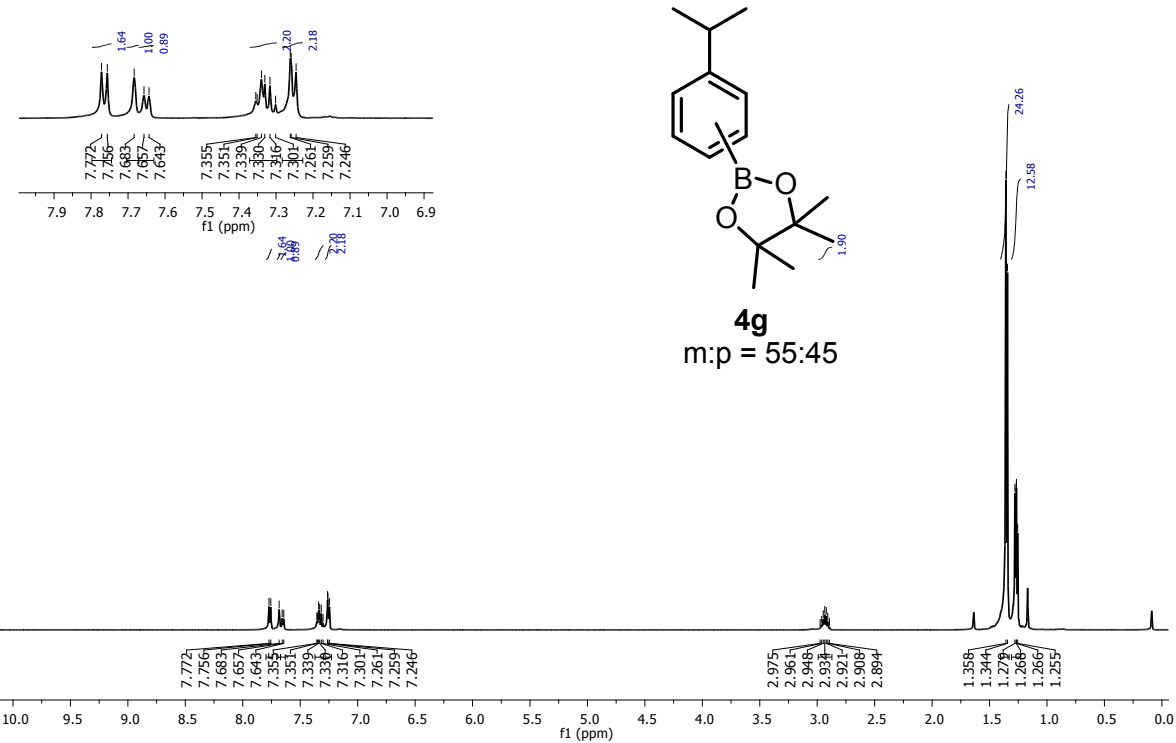


Figure S24. ¹H NMR (CDCl₃) spectrum of 2-(3-isopropylphenyl)-4,4,5,5-tetramethyl-1,3,2-dioxaborolane (**4g**).

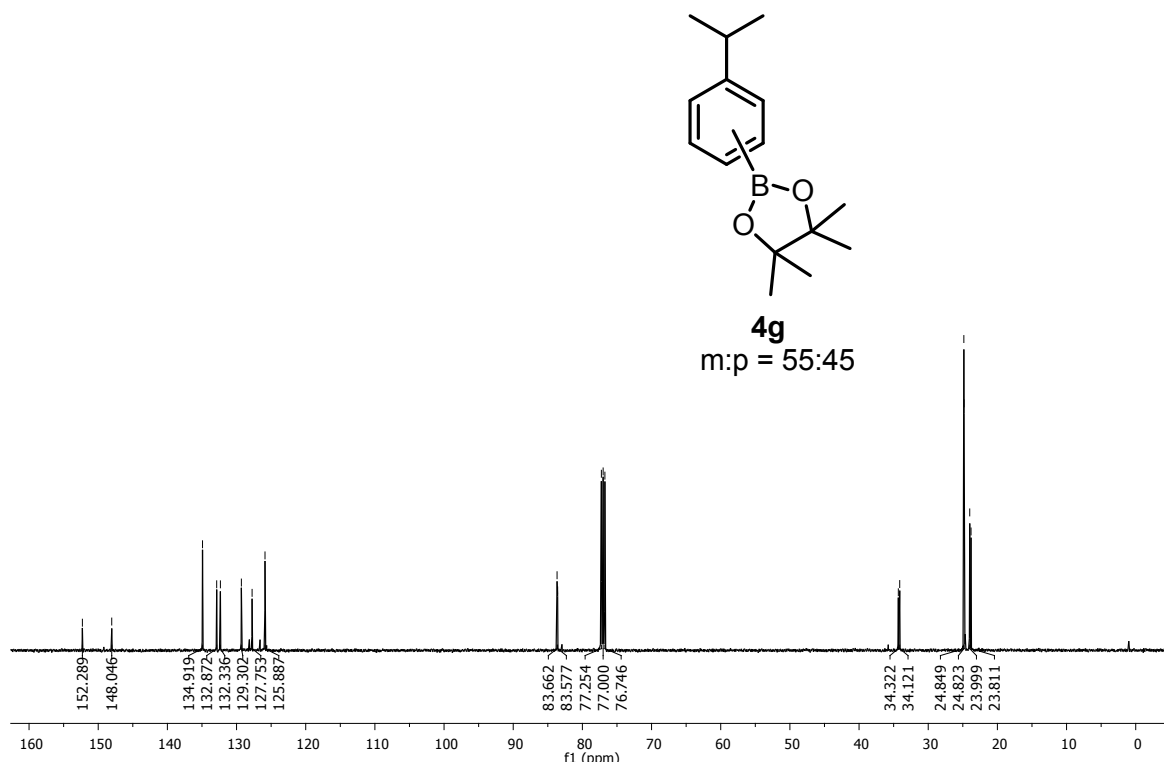


Figure S25. ¹³C NMR (CDCl₃) spectrum of 2-(3-isopropylphenyl)-4,4,5,5-tetramethyl-1,3,2-dioxaborolane (**4g**).

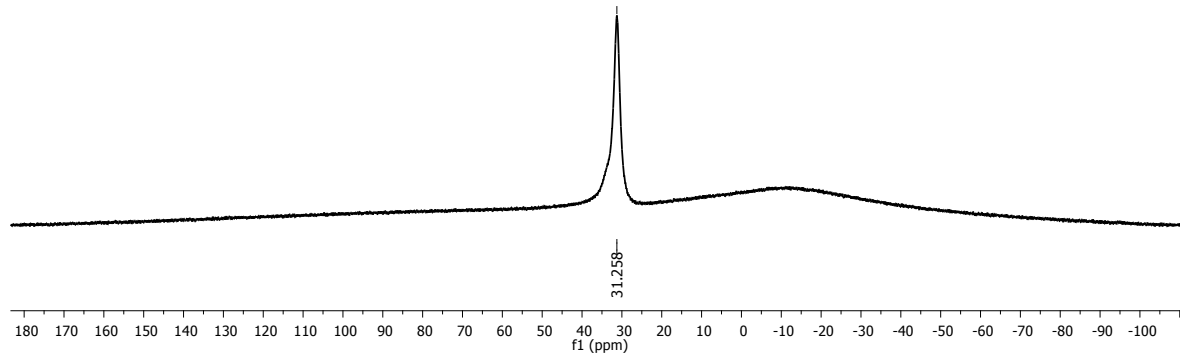
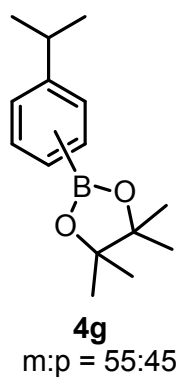


Figure S26. ^{11}B NMR (CDCl_3) spectrum of 2-(3-isopropylphenyl)-4,4,5,5-tetramethyl-1,3,2-dioxaborolane (**4g**).

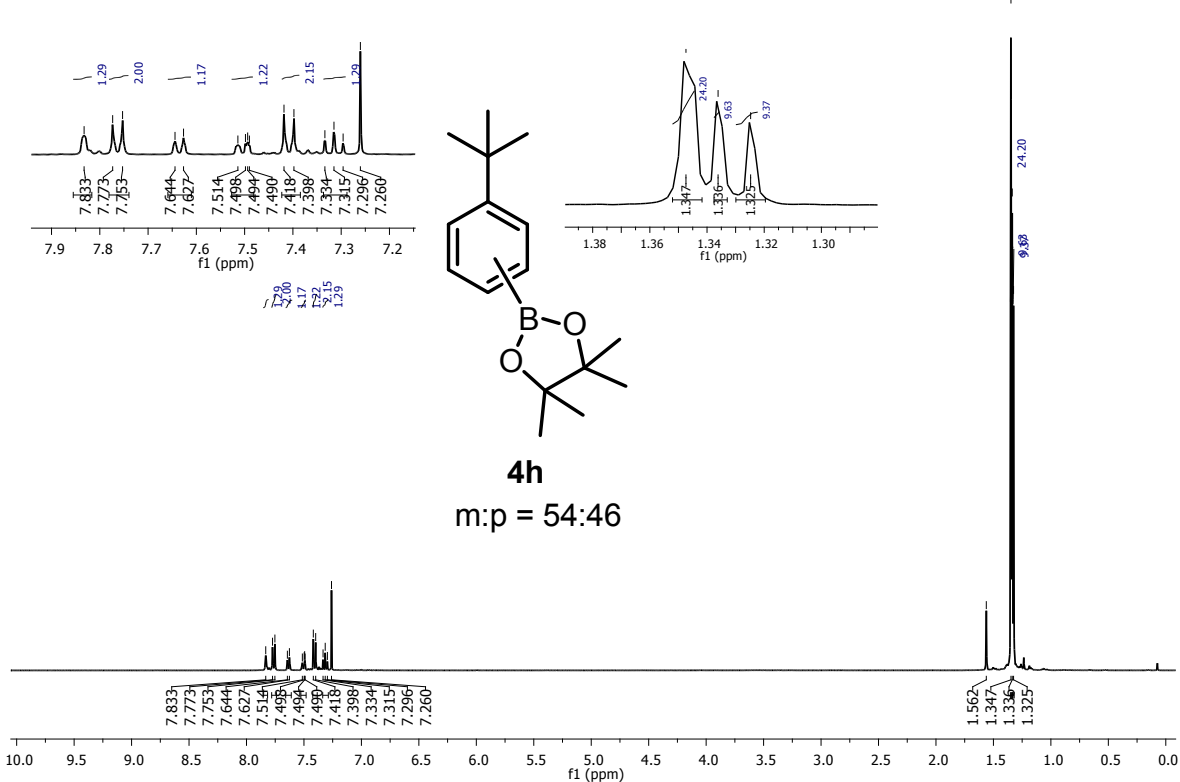


Figure S27. ^1H NMR (CDCl_3) spectrum of 2-(3-(tert-butyl)phenyl)-4,4,5,5-tetramethyl-1,3,2-dioxaborolane (**4h**).

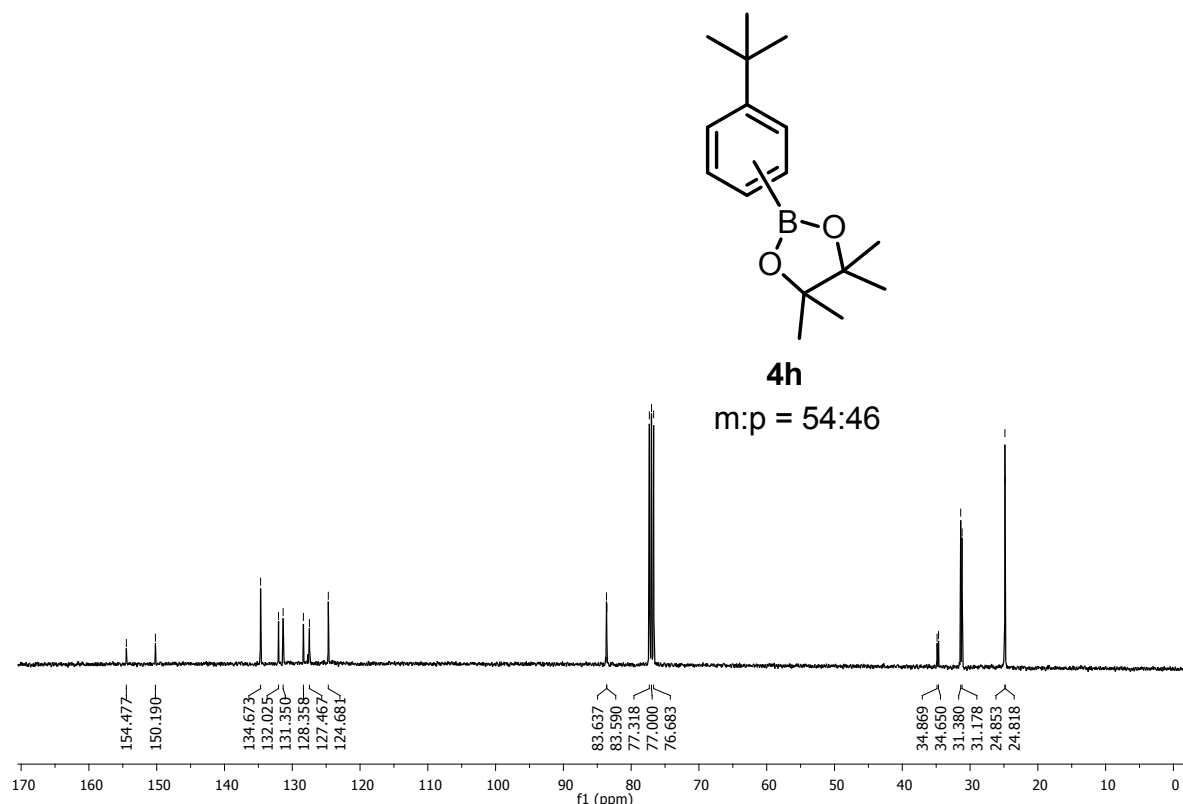


Figure S28. ^{13}C NMR (CDCl_3) spectrum of 2-(3-(tert-butyl)phenyl)-4,4,5,5-tetramethyl-1,3,2-dioxaborolane (**4h**).

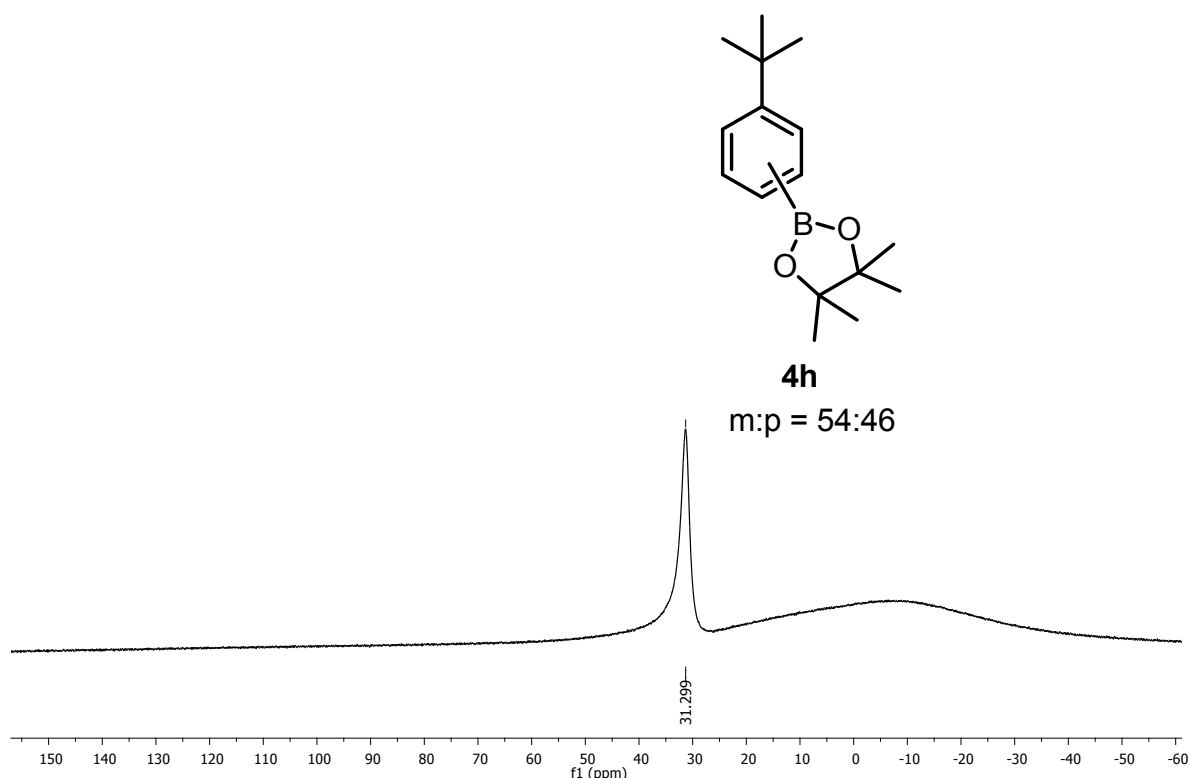


Figure S29. ^{11}B NMR (CDCl_3) spectrum of 2-(3-(tert-butyl)phenyl)-4,4,5,5-tetramethyl-1,3,2-dioxaborolane (**4h**).

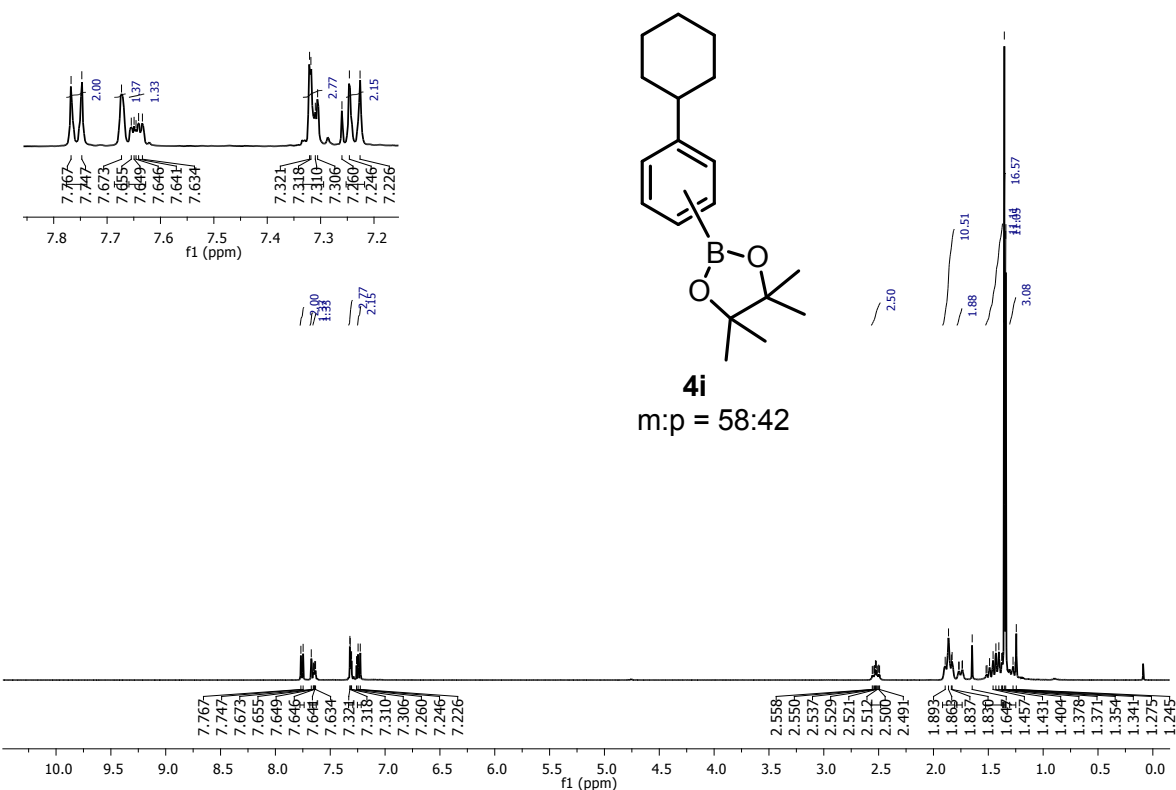


Figure S30. ¹H NMR (CDCl₃) spectrum of 2-(3-cyclohexylphenyl)-4,4,5,5-tetramethyl-1,3,2-dioxaborolane (**4i**).

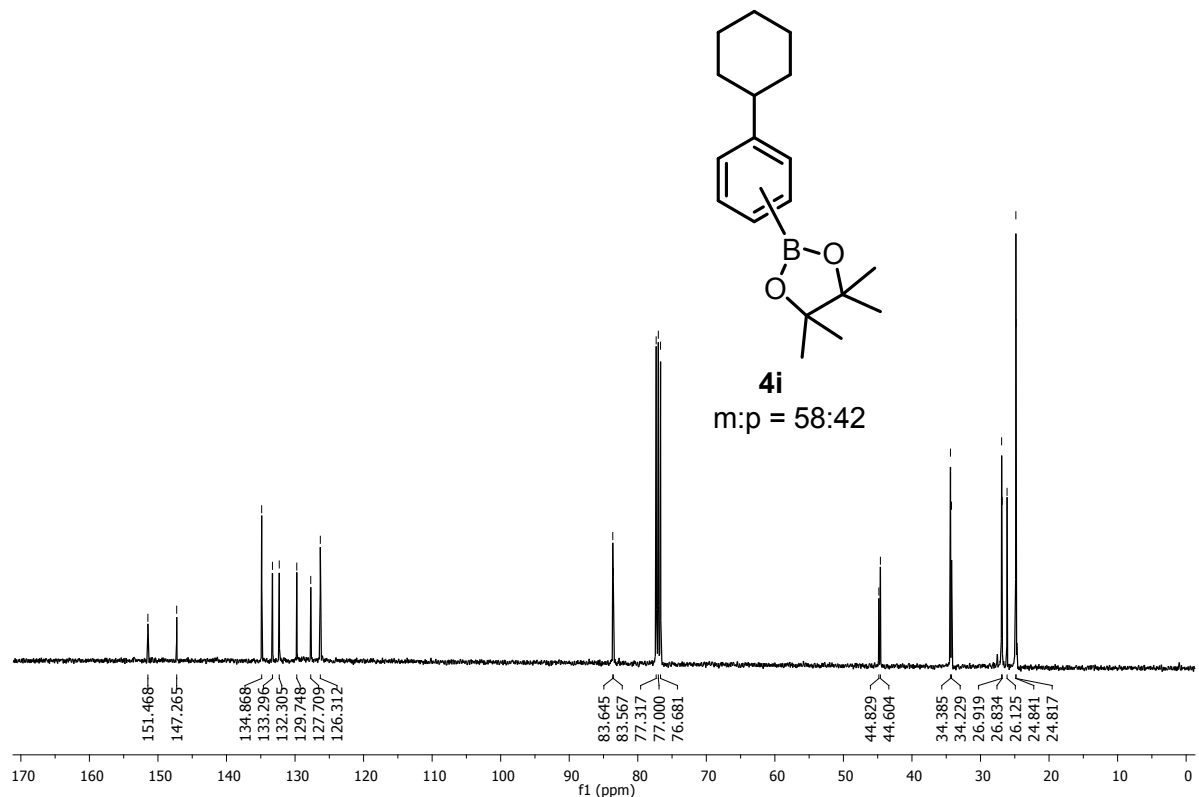


Figure S31. ¹³C NMR (CDCl₃) spectrum of 2-(3-cyclohexylphenyl)-4,4,5,5-tetramethyl-1,3,2-dioxaborolane (**4i**).

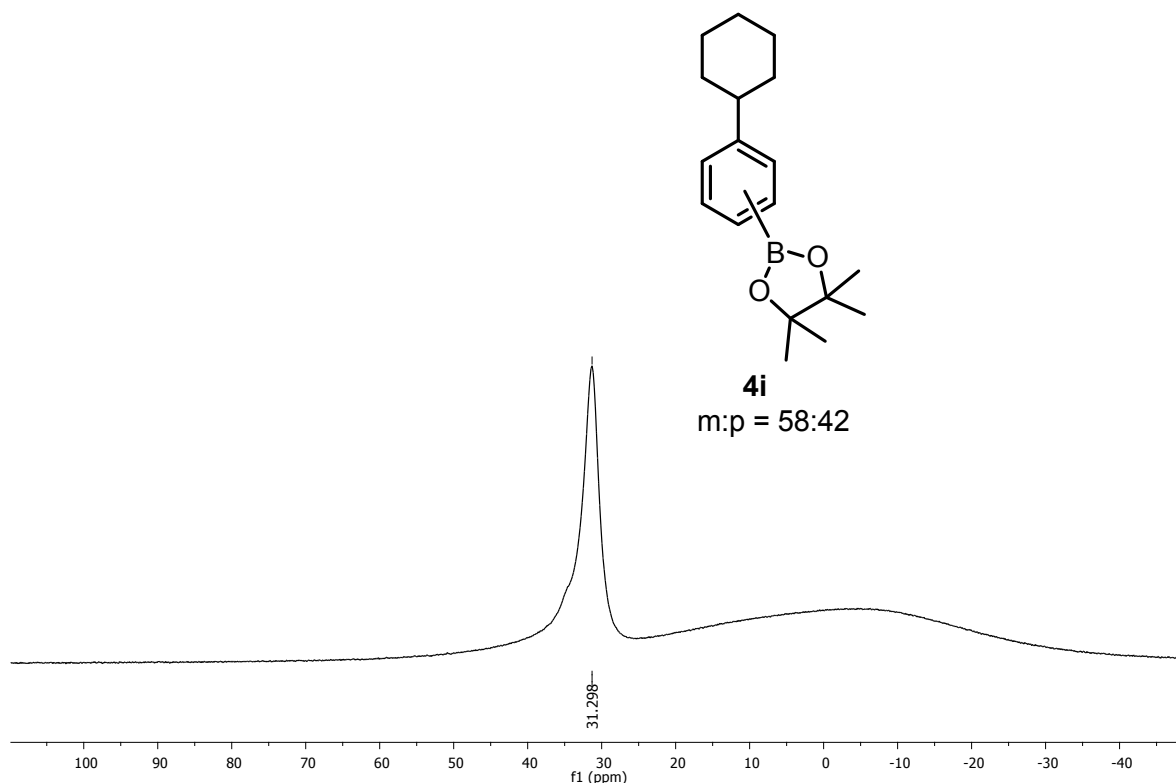


Figure S32. ^{11}B NMR (CDCl_3) spectrum of 2-(3-cyclohexylphenyl)-4,4,5,5-tetramethyl-1,3,2-dioxaborolane (**4i**).

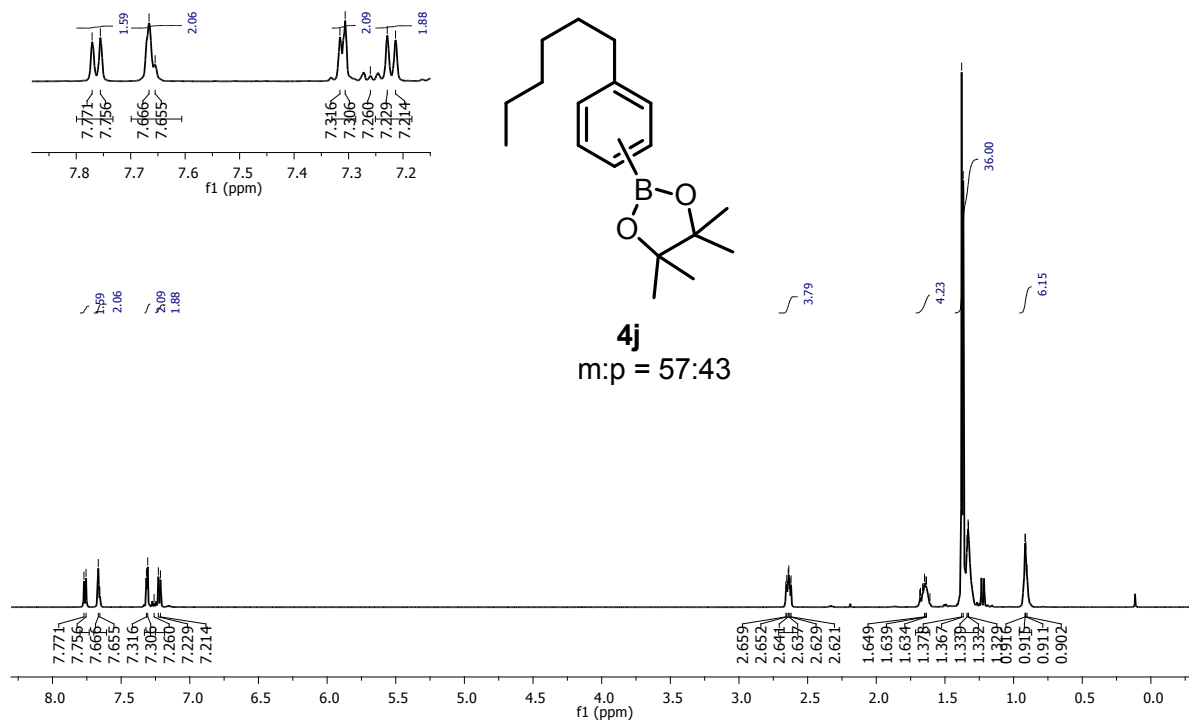


Figure S33. ^1H NMR (CDCl_3) spectrum of 2-(3-hexylphenyl)-4,4,5,5-tetramethyl-1,3,2-dioxaborolane (**4j**).

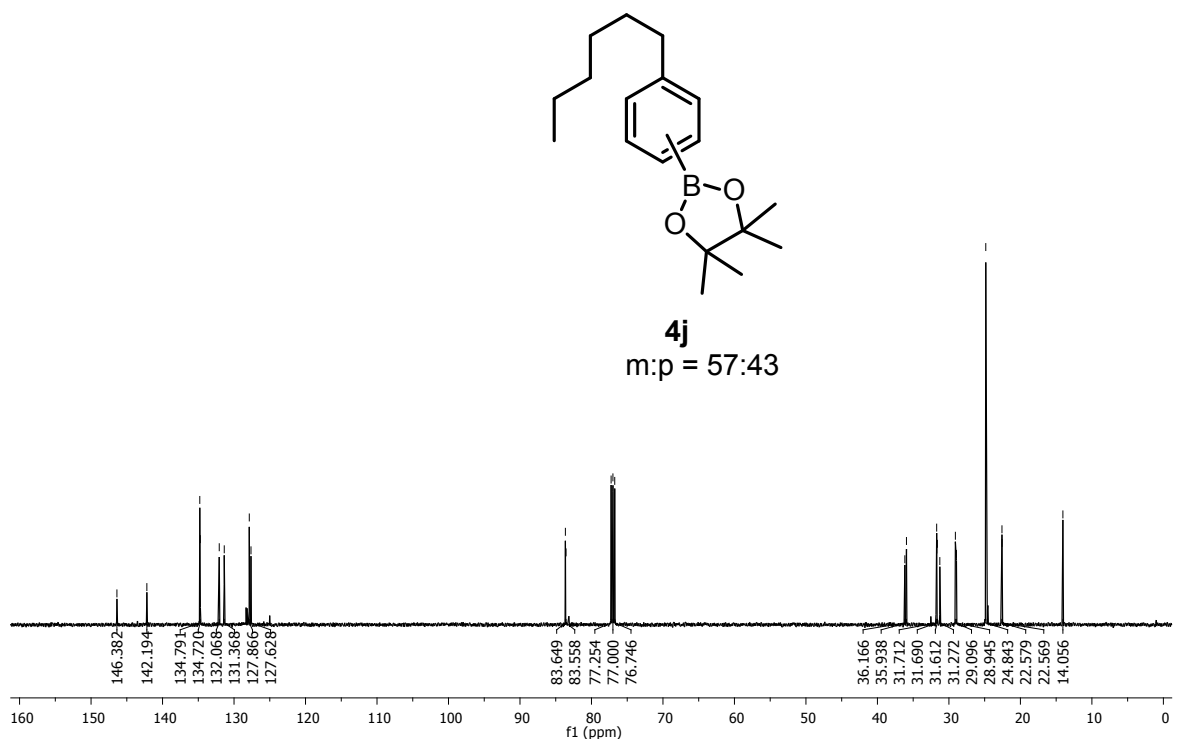


Figure S34. ^{13}C NMR (CDCl_3) spectrum of 2-(3-hexylphenyl)-4,4,5,5-tetramethyl-1,3,2-dioxaborolane (**4j**).

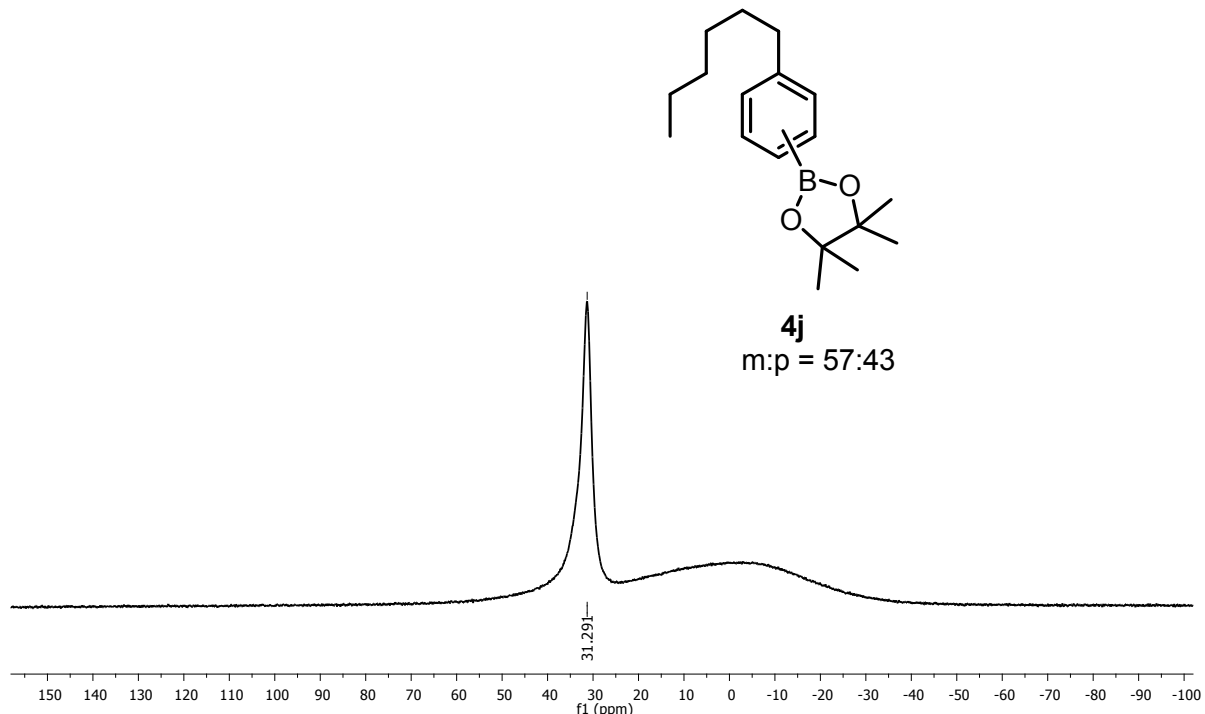


Figure S35. ^{11}B NMR (CDCl_3) spectrum of 2-(3-hexylphenyl)-4,4,5,5-tetramethyl-1,3,2-dioxaborolane (**4j**).

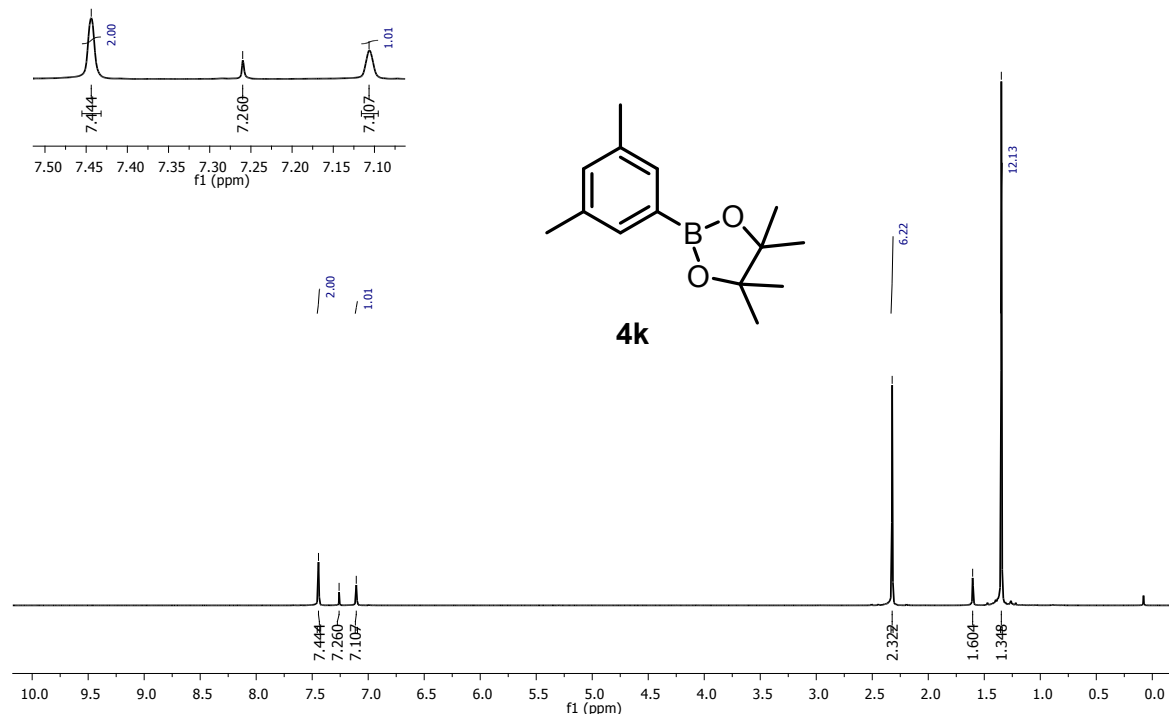


Figure S36. ¹H NMR (CDCl_3) spectrum of 2-(3,5-dimethylphenyl)-4,4,5,5-tetramethyl-1,3,2-dioxaborolane (**4k**).

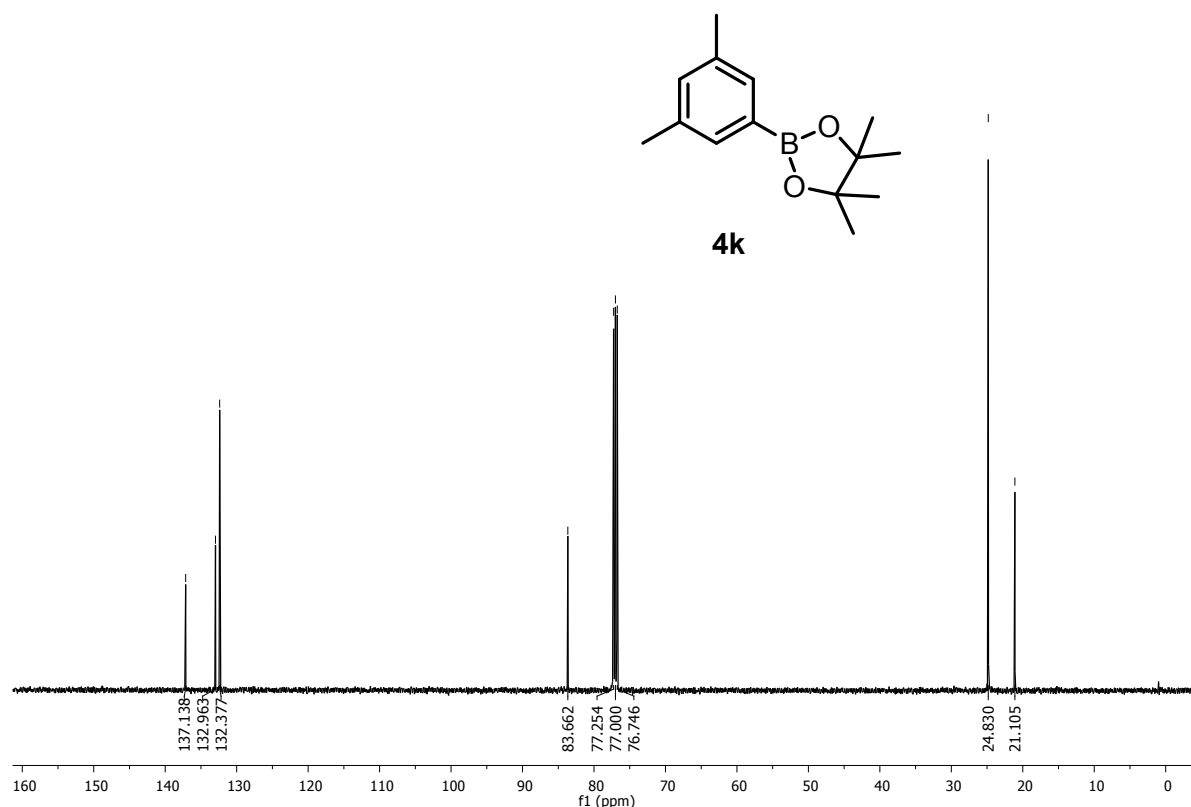


Figure S37. ¹³C NMR (CDCl_3) spectrum of 2-(3,5-dimethylphenyl)-4,4,5,5-tetramethyl-1,3,2-dioxaborolane (**4k**).

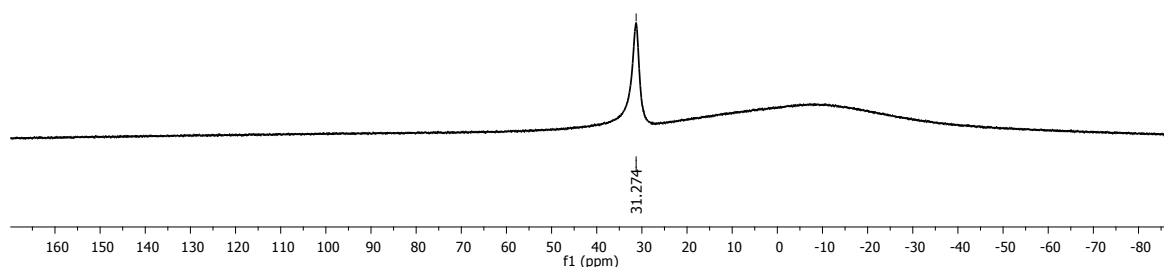
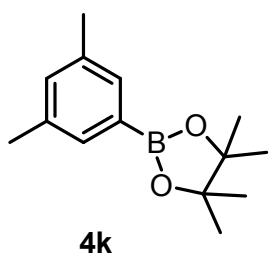


Figure S38. ^{11}B NMR (CDCl_3) spectrum of 2-(3,5-dimethylphenyl)-4,4,5,5-tetramethyl-1,3,2-dioxaborolane (**4k**).

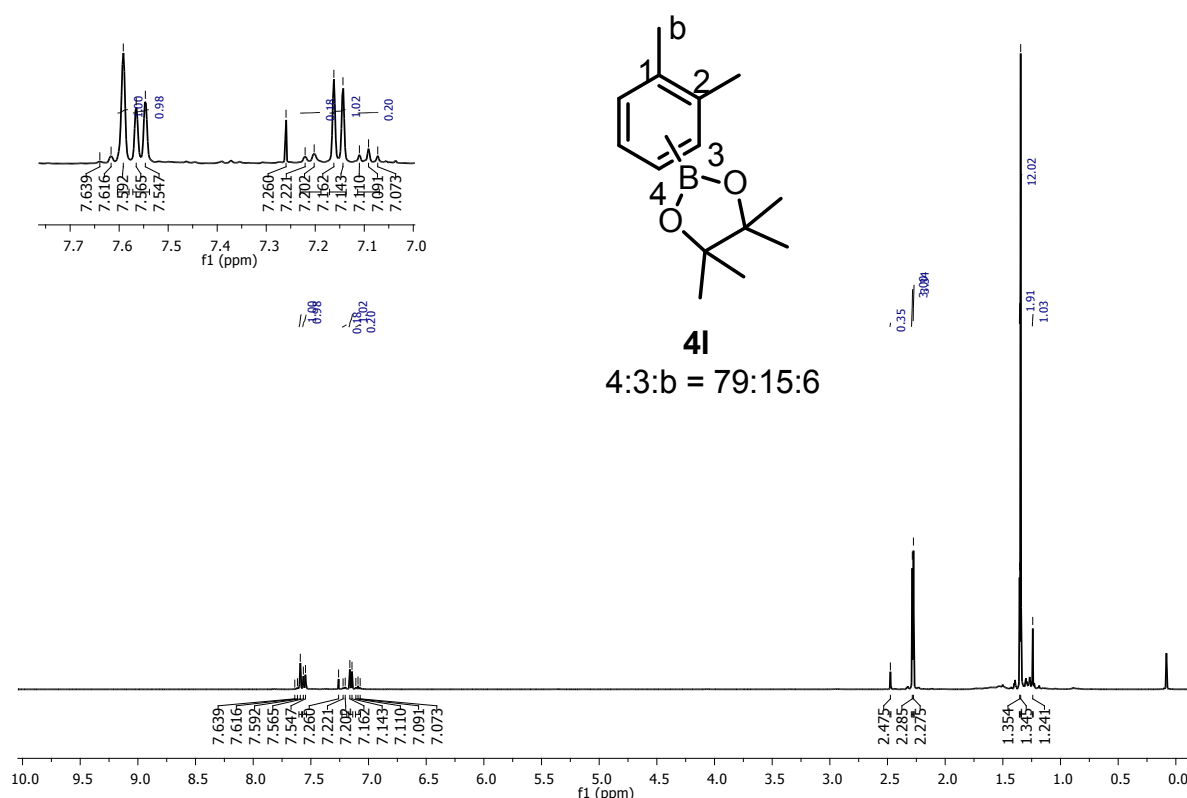


Figure S39. ^1H NMR (CDCl_3) spectrum of 2-(3,4-dimethylphenyl)-4,4,5,5-tetramethyl-1,3,2-dioxaborolane (**4l**).

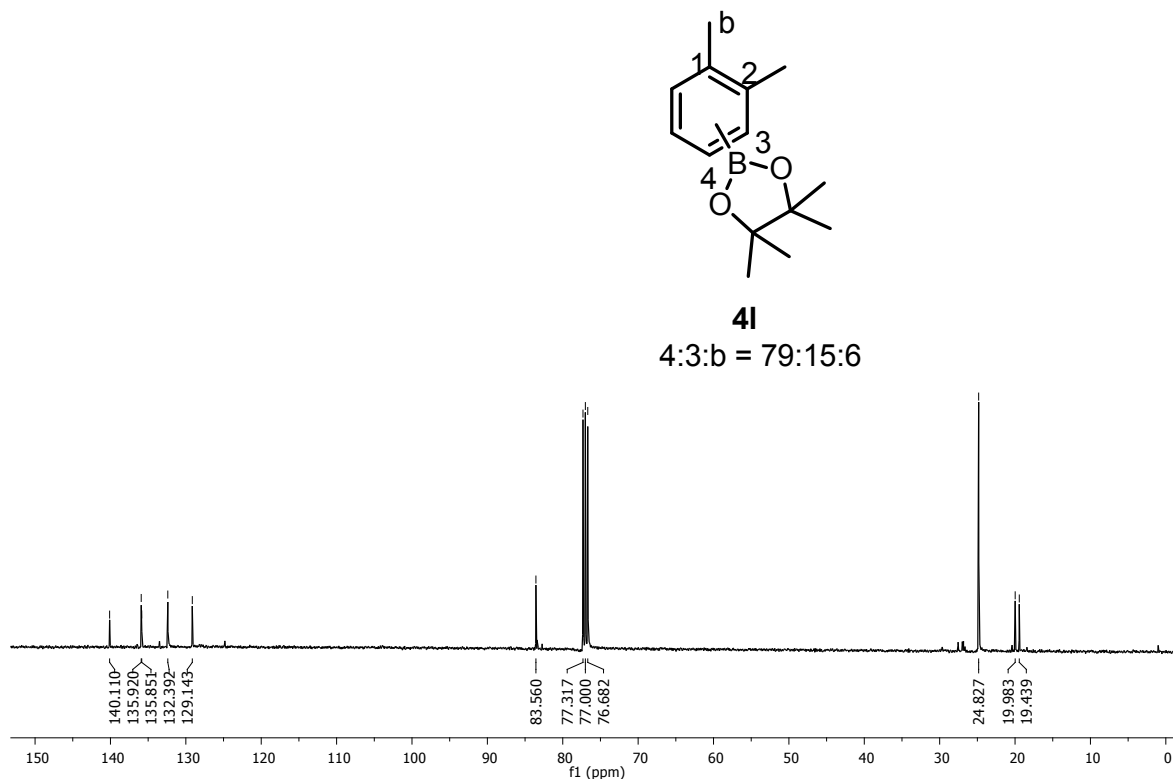


Figure S40. ^{13}C NMR (CDCl_3) spectrum of 2-(3,4-dimethylphenyl)-4,4,5,5-tetramethyl-1,3,2-dioxaborolane (**4l**).

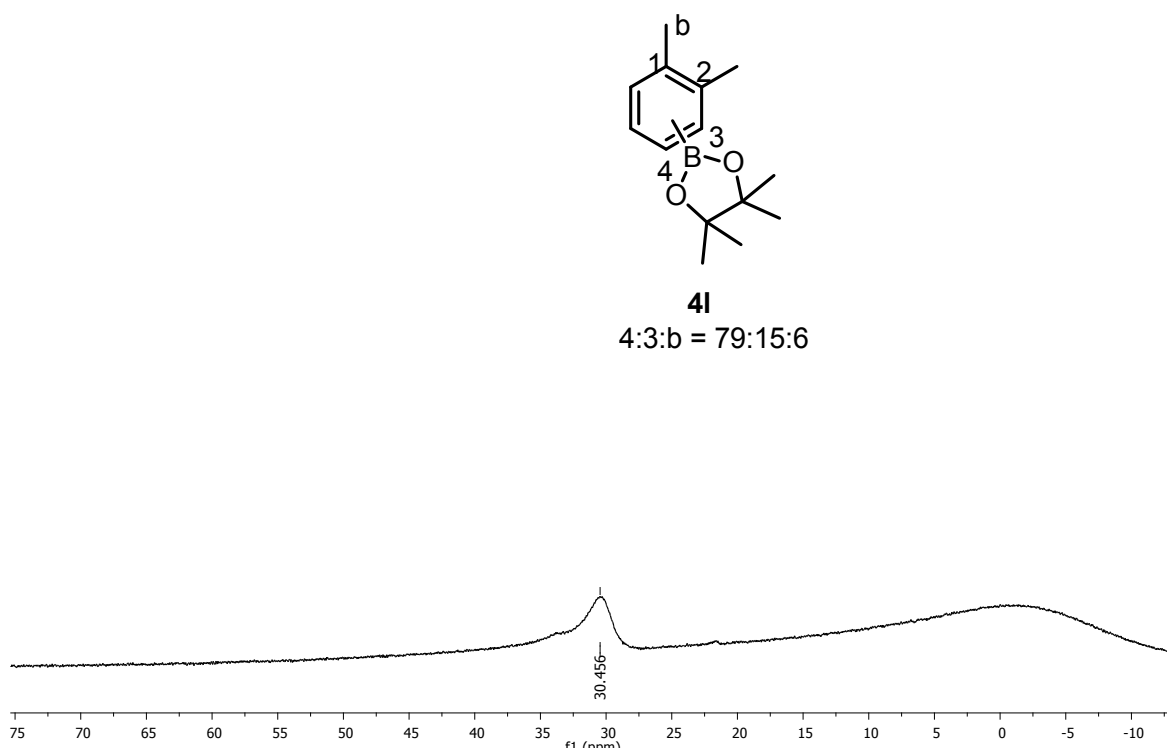


Figure S41. ^{11}B NMR (CDCl_3) spectrum of 2-(3,4-dimethylphenyl)-4,4,5,5-tetramethyl-1,3,2-dioxaborolane (**4l**).

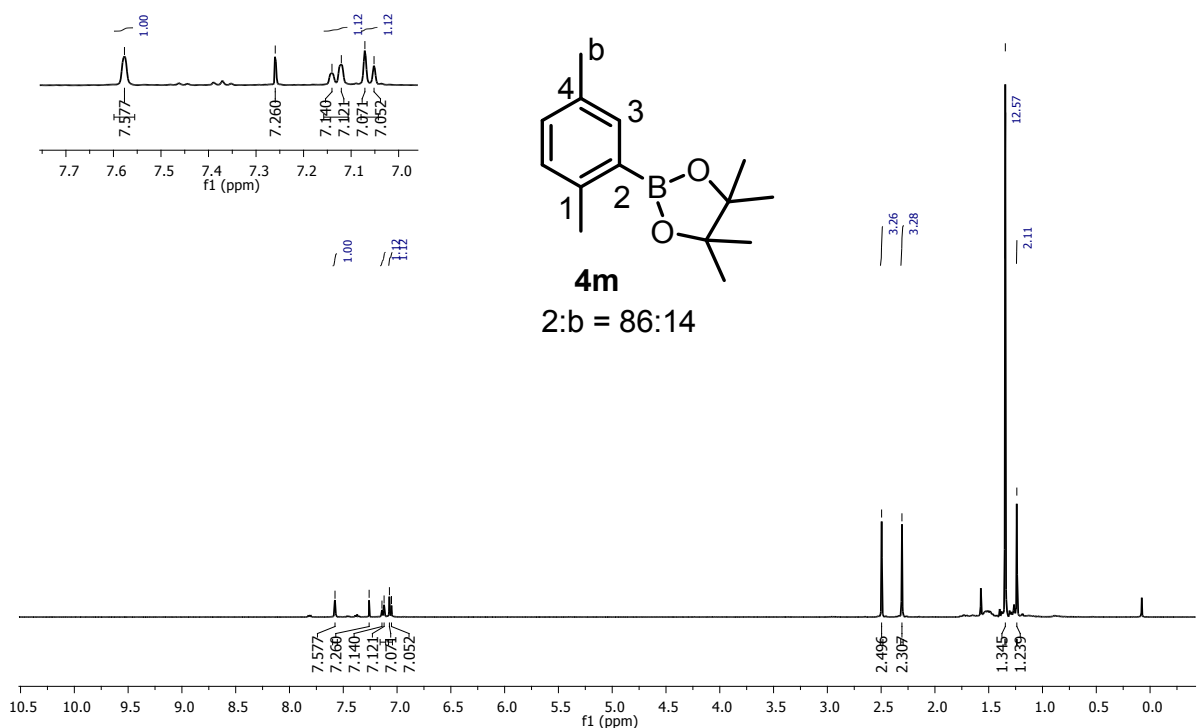


Figure S42. ¹H NMR (CDCl_3) spectrum of 2-(2,5-dimethylphenyl)-4,4,5,5-tetramethyl-1,3,2-dioxaborolane (**4m**).

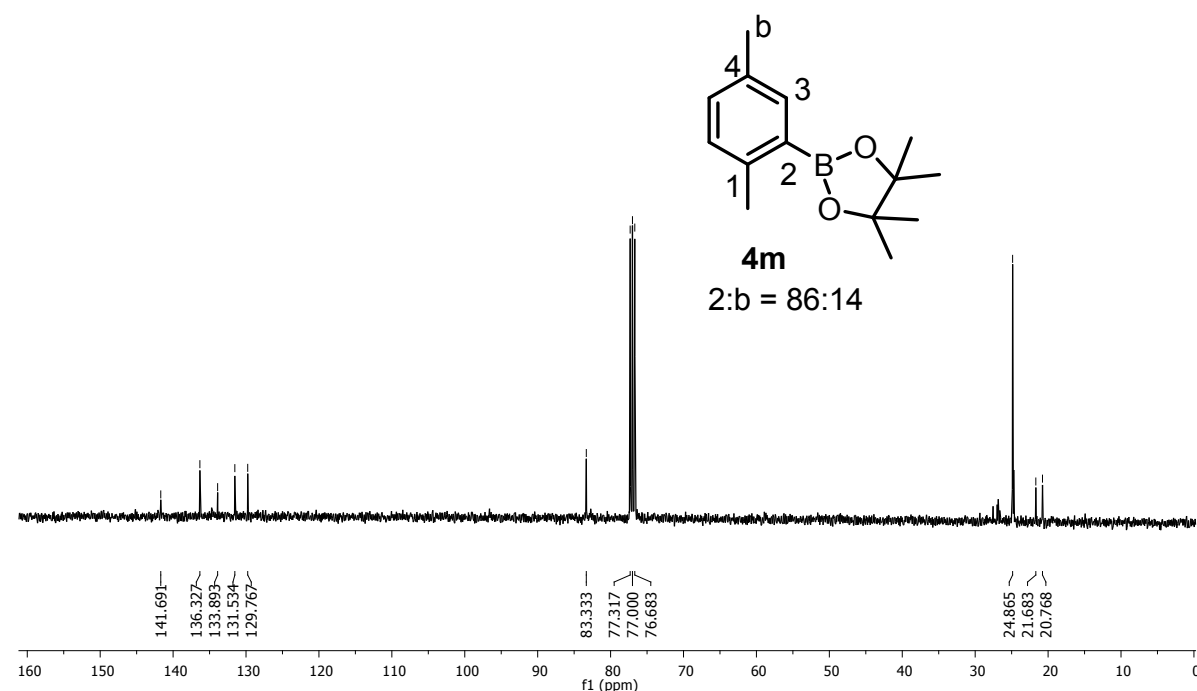


Figure S43. ¹³C NMR (CDCl_3) spectrum of 2-(2,5-dimethylphenyl)-4,4,5,5-tetramethyl-1,3,2-dioxaborolane (**4m**).

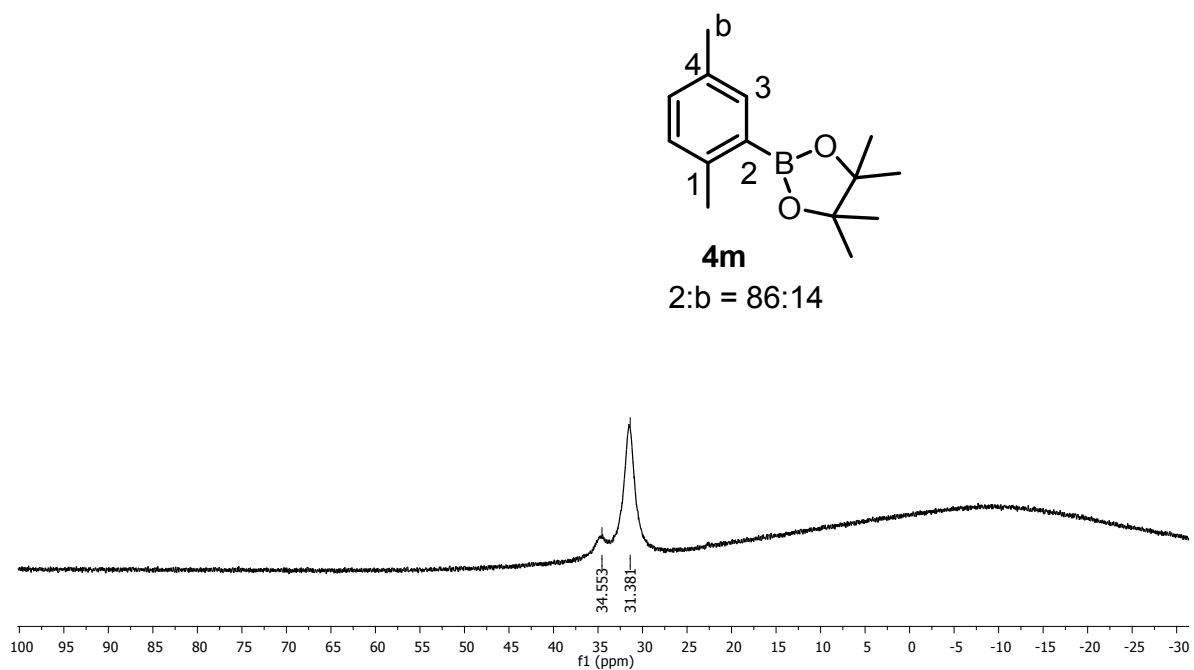


Figure S44. ^{11}B NMR (CDCl_3) spectrum of 2-(2,5-dimethylphenyl)-4,4,5,5-tetramethyl-1,3,2-dioxaborolane (**4m**).

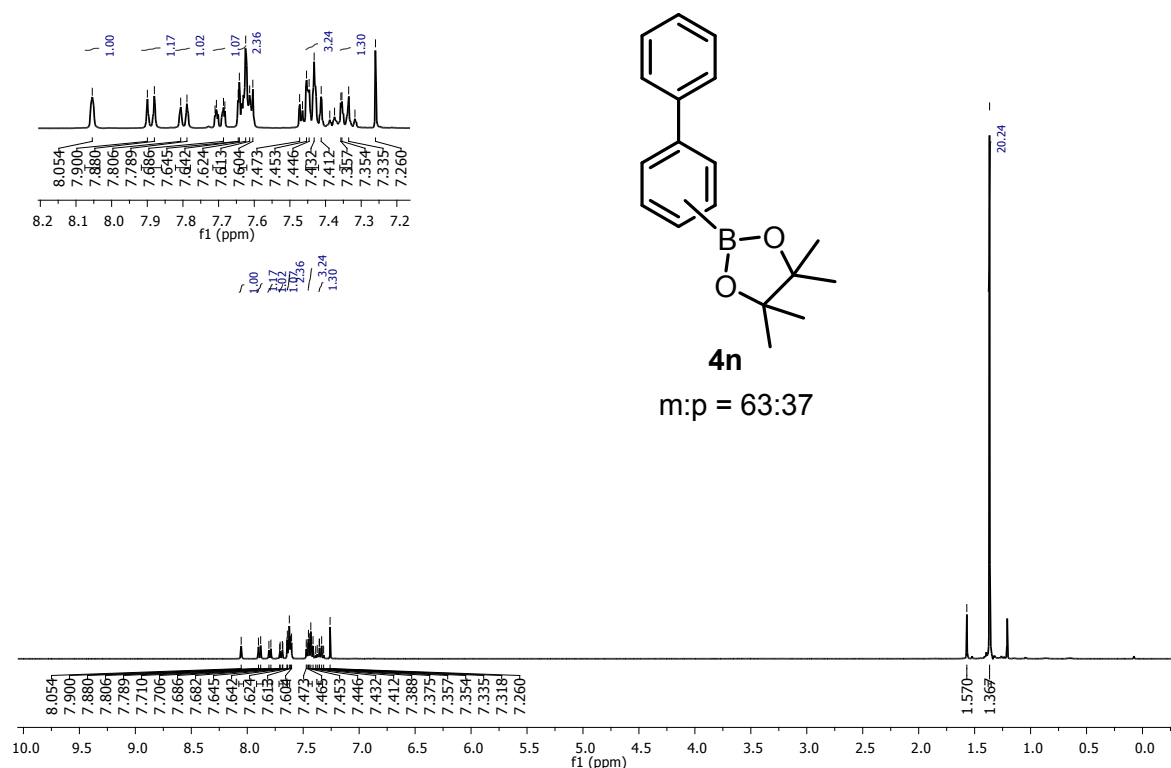


Figure S45. ^1H NMR (CDCl_3) spectrum of 2-([1,1'-biphenyl]-3-yl)-4,4,5,5-tetramethyl-1,3,2-dioxaborolane (**4n**).

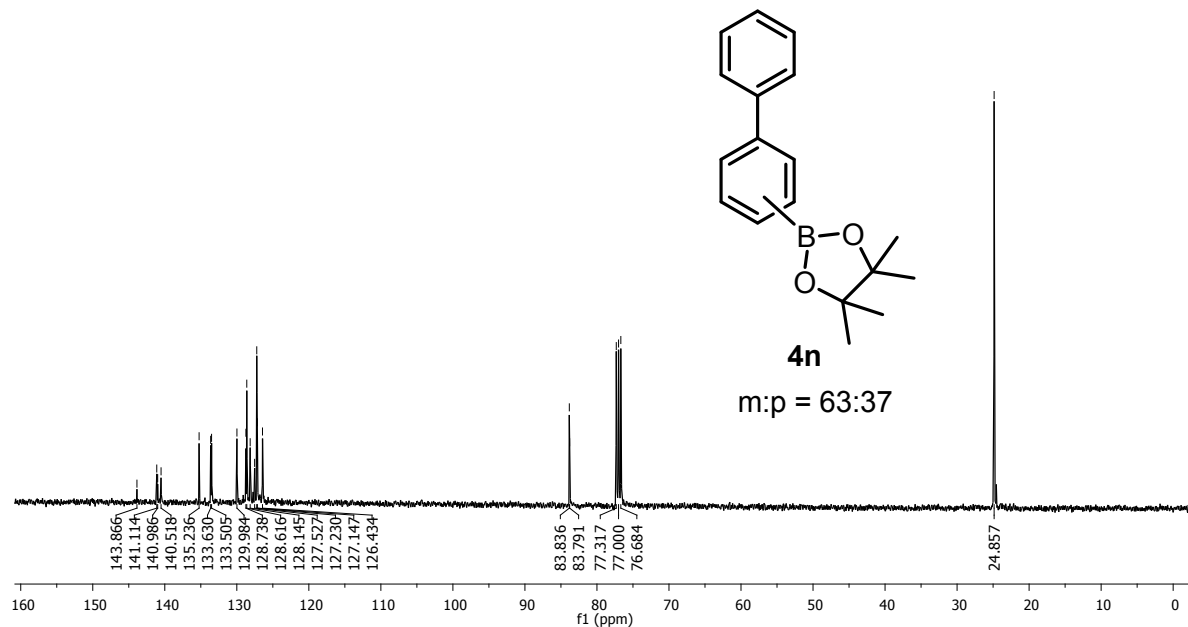


Figure S46. ^{13}C NMR (CDCl_3) spectrum of 2-([1,1'-biphenyl]-3-yl)-4,4,5,5-tetramethyl-1,3,2-dioxaborolane (**4n**).

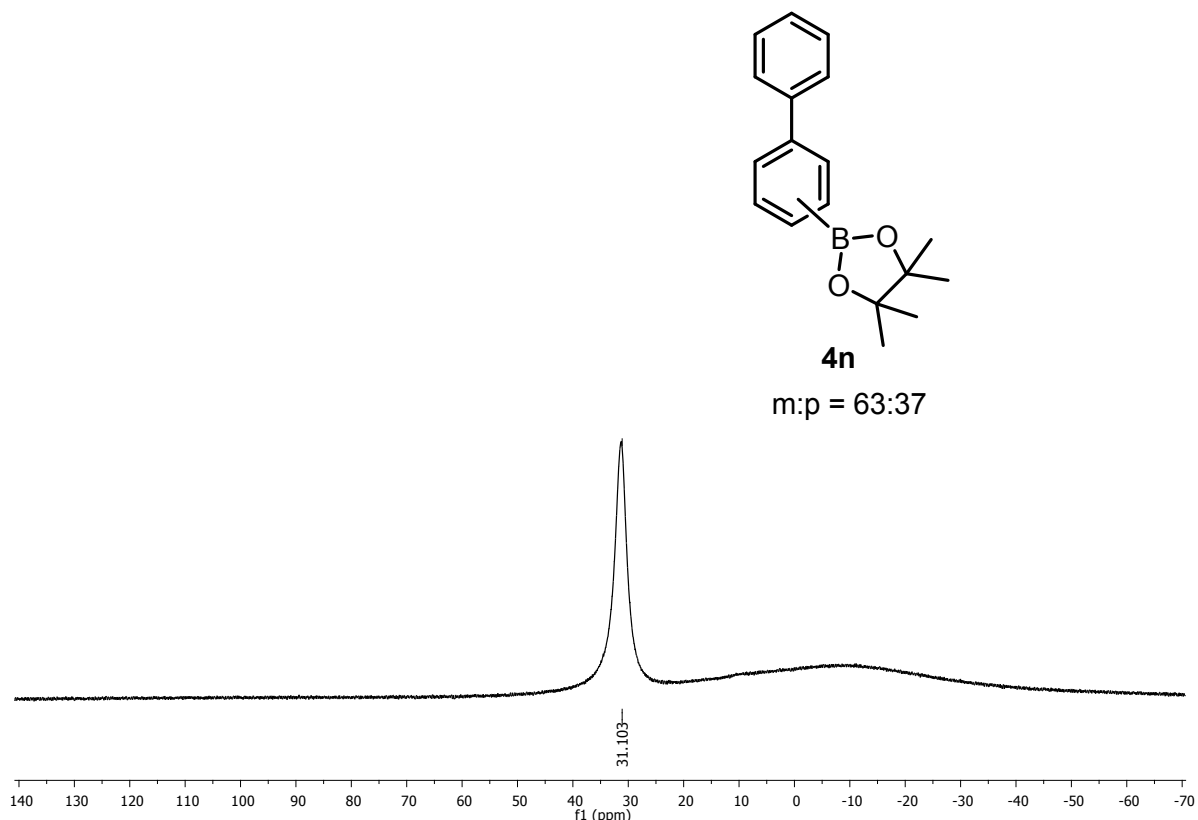


Figure S47. ^{11}B NMR (CDCl_3) spectrum of 2-([1,1'-biphenyl]-3-yl)-4,4,5,5-tetramethyl-1,3,2-dioxaborolane (**4n**).

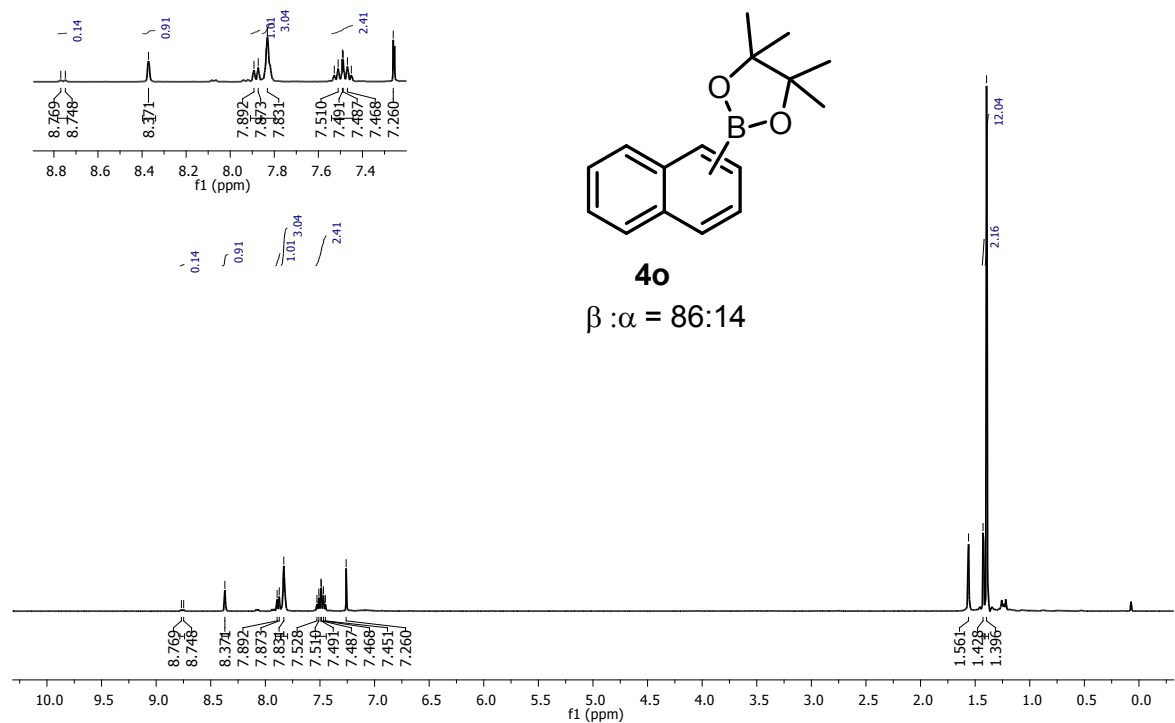


Figure S48. ¹H NMR (CDCl₃) spectrum of 4,4,5,5-tetramethyl-2-(naphthalen-2-yl)-1,3,2-dioxaborolane (**4o**).

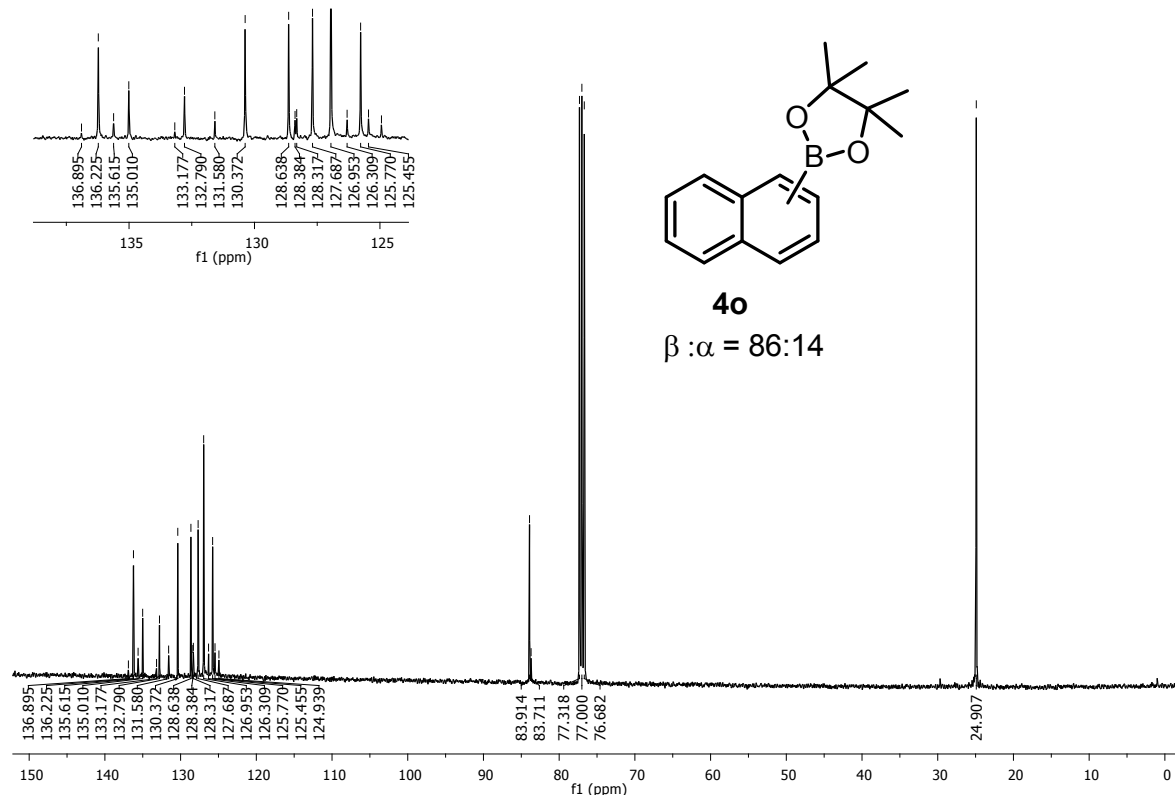


Figure S49. ¹³C NMR (CDCl₃) spectrum of 4,4,5,5-tetramethyl-2-(naphthalen-2-yl)-1,3,2-dioxaborolane (**4o**).

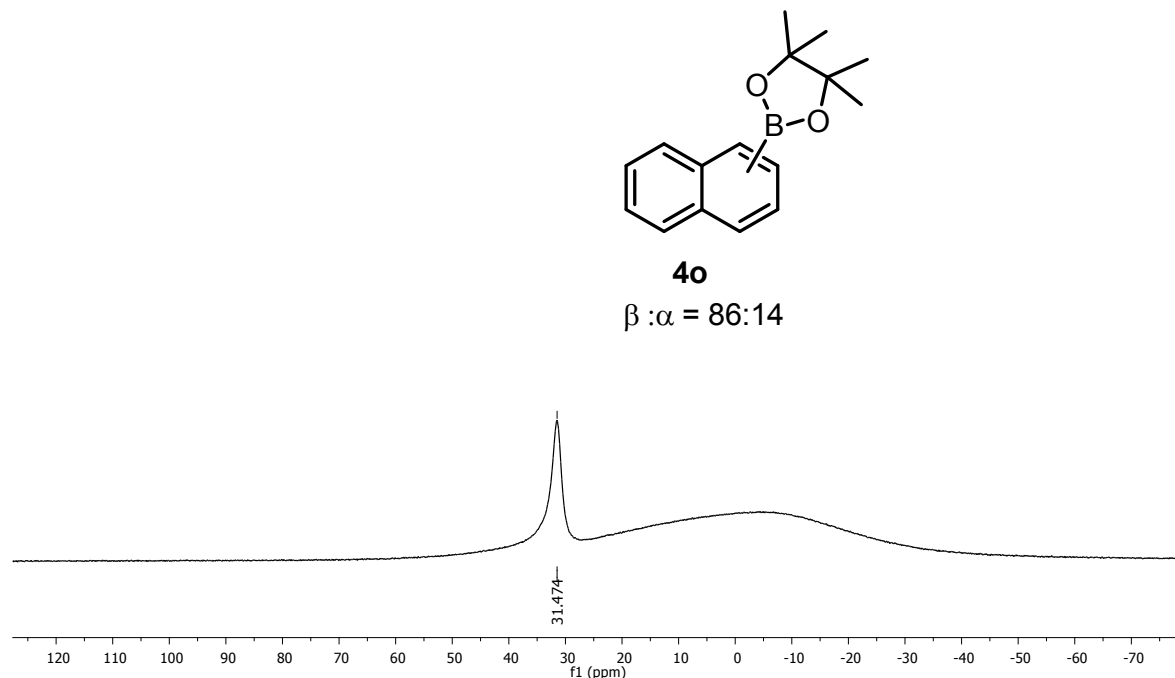


Figure S50. ^{11}B NMR (CDCl_3) spectrum of 4,4,5,5-tetramethyl-2-(naphthalen-2-yl)-1,3,2-dioxaborolane (**4o**).

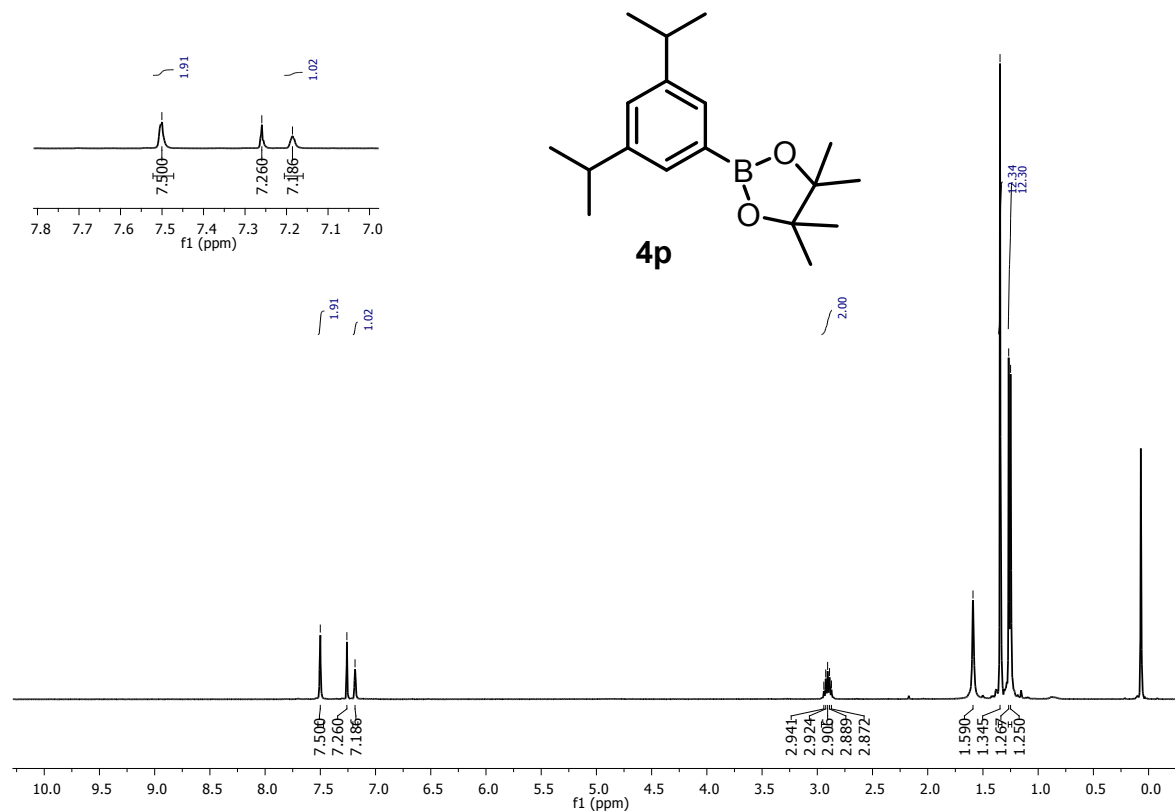


Figure S51. ^1H NMR (CDCl_3) spectrum of 2-(3,5-diisopropylphenyl)-4,4,5,5-tetramethyl-1,3,2-dioxaborolane (**4p**).

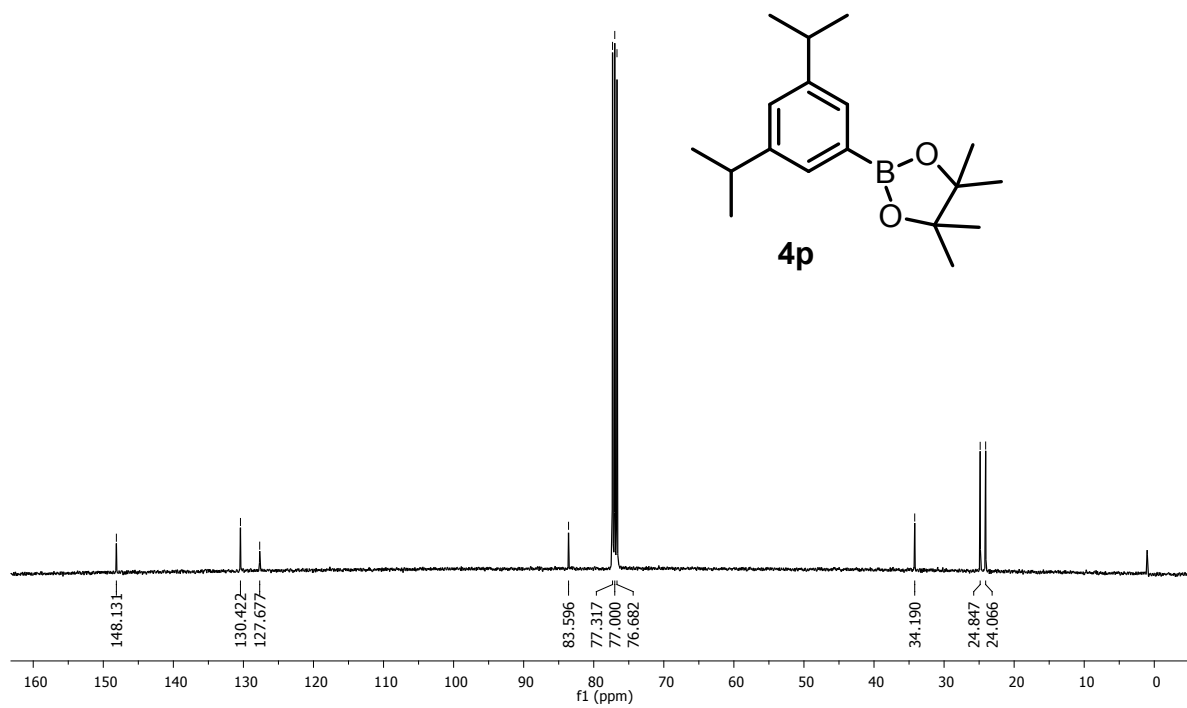


Figure S52. ^{13}C NMR (CDCl_3) spectrum of 2-(3,5-diisopropylphenyl)-4,4,5,5-tetramethyl-1,3,2-dioxaborolane (**4p**).

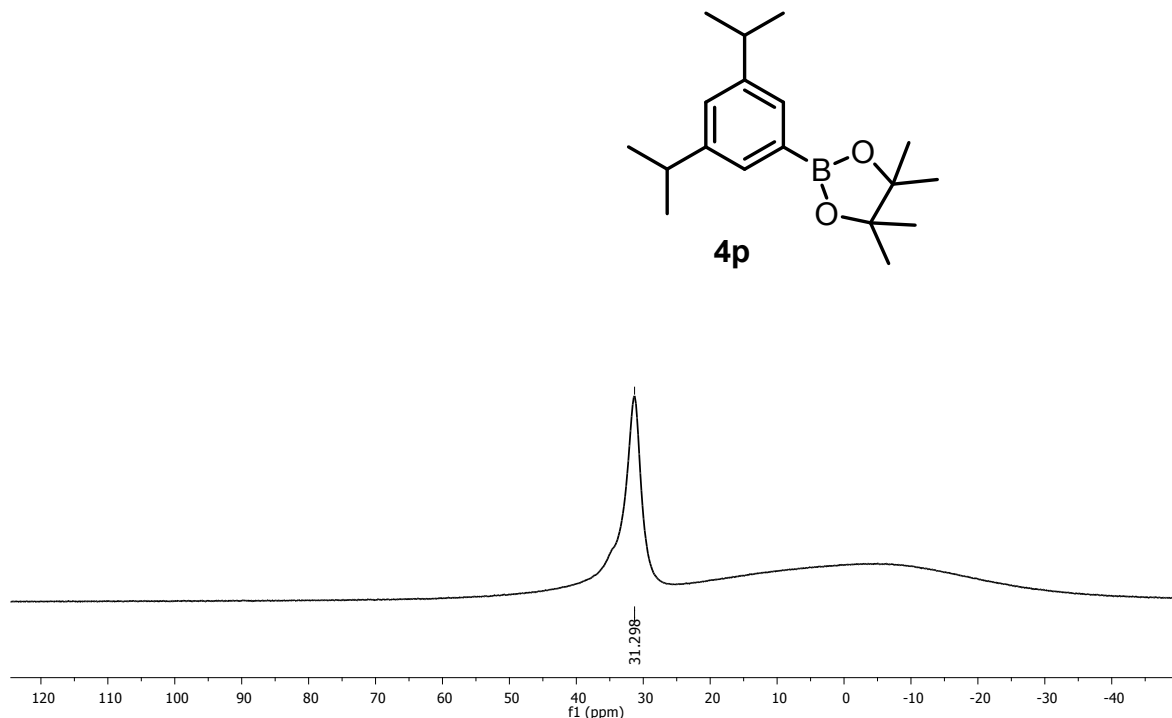


Figure S53. ^{11}B NMR (CDCl_3) spectrum of 2-(3,5-diisopropylphenyl)-4,4,5,5-tetramethyl-1,3,2-dioxaborolane (**4p**).

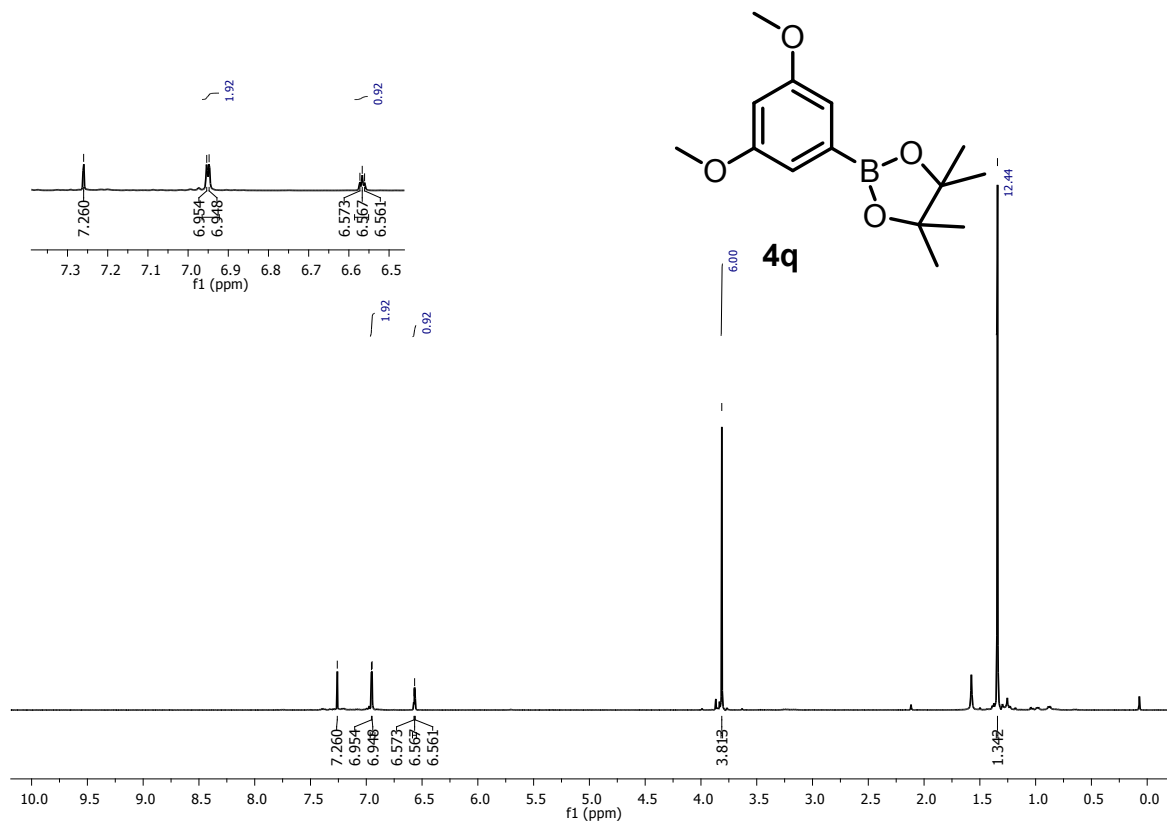


Figure S54. ^1H NMR (CDCl_3) spectrum of 2-(3,5-dimethoxyphenyl)-4,4,5,5-tetramethyl-1,3,2-dioxaborolane (**4q**).

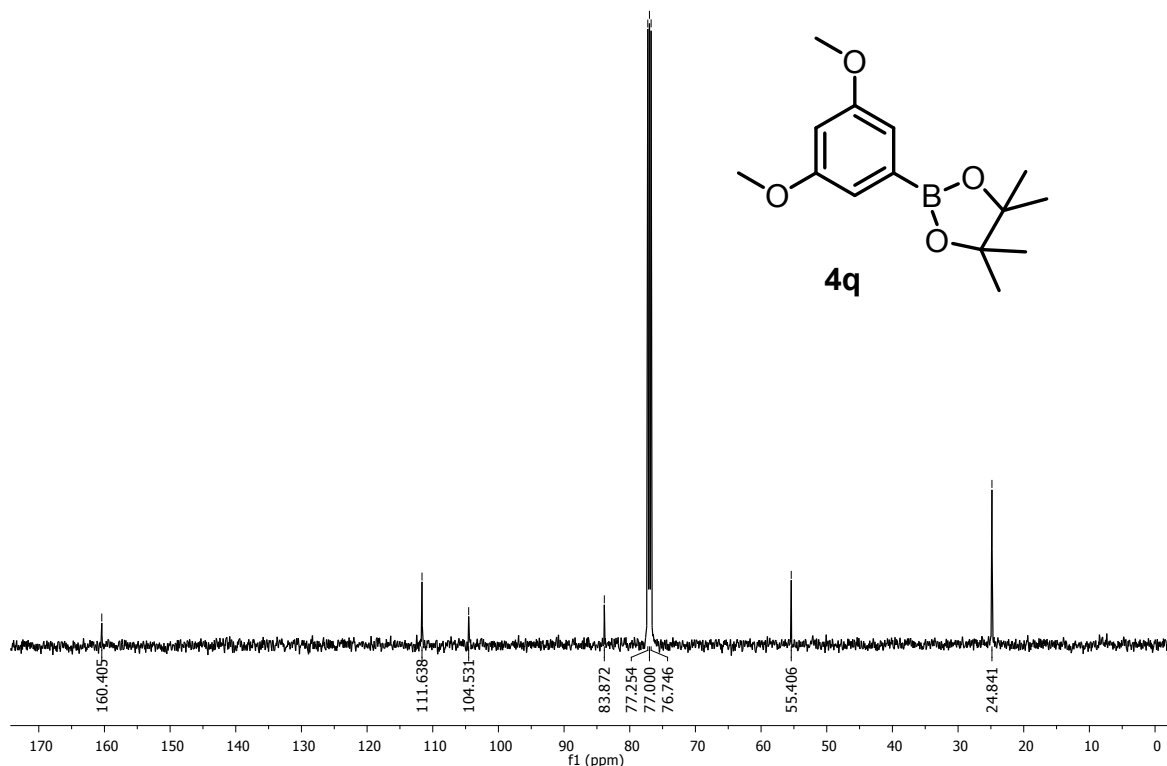


Figure S55. ^{13}C NMR (CDCl_3) spectrum of 2-(3,5-dimethoxyphenyl)-4,4,5,5-tetramethyl-1,3,2-dioxaborolane (**4q**).

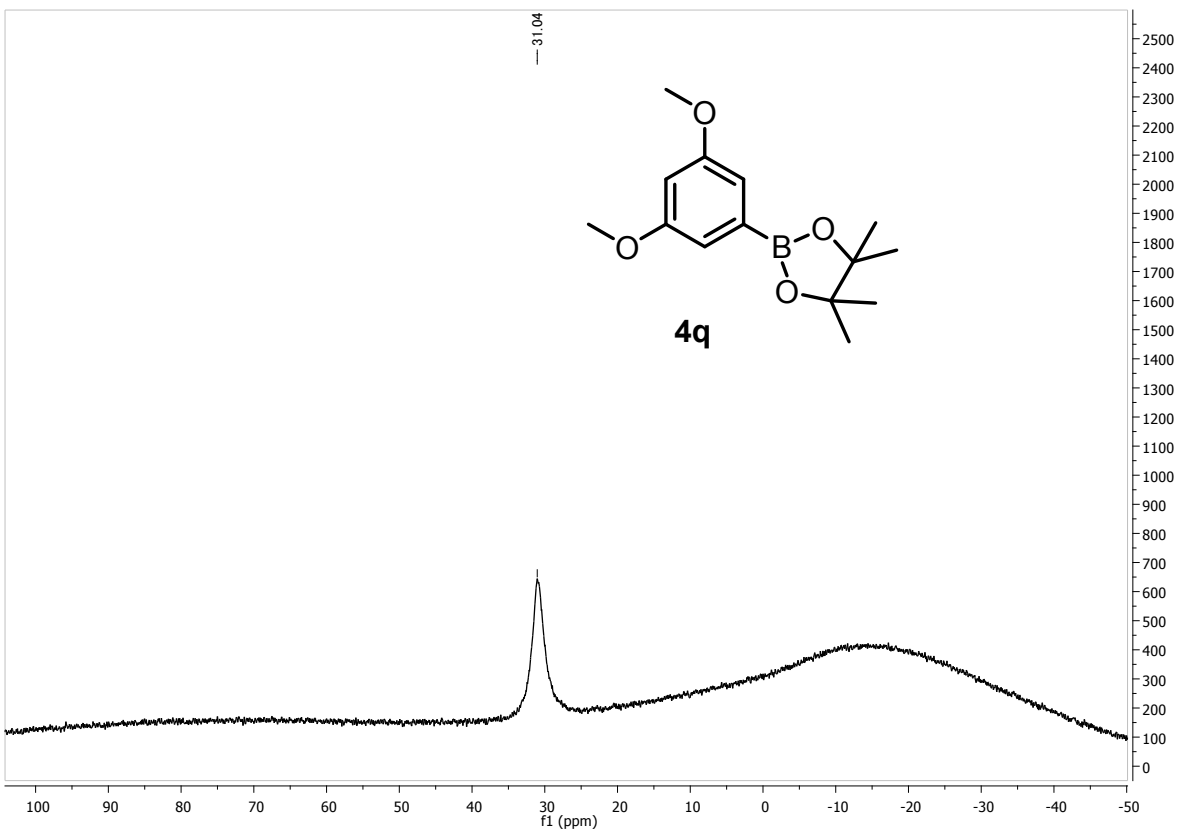


Figure S56. ^{11}B NMR (CDCl_3) spectrum of 2-(3,5-dimethoxyphenyl)-4,4,5,5-tetramethyl-1,3,2-dioxaborolane (**4q**).

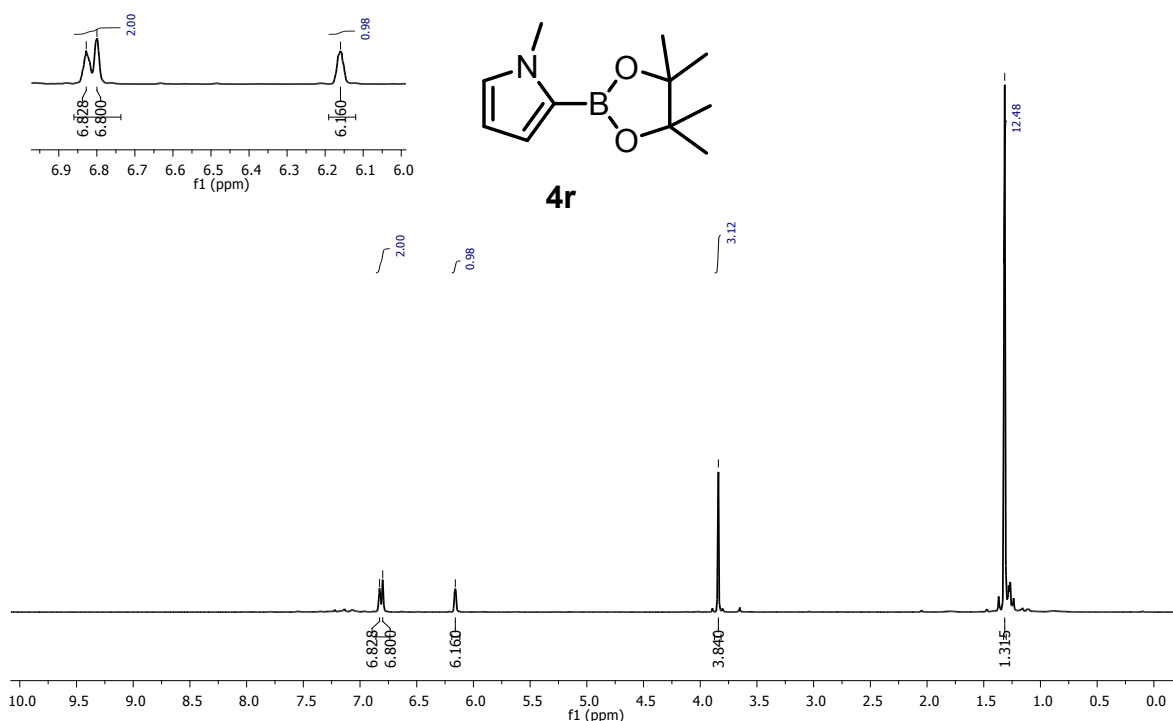


Figure S57. ^1H NMR (CDCl_3) spectrum of 1-methyl-2-(4,4,5,5-tetramethyl-1,3,2-dioxaborolan-2-yl)-1H-pyrrole (**4r**).

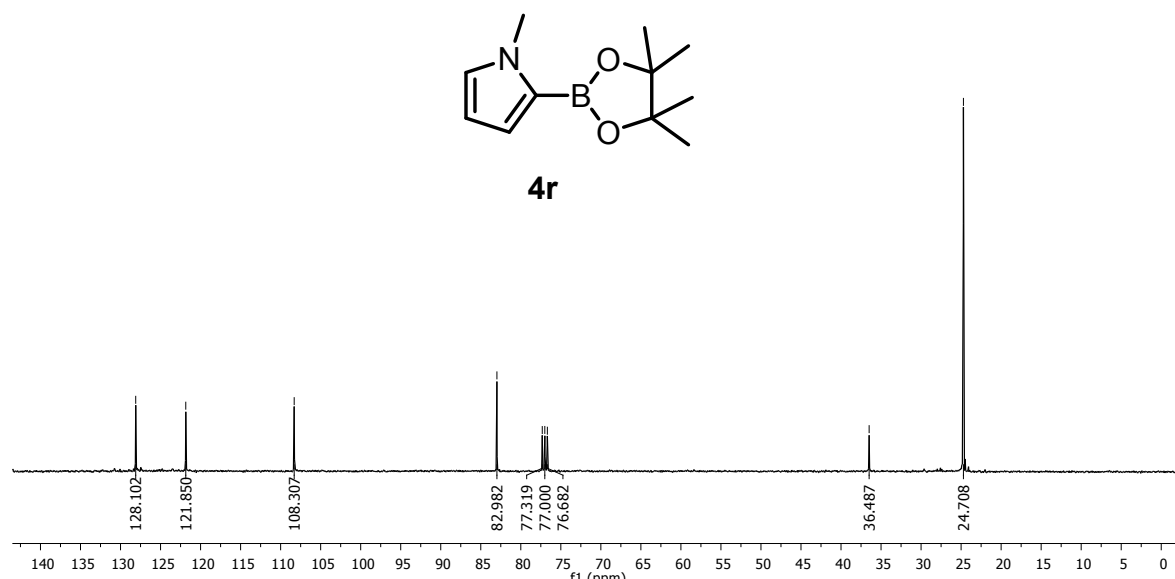


Figure S58. ^{13}C NMR (CDCl_3) spectrum of 1-methyl-2-(4,4,5,5-tetramethyl-1,3,2-dioxaborolan-2-yl)-1H-pyrrole (**4r**).

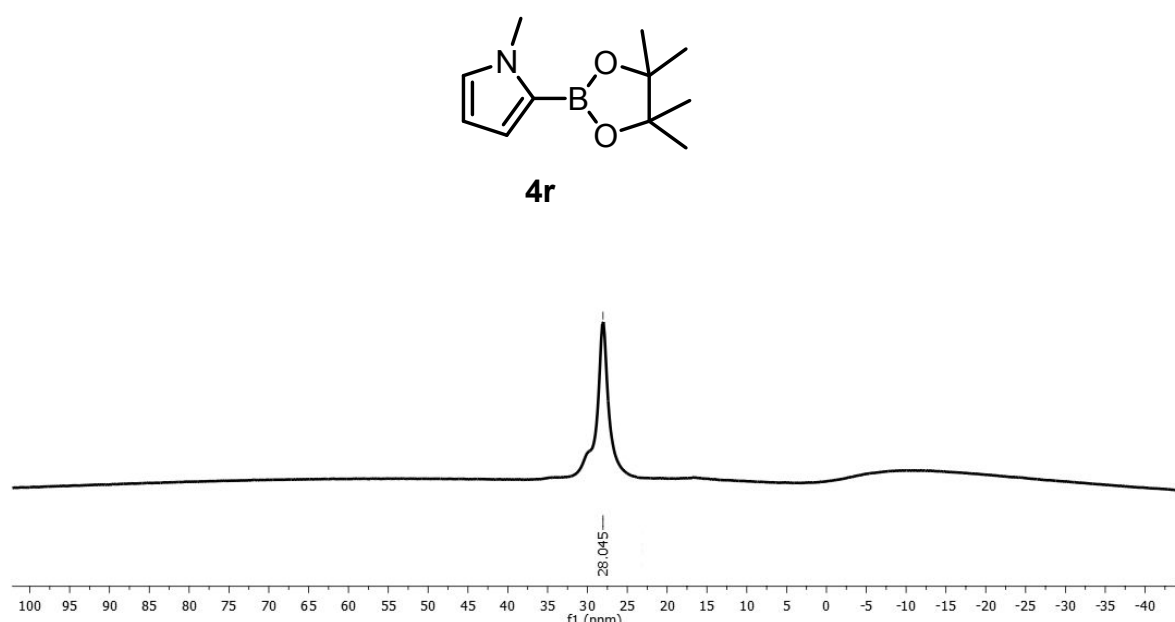


Figure S59. ^{11}B NMR (CDCl_3) spectrum of 1-methyl-2-(4,4,5,5-tetramethyl-1,3,2-dioxaborolan-2-yl)-1H-pyrrole (**4r**).

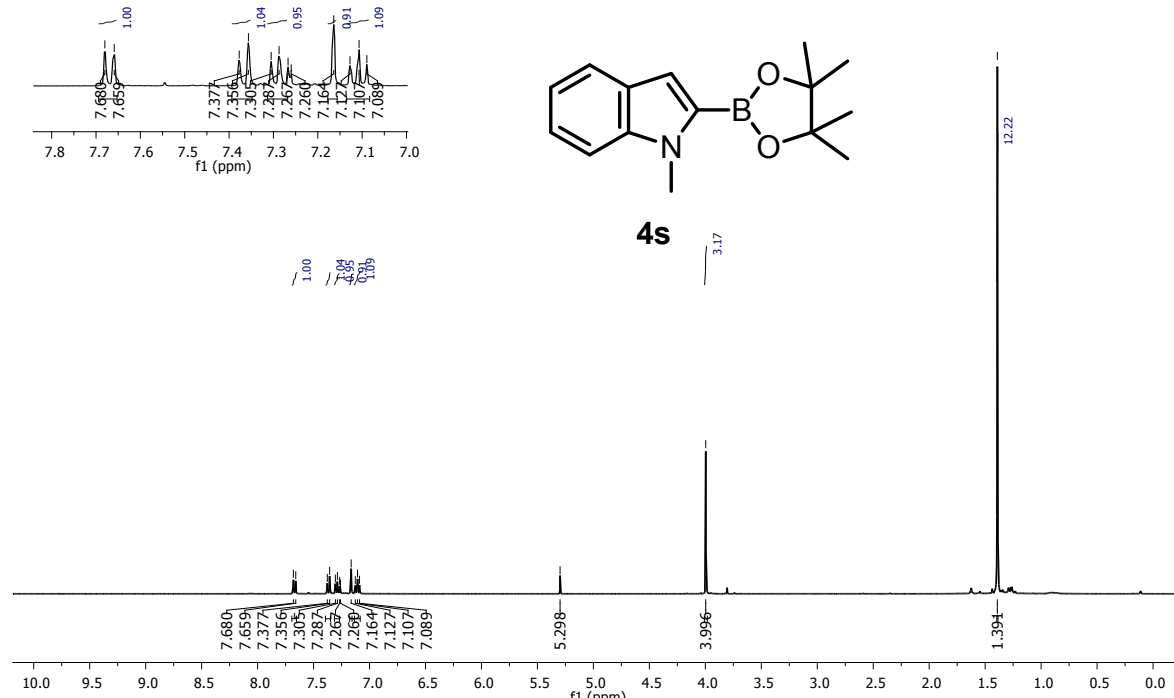


Figure S60. ¹H NMR (CDCl_3) spectrum of 1-methyl-2-(4,4,5,5-tetramethyl-1,3,2-dioxaborolan-2-yl)-1H-indole (**4s**).

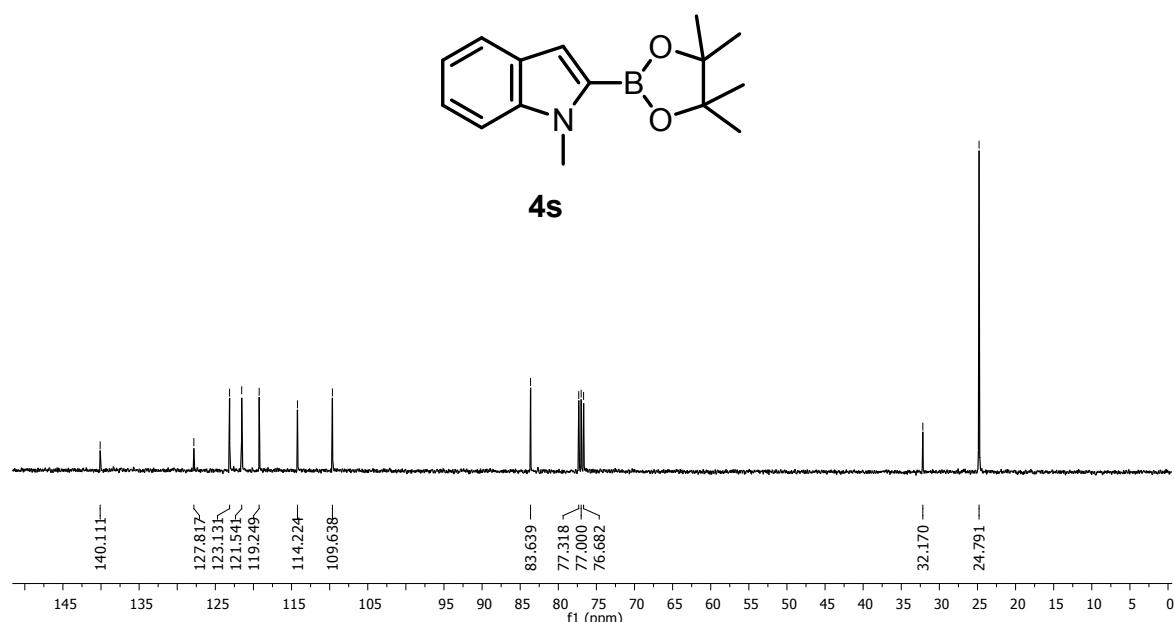
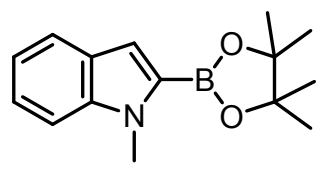


Figure S61. ¹³C NMR (CDCl_3) spectrum of 1-methyl-2-(4,4,5,5-tetramethyl-1,3,2-dioxaborolan-2-yl)-1H-indole (**4s**).



4s

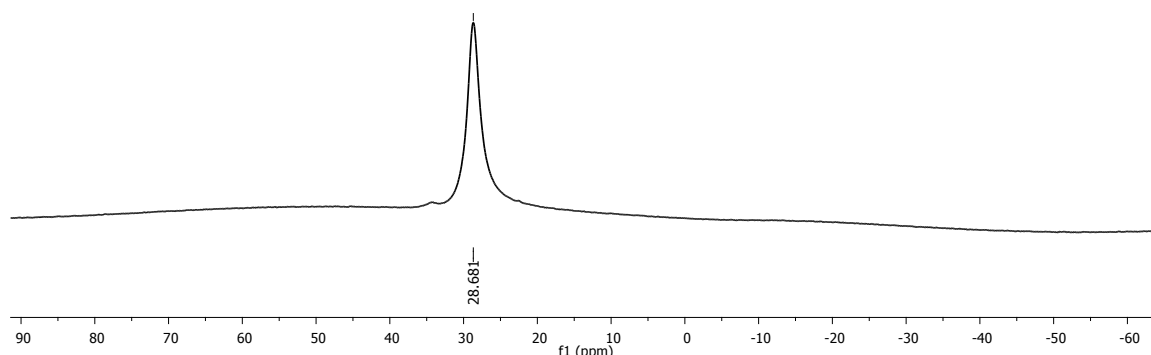


Figure S62. ^{11}B NMR (CDCl_3) spectrum of 1-methyl-2-(4,4,5,5-tetramethyl-1,3,2-dioxaborolan-2-yl)-1H-indole (**4s**).

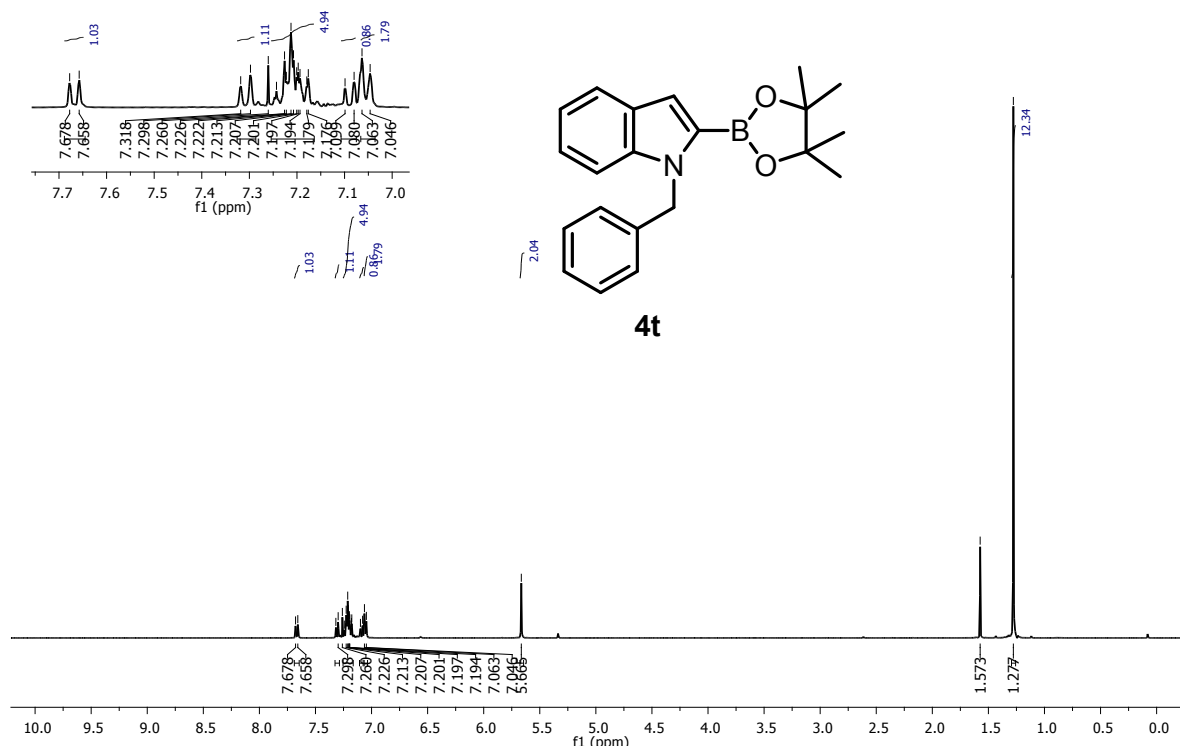


Figure S63. ^1H NMR (CDCl_3) spectrum of 1-benzyl-2-(4,4,5,5-tetramethyl-1,3,2-dioxaborolan-2-yl)-1H-indole (**4t**).

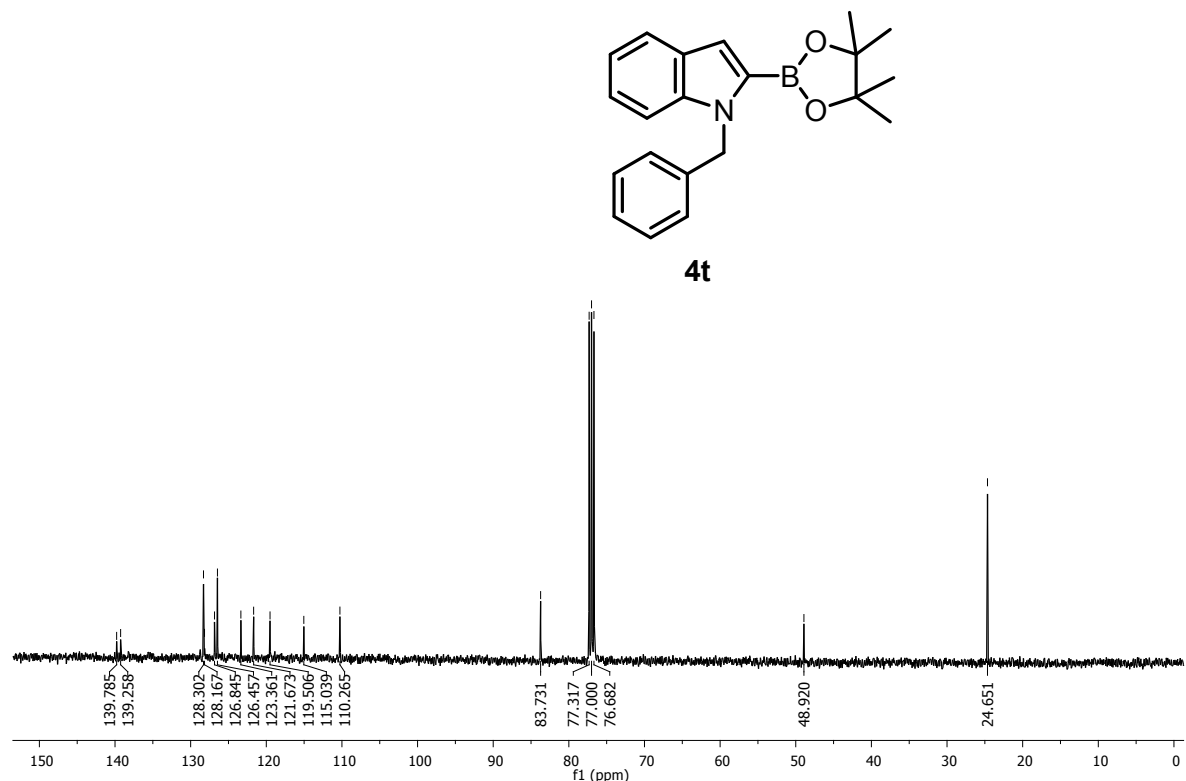


Figure S64. ^{13}C NMR (CDCl_3) spectrum of 1-benzyl-2-(4,4,5,5-tetramethyl-1,3,2-dioxaborolan-2-yl)-1H-indole (**4t**).

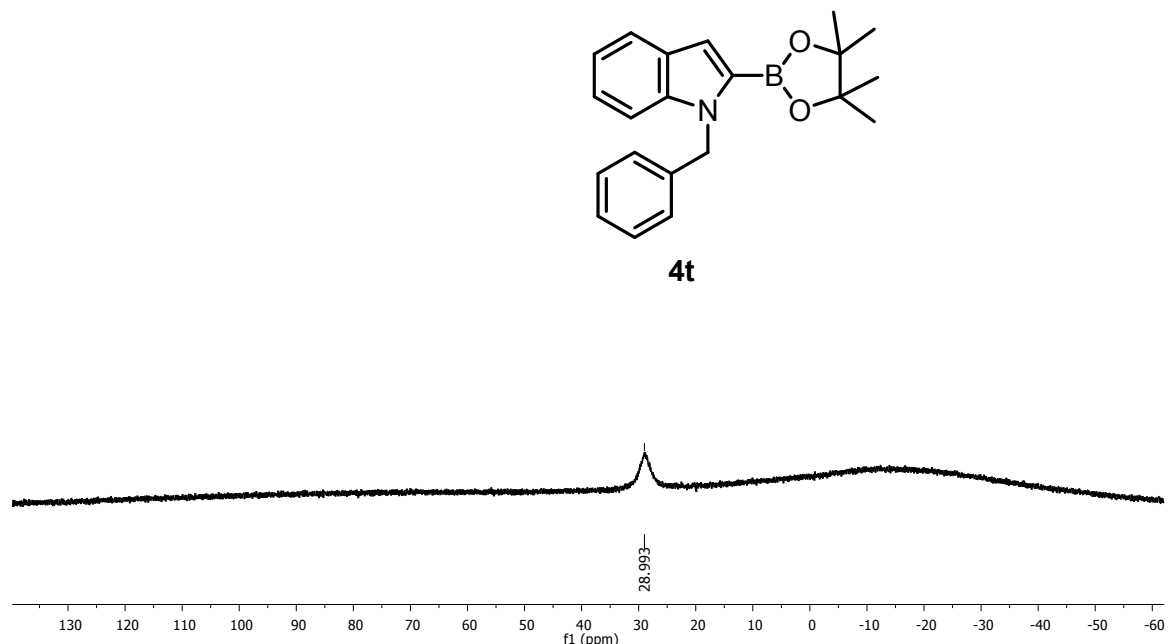


Figure S65. ^{13}C NMR (CDCl_3) spectrum of 1-benzyl-2-(4,4,5,5-tetramethyl-1,3,2-dioxaborolan-2-yl)-1H-indole (**4t**).

D) ^1H NMR spectra of stoichiometric reactions:

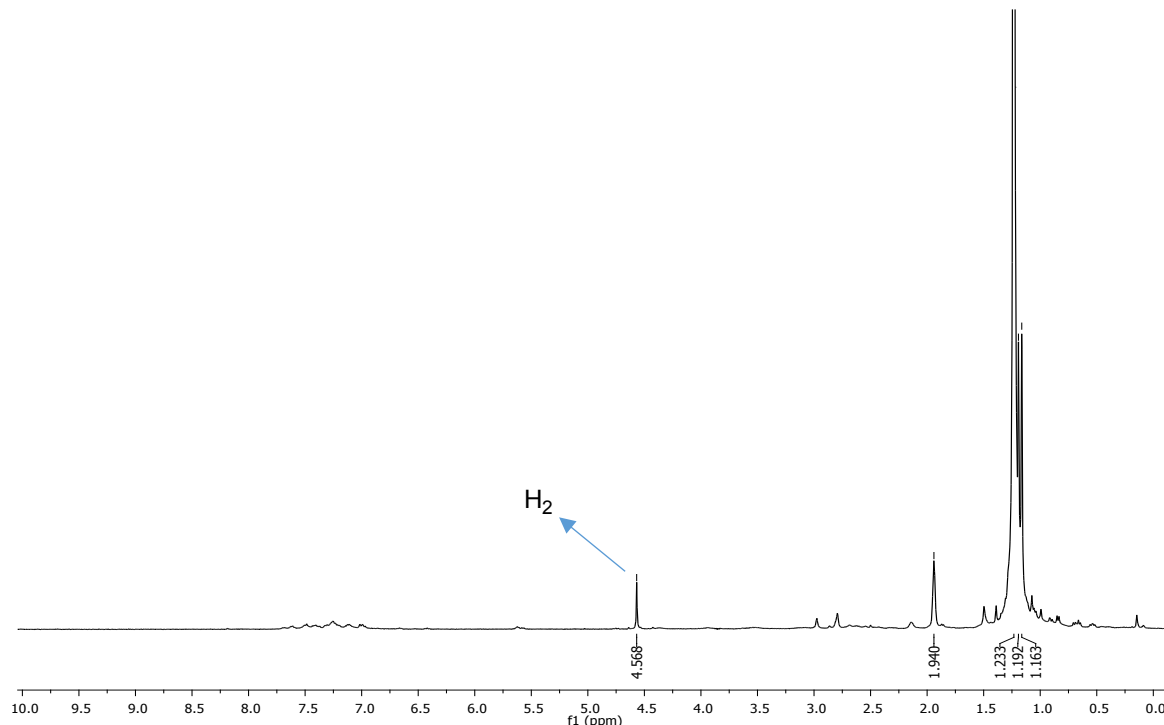


Figure S66. ^1H NMR spectrum of H_2 from reaction mixture of 1:1 ratio of Catalyst **1** and HBPin in CD_3CN using screw cap NMR tube.

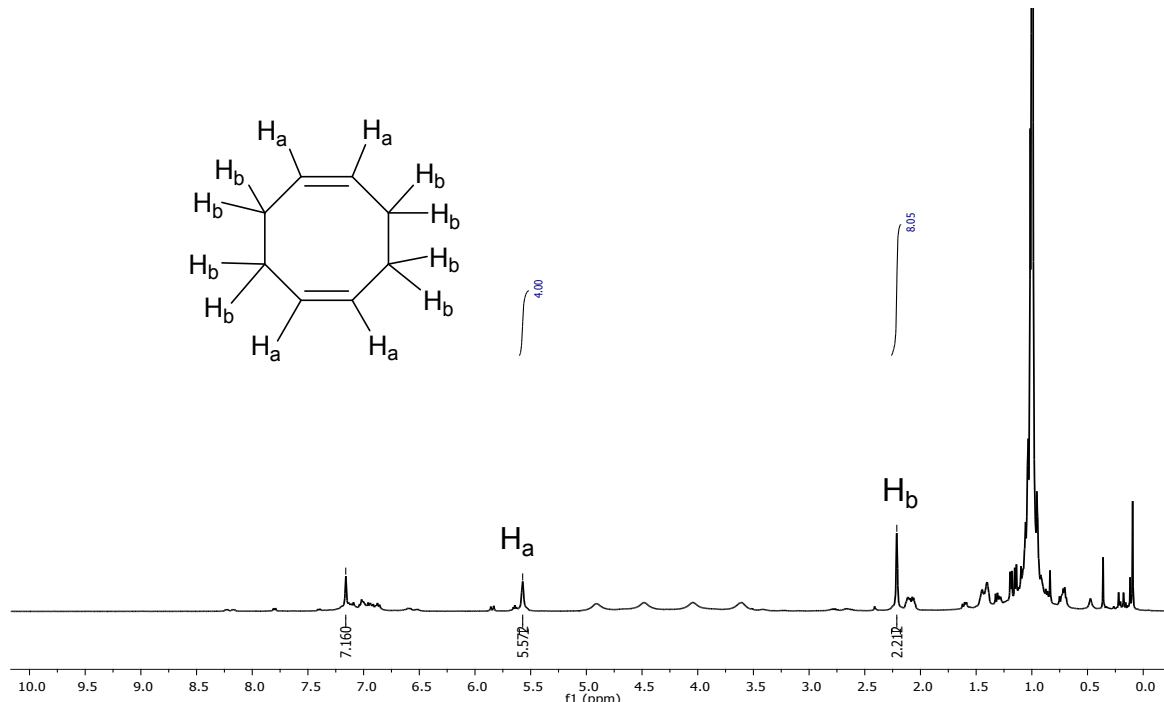


Figure S67. ^1H NMR spectrum of 1,5-cyclooctadiene from reaction mixture of 1:5 ratio of catalyst **1** and HBPin in C_6D_6 using screw cap NMR tube.

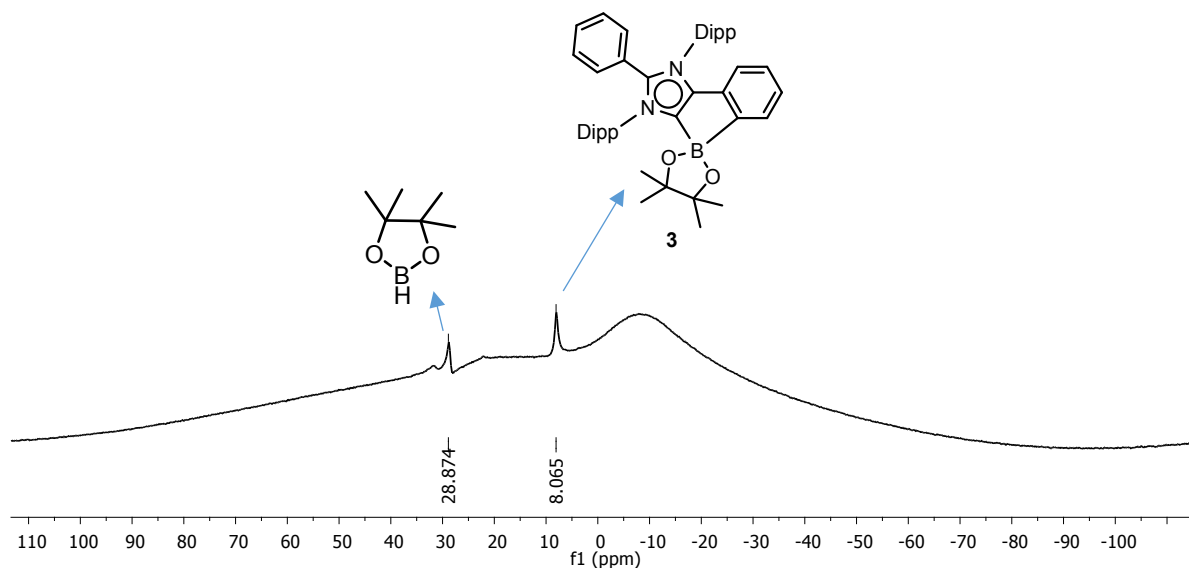


Figure S68. ^{11}B NMR spectrum of stoichiometric reaction mixture of Catalyst **1** and HBPin in C_6D_6 using screw cap NMR tube after 15 minutes.

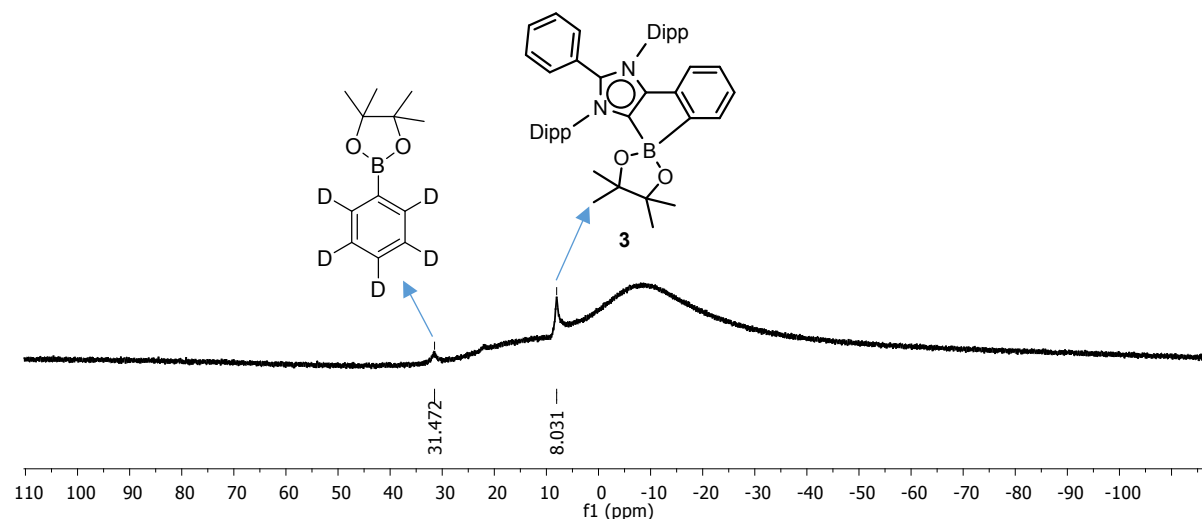


Figure S69. ^{11}B NMR spectrum of stoichiometric reaction mixture of Catalyst **1** and HBPin in C_6D_6 using screw cap NMR tube after 2 hours.

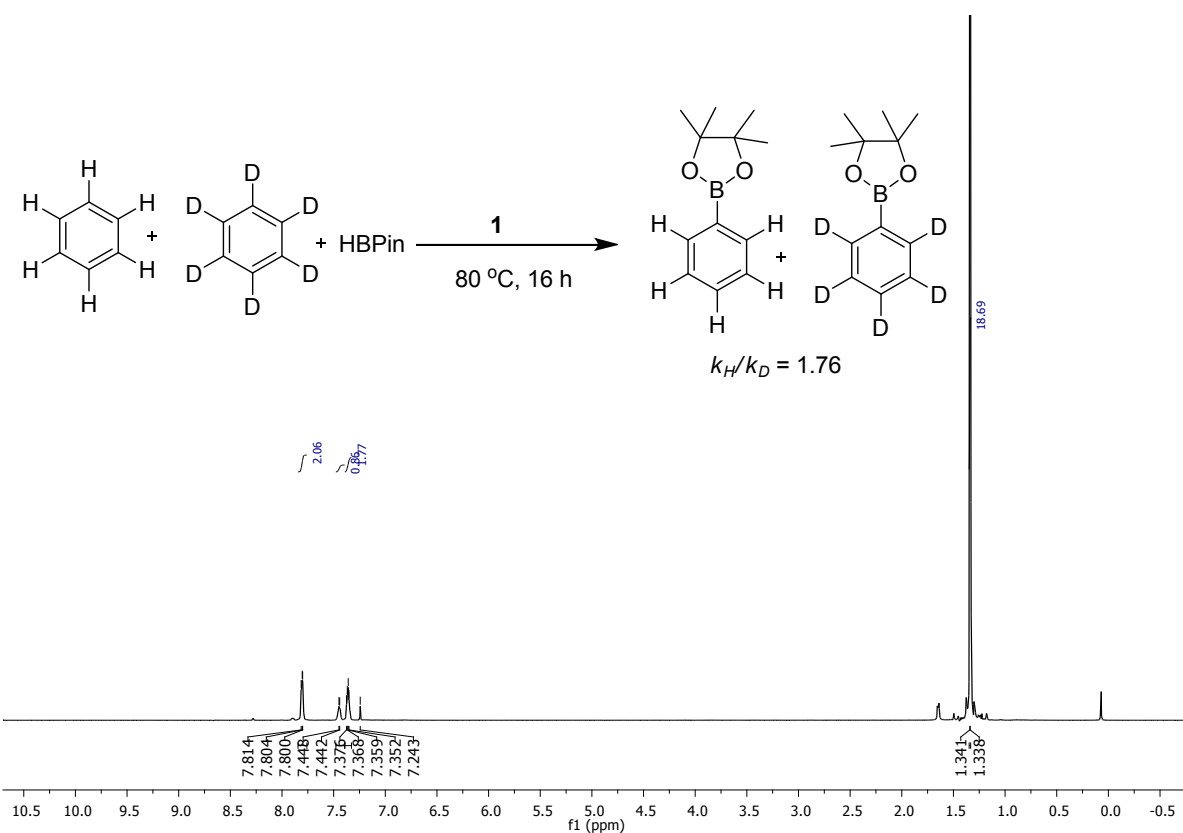


Figure S70. ^1H NMR (CDCl_3) spectrum for k_H/k_D experiment.

X-ray crystallographic details:

Suitable single crystals of **2** and **3** were selected and mounted under nitrogen atmosphere using the X-TEMP2 and intensity data were collected on a Super Nova, Dual, Cu at zero, Eos diffractometer. Both the crystals were kept at 100 K during data collection. Using Olex2,¹⁸ the structure was solved with the ShelXT¹⁹ structure solution program using Intrinsic Phasing and refined with the ShelXL²⁰ refinement package using Least Squares minimisation. All non-hydrogen atoms were refined with anisotropic displacement parameters. Crystallographic data (including structure factors) for the structures have been deposited with the Cambridge Crystallographic Data Centre. Copies of the data can be obtained free of charge from The Cambridge Crystallographic Data Centre *via* www.ccdc.cam.ac.uk/data_request/cif. CCDC 1890848 and 1890849 contains the supplementary crystallographic data of compounds **2** and **3** respectively for this paper.

E) Crystallographic and data collection parameters for **2 and **3**:**

	2	3
CCDC	1890848	1890849
Identification code	Ni_OMeNHC	Ni_HBPin_Tol
Empirical formula	C48 H58 N2 Ni1 O1,C6 H6	C45 H55 B1 N2 O2,C7 H8
Formula weight	815.78	758.85
T [K]	100.00(10)	100.00(3)
Crystal system	triclinic	triclinic
Space group	P-1	P-1
a [Å]	10.9163(5)	10.9028(3)
b [Å]	10.9742(6)	11.7027(4)
c [Å]	20.8663(9)	18.5034(5)
α [°]	95.921(4)	83.927(2)
β [°]	102.823(4)	83.272(2)
γ [°]	108.375(4)	67.576(3)

Volume [Å ³]	2272.3(2)	2162.54(12)
Z	2	2
ρ_{calcd} [g/cm ⁻³]	1.192	1.165
F[000]	876.0	820.0
μ [mm ⁻¹]	0.467	0.528
Crystal size/mm ³	0.4 × 0.3 × 0.2	0.2 × 0.15 × 0.1
Radiation	MoKα ($\lambda = 0.71073$)	CuKα ($\lambda = 1.54184$)
2θ [°] range for data collection	3.982 to 50.05	3.794 to 50.052
index ranges	-12 ≤ h ≤ 12, -13 ≤ k ≤ 13, -24 ≤ l ≤ 21	-12 ≤ h ≤ 12, -13 ≤ k ≤ 13, -21 ≤ l ≤ 21
Reflections collected	11750	15844
Independent reflections	7941 [R _{int} = 0.0301, R _{sigma} = 0.0588]	7471 [R _{int} = 0.0227, R _{sigma} = 0.0282]
Final R indexes [$I \geq 2\sigma(I)$]	R ₁ = 0.0427, wR ₂ = 0.0976	R ₁ = 0.0376, wR ₂ = 0.0939
Final R indexes [all data]	R ₁ = 0.0524, wR ₂ = 0.1050	R ₁ = 0.0421, wR ₂ = 0.0978
Data/restraints/parameters	7941/0/551	7471/0/527
Goodness-of-fit on F ²	1.044	1.031
Largest difference in peak and hole [e/ Å ³]	0.56/-0.57	0.75/-0.68

References:

1. Furukawa, T.; Tobisu, M.; Chatani, N. Nickel-Catalyzed Borylation of Arenes and Indoles via C–H Bond Cleavage. *Chem. Commun.* **2015**, *51*, 6508–6511.
2. Yan, G.; Jiang, Y.; Kuang, C.; Wang, S.; Liu, H.; Zhang, Y.; Wang, J. Nano- Fe_2O_3 -Catalyzed Direct Borylation of Arenes. *Chem. Commun.* **2010**, *46*, 3170–3172.
3. Boebel, T. A.; Hartwig, J. F. Iridium-Catalyzed Preparation of Silylboranes by Silane Borylation and Their Use in the Catalytic Borylation of Arenes. *Organometallics* **2008**, *27*, 6013–6019.
4. Dombray, T.; Werncke, C. G.; Jiang, S.; Grellier, M.; Vendier, L.; Bontemps, S.; Sortais, J. B.; Etienne, S. S.; Darcel, C. Iron-Catalyzed C-H Borylation of Arenes. *J. Am. Chem. Soc.* **2015**, *137*, 4062–4065.
5. O'Connell, D. P.; LeBlanc, D. F.; Cromley, D.; Billheimer, J.; Rader, D. J.; Bachovchin, W. W. Design and Synthesis of Boronic Acid Inhibitors of Endothelial Lipase. *Bioorg. Med. Chem. Lett.* **2012**, *22*, 1397–1401.
6. Benarous, R.; Chevreuil, F.; Ledoussal, B.; Chasset, S.; Strat, F. L. Inhibitors of viral replication, their process of preparation and their therapeutical uses. WO2014/057103 AI, PCT/EP2013/071321.
7. Rasina, D.; Otikovs, M.; Leitans, J.; Recacha, R.; Borysov, O.V.; Lapsa, I. K.; Domracheva, I.; Pantelejevs, T.; Tars, K.; Blackman, M. J.; Jaudzems, K.; Jirgensons, A. Fragment-Based Discovery of 2-Aminoquinazolin-4(3H)-ones As Novel Class Nonpeptidomimetic Inhibitors of the Plasmepsins I, II, and IV. *J. Med. Chem.* **2016**, *59*, 374–387.
8. Cho, J. Y.; Iverson, C. N.; Smith III, M. R. Steric and Chelate Directing Effects in Aromatic Borylation, *J. Am. Chem. Soc.* **2000**, *122*, 12868–12869.
9. Hu, J.; Sun, H.; Cai, W.; Pu, X.; Zhang, Y.; Shi, Z. Nickel-Catalyzed Borylation of Aryl- and Benzyltrimethylammonium Salts via C-N Bond Cleavage. *J. Org. Chem.* **2016**, *81*, 14–24.
10. Tajuddin, H.; Harrisson, P.; Bitterlich, B.; Collings, J C.; Sim, N.; Batsanov, A. S.; Cheung, M. S.; Kawamorita, S.; Maxwell, A. C.; Shukla, L.; Morris, J.; Lin, Z.; Marder, T. B.; Steel, P. G. Iridium-Catalyzed C-H Borylation of Quinolines and Unsymmetrical 1,2- Disubstituted Benzenes: Insights into Sterics and Electronic Effects on Selectivity. *Chem. Sci.* **2012**, *3*, 3505–3515.
11. Bheeter, C. B.; Chowdhury, A. D.; Adam, R.; Jackstell, R.; Beller, M. Efficient Rh-Catalyzed C–H Borylation of Arene Derivatives under Photochemical Conditions, *Org. Biomol. Chem.* **2015**, *13*, 10336–10340.
12. Vara, B. A.; Jouffroy, M.; Molander, G. A. C(sp₃)–C(sp₂) Cross-Coupling of Alkylsilicates with Borylated Aryl Bromides – An Iterative Platform to Alkylated Aryl- and Heteroaryl Boronates. *Chem. Sci.* **2017**, *8*, 530–535.

13. Chen, H. B.; Zhou, Y.; Yin, J.; Yan, J.; Ma, Y.; Wang, L.; Cao, Y.; Wang, J.; Pei, J. Single Organic Microtwist with Tunable Pitch, *Langmuir* **2009**, *25*, 5459–5462.
14. Liu, C.; Ji, C. L.; Hong, X.; Szostak, M.; Palladium-Catalyzed Decarbonylative Borylation of Carboxylic Acids: Tuning Reaction Selectivity by Computation. *Angew. Chem. Int. Ed.* **2018**, *57*, 16721–16726.
15. Cheng, Y.; Lichtenfeld, C. M.; Studer A. Metal-Free Radical Borylation of Alkyl and Aryl Iodides. *Angew. Chem. Int. Ed.* **2018**, *57*, 16832–16836.
16. Lokare, K. S.; Staples, R. J.; Odom, A. L. Synthesis, Properties, and Structure of Tethered Molybdenum Alkylidenes. *Organometallics* **2008**, *27*, 5130–5138.
17. Zernickel, A.; Du, W.; Ghorpade, S. A.; Sawant, D. N.; Makki, A. A.; Sekar, N.; Eppinger, J. Bedford-Type Palladacycle-Catalyzed Miyaura Borylation of Aryl Halides with Tetrahydroxydiboron in Water. *J. Org. Chem.* **2018**, *83*, 1842–1851.
18. Dolomanov, O. V.; Bourhis, L. J.; Gildea, R. J.; Howard, J. A. K.; Puschmann, H. OLEX2: A Complete Structure Solution, Refinement and Analysis Program. *J. Appl. Cryst.* **2009**, *42*, 339–341.
19. Sheldrick, G. M. SHELXT – Integrated Space-Group and Crystal-Structure Determination. *Acta Cryst.* **2015**, *A71*, 3–8.
20. Sheldrick, G.M. Crystal Structure Refinement with SHELXL. *Acta Cryst.* **2015**, *C71*, 3–8.